SEISMIC VERIFICATION OF MIXED EVENTS

Bernard Harris

Ocean and Atmospheric Science, Incorporated

Prepared for:

Air Force Office of Scientific Research

15 November 1975

AFOSR-TR-76-0038

OAS

OCEAN & ATMOSPHERIC SCIENCE, INC.
145 PALISADE STREET
DOBBS FERRY, NEW YORK 10522
914-693-9001

TR 75-271

FINAL REPORT

SEISMIC VERIFICATION OF

MIXED EVENTS

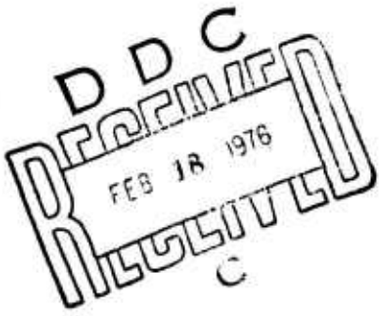

by

Dr. Bernard Harris

Submitted under Contract No. F44620-74-C-0066

Prepared for:

Air Force Office of Scientific Research
1400 Wilson Boulevard
Arlington, Virginia 22209

November 15, 1975

Form Approved
Budget Bureau No. 22-R0293

OAS

OCEAN & ATMOSPHERIC SCIENCE, INC.
145 PALISADE STREET
DOBBS FERRY, NEW YORK 10522
914-693-9001

FINAL REPORT

For Period April 1, 1974 to April 1, 1975

Sponsored by
Advanced Research Projects Agency
ARPA Order No. 1827

ARPA Order Number:	1827
Program Code Number:	4F10
Name of Contractor:	Ocean & Atmospheric Science, Inc.
Effective Date of Contract:	April 1, 1974
Contract Expiration Date:	March 31, 1975
Amount of Contract Dollars:	$128,579
Contract Number:	F44620-74-C-0066
Principal Investigator and Phone Number:	Dr. Bernard Harris (914) 693-9001
Program Manager and Phone Number:	Dr. Bernard Harris (914) 693-9001
Short Title of Work:	Seismic Verification of Mixed Events

This research was supported by the Advanced Research Projects Agency of the Department of Defense and was monitored by the Air Force Office of Scientific Research under Contract No. F44620-74-C-0066.

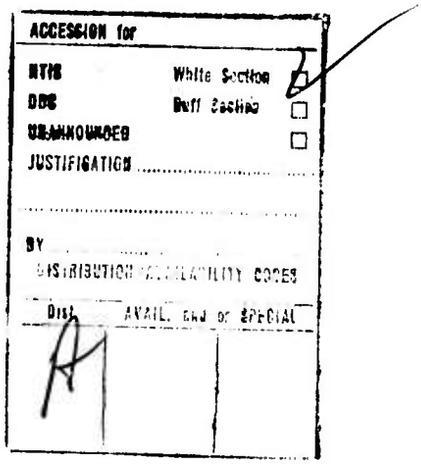

UNCLASSIFIED

SECURITY CLASSIFICATION OF THIS PAGE (When Data Entered)

REPORT DOCUMENTATION PAGE		READ INSTRUCTIONS BEFORE COMPLETING FORM
1. REPORT NUMBER AFOSR - TR - 76 - 0038	2. GOVT ACCESSION NO.	3. RECIPIENT'S CATALOG NUMBER
4. TITLE (and Subtitle) FINAL REPORT: SEISMIC VERIFICATION OF MIXED EVENTS		5. TYPE OF REPORT & PERIOD COVERED Final Report April 1, 74 - April 1, 75 6. PERFORMING ORG. REPORT NUMBER TR 75-271
7. AUTHOR(s) Dr. Bernard Harris		8. CONTRACT OR GRANT NUMBER(s) F44620-74-C-0066
9. PERFORMING ORGANIZATION NAME AND ADDRESS Ocean & Atmospheric Science, Inc. 145 Palisade Street, Dobbs Ferry, NY 10522		10. PROGRAM ELEMENT, PROJECT, TASK AREA & WORK UNIT NUMBERS 62701E AO 1827
11. CONTROLLING OFFICE NAME AND ADDRESS Advanced Research Projects Agency/NMR 1400 Wilson Boulevard Arlington, Virginia 22209		12. REPORT DATE November 15, 1975 13. NUMBER OF PAGES 159
14. MONITORING AGENCY NAME & ADDRESS (if different from Controlling Office) Air Force Office of Scientific Research 1400 Wilson Boulevard Arlington, Virginia 22209		15. SECURITY CLASS. (of this report) UNCLASSIFIED 15a. DECLASSIFICATION/DOWNGRADING SCHEDULE

16. DISTRIBUTION STATEMENT (of this Report)

Approved for public release; distribution unlimited

17. DISTRIBUTION STATEMENT (of the abstract entered in Block 20, if different from Report)

18. SUPPLEMENTARY NOTES

Nuclear seismic discrimination; surface waves; ellipticity; mixed events

19. KEY WORDS (Continue on reverse side if necessary and identify by block number)

Nuclear seismic discrimination; surface waves; ellipticity; mixed events; Love waves; Rayleigh waves

20. ABSTRACT (Continue on reverse side if necessary and identify by block number)

The limitations of polarization and azimuthal filters for sorting mixed event seismic signals was quantified and a combined data processing technique, the Ellipticity Filter, was proposed. The algorithms for instrumenting the Ellipticity Filter concept for both noise-free and noise-present models were developed. The

DD FORM 1 JAN 73 1473 EDITION OF 1 NOV 65 IS OBSOLETE

UNCLASSIFIED

SECURITY CLASSIFICATION OF THIS PAGE (When Data Entered)

superiority of the Ellipticity Filter, however, requires the accurate calibration of the seismological stations. This problem was experimentally examined and the differences of the seismic instrumentation noted. Since considerable improvements in the VLP seismological stations have been recently achieved, it is recommended that the Ellipticity Filter technique be tested using current data.

Summary

This is the final report describing the work performed on Contract No. F44620-74-C-0066 during the period April 1, 1974 to April 1, 1975. The purpose of this effort is to:

1. Establish a classification technique for mixed seismic events,
2. Establish a computer model(s) for these classification techniques,
3. Evaluate the azimuthal and polarization filters and array processing methods as a combined data processing technique and its usefulness as a discriminate criterion.

Seismic verification of underground nuclear explosions requires the classification of seismic events from observations made at teleseismic distances. For single events, considerable success has been achieved by examining the characteristics of the body and surface waves and applying such single event classifiers as the M_s:m_b ratio. For mixed events, the key problem is to free the surface waves of the event from the overlapping events and interferences to permit single event classifiers to be used.

The decomposition of mixed events into the multipath and interference components has been done, in the past, by groups under Lynn Sykes and S.S. Alexander, using such techniques as the Polarization and Azimuthal Filters. For polarization-type filters, the

basis of the decomposition is a phase difference sort, such as the phase difference between the radial horizontal and vertical components of a Rayleigh wave. For azimuthal-type filters, the basis of the decomposition is a frequency domain sort based on the amplitude ratio of the horizontal seismometer signals. Azimuthal filtering can also be based on array techniques such as the high resolution f-k methods, but these are not considered here.

A performance evaluation of the Polarization and Azimuthal Filters shows that they can have only limited success in a mixed event situation because:

1. They are essentially sorting and not filtering techniques,

2. The multipath components of the mixed events must be non-overlapping in frequency-time space.

To avoid these limitations, the Ellipticity Filter was proposed. The Ellipticity Filter, because the ellipticity of the Rayleigh wave components is used as a constraint, is a structural approach which permits quantified relations to be written between the amplitudes, phases, and azimuths of the multipath signals. Perturbations due to unstructured components such as noise can be minimized by means of auxiliary relationships. Moreover, matched filter processing can be included by interrelating the components at different

frequencies. The overall result is a unified processing technique which should prove much superior to the fragmented approaches previously used.

The superiority of the Ellipticity Filter, however, requires accurate calibration of the seismological stations in both amplitude and phase shift as a function of frequency. Until recently, the presence of substantial drift in the frequency response of the instrumentation prevented attainment of accuracies much better than ten percent. A considerable effort was, therefore, necessarily directed toward the attainment of accurate calibration in the presence of such drift. This effort was not successful either because the sites were not calibrated frequently enough for the complex transfer function to be determined or because the drift was unpredictable.

Since this situation has now been alleviated by the development and site emplacement of better electronics, it is recommended that the Ellipticity Filter technqiue be tested using current instrumentation. The results should be not only a good method for coping with the mixed event situation, but lead to a better seismological understanding of earth physics through the more accurate measurement of ellipticity.

TABLE OF CONTENTS

TABLE OF CONTENTS (Continued)

TABLE OF CONTENTS (Continued)

TABLE OF CONTENTS (Continued)

LIST OF FIGURES

LIST OF FIGURES (Continued)

LIST OF TABLES

SECTION I

PERFORMANCE EVALUATION OF AZIMUTHAL AND POLARIZATION FILTERS FOR SEISMIC APPLICATIONS

The decomposition of mixed events into the multipath components has been done, in the past, using such techniques as the Polarization and Azimuthal Filters. The performance of these filters is considered here in detail. The evaluation shows that Polarization and Azimuthal Filters are limited in a mixed event situation because they do not fully exploit the structure of the horizontal and vertical components of the multipath. The result is that these techniques can be successful only if the events are non-overlapping in frequency-time space. For this reason, the Ellipticity Filter is superior.

1.0 Introduction

A mixed event situation occurs when the surface seismic waves of a target event arrive at a seismological station at the same time as the seismic waves of other events, such as the coda of an earthquake. In some mixed situations, the arrivals are not simultaneous at all stations and the events can be resolved. In other situations, however, the mixed event itself must be resolved using the composite event data. The purpose of this decomposition of the composite event is to determine such features as the magnitude of the target event so that classifiers such as the $M_s : m_b$ ratio can be used effectively.

The decomposition of a mixed event can be easily done when the component events fortuitously do not occupy the same frequency bin during the same time interval. In such instances, the basic events can be separated from each other when:

1. there are physical differences between the events that can be used as the basis for the sort,
2. the background noise level is low enough so that the sorting process is not excessively interfered with.

Physical differences that can be used as a basis for a sorting procedure are polarization and azimuth. These are encompassed in such techniques as Choy and McCamy's Polarization and Azimuthal

Filters[1,2]. Similar techniques are encompassed in the REMODE system of Sax and Mims[3,4] as well as in non-seismic systems such as those associated with radio and underwater sound systems.

It is to be emphasized that, in order for these techniques to be successful, the events which are mixed must not occupy the same frequency bin at the same time. In addition, the background noise level must be low to permit the necessary non-linear processing.

The magnitude of these problems can be roughly quantified using general principles. At the decision point of the sort, the non-linear sorting operation, because it is a non-linear process, requires a signal-to-noise ratio threshold of 10 to 20 dB for the sorting to be successful. That is, the ratio of the desired event power level to the background noise power level on a per frequency bin basis should exceed about 10 dB for any reasonable performance, and 20 dB for excellent performance. Below 10 dB, one usually has the problem of deciding if the performance is good enough, but above 20 dB most non-linear operations are relatively clean. Now, if there are about a half dozen independent frequency bins over the frequency range of interest, this implies that the desired signal to background noise level should exceed about 4 dB for the sort of reasonable performance and 12 dB for excellent performance. These results will be more fully quantified later.

The requirement of a good signal to background noise level can be alleviated, to some extent, by using the long period, high-gain seismometer stations developed by Lamont-Doherty Geological Observatory[5]. These long-period, high-gain seismometer stations have their peak magnification centered about the earth noise minimum near 40 seconds and permit observation of very long-period surface waves from about 25 to 60 seconds[6,7,8]. As few as three of these stations are capable of detection, by direct instpection alone, roughly 60 percent of all events on a world-wide basis whose magnitudes are greater than $m_b = 4.0$[9]. With such a reduced noise background, the remaining difficulty is primarily the mixed event problem or the detection of a desired signal in the presence of other signals such as coda.

It is to be recognized, of course, that the potential reduction in the noise level by using the VLP stations may not mean that the Polarization and Azimuthal Filter techniques are optimum in the VLP signal range. The first reason is that the reduction in background noise levels for the VLP instrumentation may be accompanied, at some sites, by a reduction in amplitude for the events of interest. Thus, the desired signal to background noise level improvement may not be as great as originally conjectured. The second reason is that the use of longer period signals can result in more frequency-time overlaps of the desired event and the interference. For signals having

periods from 25 to 60 seconds, the time aperture for evaluating the spectral components is limited to about 200 seconds. This is the duration over which the multipath propagation is stable[10]. There are, thus, only six independent frequency bins and the probability of the desired event and the interfering event randomly occupying the same frequency bin is 1/6th.

When this simultaneous occupancy occurs, the interfering event, when large, will usually suppress the desired event unless fortuitously structured. If the critical duration of the desired event is 600 seconds, only $(5/6)^3$ or 0.58 or about half the time will the desired event remain unobscured by the interference. If the critical duration is longer, the performance is, of course, worse.

The problem is that the desired event and the interference must be frequency separable. However, at least half the time, for VLP signals, this frequency separation will not be present and both the Polarization and Azimuthal filter techniques will fail. This is the reason the Ellipticity Filter has been proposed as a technique which will operate whether or not the events' frequencies overlap[11, 12].

2.0 Polarization Filter

The Polarization Filter, as developed by Choy and McCamy[1], separates a Rayleigh wave from Love waves by retaining and recombining only those signals which possess the desired attribute of a ninety degree phase shift between corresponding frequency-time bin components of the vertical and horizontal outputs of a three-axis seismometer site. The specific procedure is to select time windows of about two-hundred seconds duration. This is long enough to have about a half-dozen independent frequency bins over the VLP range of interest (25 to 60 seconds) but short enough so that the multipath is somewhat stable. The descrete Fourier Transforms of the selected horizontal and the vertical seismometer outputs are then computed for over-lapping, time-shifted windows. Ideally, the selected horizontal component is the radial component, when the azimuth is known, or the corresponding radial component when a particular azimuth is being tested. However, the selection should not be too critical of azimuth provided the desired horizontal component is not near tangential.

For each frequency component in the VLP range, the phase difference between the vertical and selected horizontal output is evaluated. Each frequency component is then either passed or attenuated based on the value of this phase difference.

Rather than using a pass or stop criterion, Choy and McCamy used a filter function with a monotonic fall-off which depended on the absolute value of the phase difference between the vertical and the selected horizontal component. The particular filter function used by Choy and McCamy is

$$F = \sin^{2N}\left[\phi_z(\omega) - \phi_h(\omega)\right]$$

in which $\phi_z(\omega)$ and $\phi_h(\omega)$ are the phases of the selected vertical and horizontal component.

As will be seen, the exact filter function is relatively unimportant although one could optimize the functional form depending upon the the expected relative amplitudes of the desired signal, interference, and background noise. Since the basic interest is in separating out a desired signal when the interference is high and the background noise level low, a near rectangular filter is optimum. In this sense, this filter function is equivalent to passing all frequency components whose phase angle differences from the 90° criterion are less than some Δ and stopping all frequency components whose difference exceeds Δ. For the filter function used by Choy and McCamy, the pass range Δ depends on the exponent N, large N corresponding to a smaller Δ.

The filter output is calculated by multiplying each Fourier component of the signal by the filter function, F . The output frequency-time bin representations of the passed signal are then transformed back into the time domain, if desired, and smoothed, The resulting signal is, thus, composed of frequency-time bin signals whose phase differences between the vertical and horizontal are near ninety degrees - as for a pure Rayleigh wave.

2.1 Suggested Improvements in the Polarization Filter

The suggested improvement in the Polarization Filter is to configure an Ellipticity Filter. More modest improvements are possible depending on the specific multipath components present.

2.1.1 Rayleigh-Love Wave Mixed Event

The Polarization Filter was originally configured to separate Rayleigh from Love waves. Since Love waves are horizontally polarized with no vertical component of motion, a mixed signal will pass only at those frequencies where the Rayleigh wave dominates, or where the horizontal components of the Rayleigh and Love signals are, by chance, completely in phase or out of phase. The situation is as shown below.

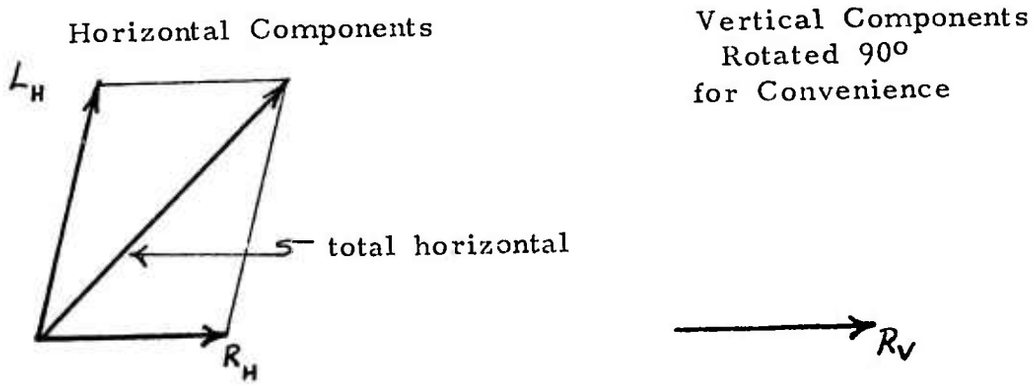

What the filter does is separate mixed Rayleigh and Love waves which do not occupy the same frequency-time bin at the same time.

The Polarization Filter could be improved for this mixed event situation by:

1. For each frequency bin, test the amplitude as well as the phase. Only those frequency bins in which there is both significant horizontal and vertical components should be considered to have a Rayleigh wave component. This would eliminate some background noise as well as the happenstance in which the Love wave component, albeit alone in a frequency bin, appeared to be a Rayleigh wave because of a near ninety degree relative phase angle with a corresponding vertical noise component.

2. A further refinement is to consider only those frequency components to be a Rayleigh wave in which the ratio of the horizontal to vertical component is within the allowed range of ellipticity values (including measurement errors), including amplitude as well as phase.

This latter refinement, of course, would bring the performance of the polarization Filter closer to that of the Ellipticity Filter. Then, the Polarization Filter would separate Rayleigh from Love waves even for the happenstance situations, provided the waves did not occupy the same frequency-time bin. Complete rejection, and thus error, would occur if any significant portion of these waves did overlap. The Ellipticity Filter would separate the signals even with an overlap condition.

2.1.2 Rayleigh-Rayleigh Wave Mixed Events

While the Polarization Filter was not designed to handle Rayleigh-Rayleigh wave mixed events, it is desirable to examine this situation to determine if it could be adapted to do so.

Pure Rayleigh waves have the characteristic that the vertical components are always $\pm 90^{\circ}$ out of phase with both horizontal components. If the two Rayleigh waves do not overlap in the frequency-time bins, it will be quite evident that two Rayleigh waves are present. The basis of the sort can then be:

1. The smooth behavior of the instantaneous frequency with time,
2. The smooth behavior of the instantaneous amplitude with time.

When two Rayleigh waves are present in one frequency-time bin, the composite signal is as shown below.

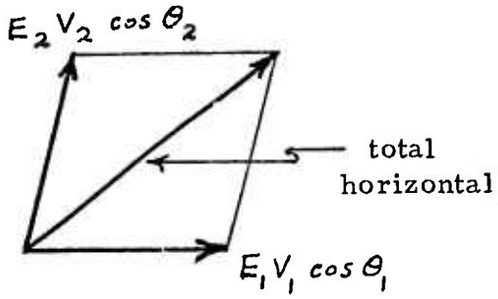

Horizontal Components

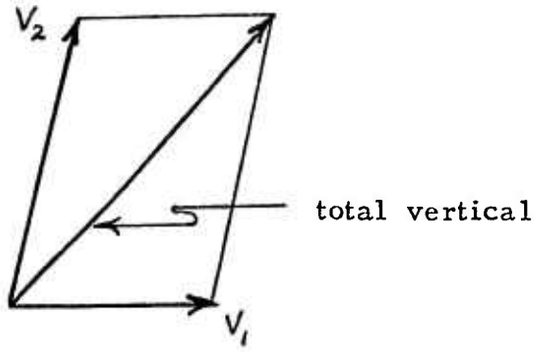

Vertical Components Rotated 90 degrees

V_1, V_2 are the vertical components

E_1, E_2 are the ellipticities of the two Rayleigh waves, since these may be bearing dependent.

θ_1, θ_2 are the corresponding bearings.

When the two waves are from the same azimuth, the total horizontal component will be 90 degrees with respect to the total vertical component. There is no way to separate this type of mixed event using a single seismological station. If the azimuths differ significantly, however, the mixed signal will be identifiable as not being a single Rayleigh event, provided the azimuth difference is not closely compensated by a change in ellipticity. It will not be possible to determine, however, if the mixed event is Rayleigh-Rayleigh or Rayleigh-Love unless the time behavior is examined and/or the range of potential ellipticity values is considered and/or the bearing is known.

What the filter does do is to help separate mixed Rayleigh waves which do not occupy the same frequency bin at the same time and reject mixed Rayleigh waves which do occupy the same frequency bin at the same time -- provided they are not from the same azimuth.

2.1.3 Love-Love Wave Mixed Events

Mixed signals, comprised of only Love waves, will not pass at all because the Polarization Filter is dependent on the phase difference between vertical and horizontal components. Since Love waves are horizontally polarized and have no vertical component, the filter will reject the entire record unless the vertical background noise fortuitously resembles the equivalent vertical Rayleigh component. A direct amplitude test should resolve this situation.

2.2 Performance Evaluation of the Polarization Filter

The Polarization Filter is a technique for sorting out Rayleigh waves in a mixed event situation. The basis of the sort is that the horizontal and vertical components of a Rayleigh wave have a ninety degree phase difference. When interference is present, the corresponding phase difference is usually not ninety degrees so that the presence of the interference can be recognized.

In the Polarization Filter, the two input signals are Fourier transformed, using a high speed algorithm such as the FFT, and the complex outputs of the corresponding frequency and phase compared. In the absence of interference, the desired signals are perturbed by the additive background noise to give the total observed signals. Thus, the two observed signals are related to the desired signal by

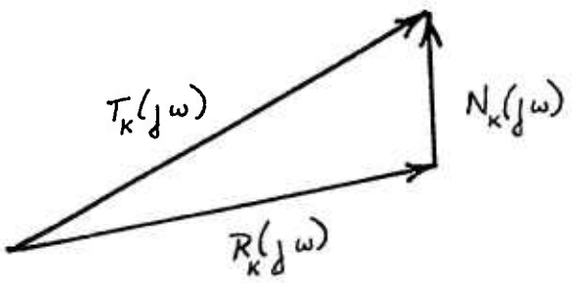

$K = 1, 2$

$$T_1(j\omega) = R_1(j\omega) + N_1(j\omega)$$
$$T_2(j\omega) = R_2(j\omega) + N_2(j\omega)$$

in which $R_1(j\omega)$ and $R_2(j\omega)$ are the desired Rayleigh wave components

$N_1(j\omega)$ and $N_2(j\omega)$ are the background noises of each seismometer output.

The corresponding phase angles of the two observed signals are

$$\varphi_1 = \arctan \frac{\mathrm{Im}\, T_1(j\omega)}{\mathrm{Re}\, T_1(j\omega)}$$

$$\varphi_2 = \arctan \frac{\mathrm{Im}\, T_2(j\omega)}{\mathrm{Re}\, T_2(j\omega)}$$

The performance of the Polarization Filter is easily understood from the following simplified analysis based on the background noise being small. The observed phase angles

$$\hat{\varphi}_K = \arctan \frac{\mathrm{Im}\, T_K(j\omega)}{\mathrm{Re}\, T_K(j\omega)} ; \qquad K = 1, 2$$

differ from the true phase angle in the absence of noise

$$\bar{\varphi}_K = \arctan \frac{\mathrm{Im}\, R_K(j\omega)}{\mathrm{Re}\, R_K(j\omega)}$$

by an amount

$$\Delta\varphi_k = \hat{\varphi}_K - \bar{\varphi}_K$$

or

$$\Delta\varphi_K = \arctan \frac{\mathrm{Im}\, T_K(j\omega)}{\mathrm{Re}\, T_K(j\omega)} - \arctan \frac{\mathrm{Im}\, R_K(j\omega)}{\mathrm{Re}\, R_K(j\omega)}$$

$$= \arctan \frac{\left[\frac{\mathrm{Im}\, T_K(j\omega)}{\mathrm{Re}\, T_K(j\omega)} - \frac{\mathrm{Im}\, R_K(j\omega)}{\mathrm{Re}\, R_K(j\omega)}\right]}{\left[1 + \frac{\mathrm{Im}\, T_K(j\omega)}{\mathrm{Re}\, T_K(j\omega)} \frac{\mathrm{Im}\, R_K(j\omega)}{\mathrm{Re}\, R_K(j\omega)}\right]}$$

$$\approx \frac{\frac{\mathrm{Im}\, T_K(j\omega)}{\mathrm{Re}\, T_K(j\omega)} - \frac{\mathrm{Im}\, R_K(j\omega)}{\mathrm{Re}\, R_K(j\omega)}}{1 + \frac{\mathrm{Im}\, T_K(j\omega)}{\mathrm{Re}\, T_K(j\omega)} \frac{\mathrm{Im}\, R_K(j\omega)}{\mathrm{Re}\, R_K(j\omega)}}$$

the approximation being based on

$$\arctan \Delta\varphi_K \approx \Delta\varphi_K$$

when the error in the angle is small.

In the form

$$\Delta\varphi_K \approx \frac{\mathrm{Im}\, T_K(j\omega)\, \mathrm{Re}\, R_K(j\omega) - \mathrm{Im}\, R_K(j\omega)\, \mathrm{Re}\, T_K(j\omega)}{\mathrm{Re}\, T_K(j\omega)\, \mathrm{Re}\, R_K(j\omega) + \mathrm{Im}\, T_K(j\omega)\, \mathrm{Im}\, R_K(j\omega)}$$

the denominator is bounded even when $\mathrm{Re}\, R_K(j\omega)$ is zero and the true angle is $\pi/2$. Moreover, the denominator is given by

$$[\mathrm{Re}\, R_K(j\omega)]^2 + [\mathrm{Im}\, R_K(j\omega)]^2 + \mathrm{Re}\, R_K(j\omega)\, \mathrm{Re}\, N_K(j\omega) + \mathrm{Im}\, R_K(j\omega)\, \mathrm{Im}\, N_K(j\omega)$$

which, for low noise levels, is simply $|R_K(j\omega)|^2 \approx R_K^2$.

The numerator is

$$Re\, R_K(j\omega)\, Im\, N_K(j\omega) - Im\, R_K(j\omega)\, Re\, N_K(j\omega)$$

so that

$$\Delta\varphi_K = \frac{\cos\bar{\varphi}_K\, Im\, N_K(j\omega) - \sin\varphi_K\, Re\, N_K(j\omega)}{R_K}$$

in which R_K is the amplitude of the desired component.

One notes that, for Gaussian noise, the inphase and quadrature noise components, $Re\, N_K(j\omega)$, $Im\, N_K(j\omega)$ are Gaussian. Hence, the distribution of the phase angle error is Gaussian since it is the sum or difference of two weighted Gaussian distributions.

The mean value of the Gaussian distribution is zero, since the expected value (denoted by brackets) is

$$\langle \Delta\varphi_K \rangle = \frac{\cos\bar{\varphi}_K \langle Im\, N_K(j\omega)\rangle - \sin\bar{\varphi}_K \langle Re\, N_K(j\omega)\rangle}{R_K}$$

$$= 0$$

The variance is

$$\sigma_{\varphi_K} = \langle(\Delta\varphi_K)^2\rangle = \frac{\cos^2\bar{\varphi}_K \langle[Im\, N_K(j\omega)]^2\rangle + \sin^2\bar{\varphi}_K \langle[Re\, N_K(j\omega)]^2\rangle}{R_K^2}$$

since the crossterm is zero - i.e., $\langle Im\, N_K(j\omega)\, Re\, N_K(j\omega)\rangle = 0$.

If the noise has a level, σ_{nK}^2

$$\langle [\mathrm{Im}\, N_K(j\omega)]^2 \rangle = \langle [\mathrm{Re}\, N_K(j\omega)]^2 \rangle = \sigma_{nK}^2$$

then

$$\sigma_{\varphi_K}^2 = \sigma_{nK}^2 / R_K^2$$

Thus, the error in one phase angle is Gaussian with zero mean and variance

$$\sigma_{\varphi_1}^2 = \frac{\sigma_{n1}^2}{R_1^2} = nsr_1$$

For the other phase angle, the error is also Gaussian with zero mean, but variance

$$\sigma_{\varphi_2}^2 = \frac{\sigma_{n2}^2}{R_2^2} = nsr_2$$

The variances of the phase angle error are thus proportional to the noise-to-signal ratios (nsr) when the noise levels are small. The difference angle, which is the argument of the filter function, is thus normal with zero mean as well. When the snr in both seismometer signals are about the same, the variance is twice the nsr of one of the inputs; when the snr is much smaller for one seismometer signal than is the other, the variance is the largest noise-to-signal ratio. In general

$$\sigma_{\varphi}^2 = nsr_1 + nsr_2$$

for the difference angle.

The filter function, $F(j\omega, \varphi)$, can have a variety of forms, one being that selected by Choy and McCamy.

$$F(j\omega, \varphi) = \sin^{2N}(\varphi_1 - \varphi_2)$$

However, the basic effect of the filter function is to pass all signals for which

$$|\varphi_1 - \varphi_2| \leq \Delta$$

and inhibit all other signals. The performance of the system can thus be adequately described by:

1. An equivalent rectangular filter function, $\pm \Delta$ wide
2. The operating characteristics in terms of the probability of accepting a desired signal p(A/D) vs the probability of accepting interference p(A/I).

This characterization will be done in the next two sections.

2.2.1 The Equivalent Rectangular Filter Function

There are several ways an equivalent rectangular filter function can be defined. The most rigorous definitions depend on the statistics of the interference to desired signal level and the attenuation required to render the interference significantly below the desired signal level. This approach is a little too involved for the general considerations of interest here.

Instead, three reasonable definitions will be considered and the results shown to be essentially the same.

1. RMS Window
2. Integrated Shape Window
3. Six dB Level Window

The equivalent rectangular filter function can be based on an "rms window" defined as

$$\Delta^2 = \frac{\int_0^{\frac{\pi}{2}} \theta^2 \cos^{2N}\theta \, d\theta}{\int_0^{\pi/2} \cos^{2N}\theta \, d\theta}$$

Since

$$\int_0^{\pi/2} \cos^{2N} d\theta = \frac{(2N-1)!!}{(2N)!!} \cdot \frac{\pi}{2}$$

$$= \frac{1 \cdot 3 \cdot 5 \cdots (2N-1)}{2 \cdot 4 \cdot 6 \cdots (2N)} \cdot \frac{\pi}{2}$$

and

$$\int_0^{\pi/2} \theta^2 \cos^{2N}\theta \, d\theta = -\frac{1}{2N^2}\int_0^{\pi/2} \cos^{2N}\theta \, d\theta + \frac{2N-1}{2N}\int_0^{\pi/2} \theta^2 \cos^{2N-2}\theta \, d\theta$$

the equivalent Δ can be solved for by iteration.

With equal intuition, an integrated shape window can be defined as

$$\Delta = \int_0^{\pi/2} \cos^{2N}\theta \, d\theta$$

so that the areas are equal, Then

$$\Delta = \frac{1.3.5\ldots(2N-1)}{2.4.6\ldots(2N)} \cdot \frac{\pi}{2}$$

With equal intuition, a third definition can be used, the 6 dB level window

$$\cos^{2N}\Delta = 1/2$$

$$\Delta = \cos^{-1}(1/2)^{1/2N}$$

The results are shown in Table I. The different definitions do not lead to significantly different results.

Experimentally, N=4 was found satisfactory for the few evaluations made with data[1]. This corresponds to passing signals whose phase difference between the vertical and horizontal is within ± 20 degrees of 90 degrees. One also notes that the effective aperture is not a strong function of N for large N .

Table I: Equivalent Rectangular Filters for the Power Law Sine Window

N	RMS		Integrated Shape Δ	6 dB Δ
	Δ radians	Δ degrees		
1	0.5678	32.53	45.00^{o}	45.00^{o}
2	0.4444	25.46	33.75^{o}	32.77^{o}
3	0.3767	21.58	28.13^{o}	27.01^{o}
4	0.3327	19.06	24.61^{o}	23.51^{o}
5	0.3011	17.25	22.15^{o}	21.09^{o}

Note: Δ is a "half" window definition.

2.2.2 Operating Characteristics

The probability of accepting the desired signal is

$$P(A/D) = \int_{-\Delta}^{+\Delta} \frac{e^{-\varphi^2/2\,(nsr_1 + nsr_2)}}{\sqrt{2\pi\,(nsr_1 + nsr_2}} \, d\varphi$$

$$= 2\int_{0}^{\Delta/(nsr_1 + nsr_2)^{1/2}} \frac{e^{-\frac{x^2}{2}}}{\sqrt{2\pi}} \, dx$$

$$= 2\left[\int_{0}^{\infty} \frac{e^{-x^2/2}}{\sqrt{2\pi}} \, dx - \int_{\Delta/(nsr_1 + nsr_2)^{1/2}}^{\infty} \frac{e^{-x^2/2}}{\sqrt{2\pi}} \, dx\right]$$

$$= 1 - 2\,\mathrm{erfc}\left[\frac{\Delta}{(nsr_1 + nsr_2)^{1/2}}\right]$$

in which erfc is the complement of the error function

$$\mathrm{erfc}\,(x) = \int_{x}^{\infty} \frac{e^{-x^2/2}}{\sqrt{2\pi}} \, dx$$

The interference, when present, is assumed to be much larger than the signal. The corresponding phase angle φ then has almost a uniform distribution. The probability of improperly accepting the

interference is then

$$P(A/I) = 2\int_0^{\infty} \frac{d\phi}{2\pi}$$

$$= \frac{\Delta}{\pi}$$

These two expressions give the operating characteristics of the Polarization Filter

$$P(A/D) = \left[1 - 2\,\mathrm{erfc}\left(\frac{\Delta}{(nsr_1 + nsr_2)^{1/2}}\right)\right]$$

$$P(A/I) = \frac{\Delta}{\pi}$$

or

$$P(A/D) = \left\{1 - 2\,\mathrm{erfc}\left[\frac{\pi P(A/I)}{(nsr_1 + nsr_2)^{1/2}}\right]\right\}$$

The difficulty in obtaining satisfactory performance from the Polarization Filter can be seen from Figure 1. Signal-to-noise ratios of about 20 dB are required for satisfactory performance. The key advantage of the Polarization Filter can also be seen. The non-linear processing will reject very high levels of interference.

This performance threshold can be described analytically. When $P(A/I)$ is to be small

$$\mathrm{erfc}\,\frac{\pi P(A/I)}{(nsr_1 + nsr_2)^{1/2}} \approx \frac{1}{2} - \sqrt{\frac{\pi}{2}}\,\frac{P(A/I)}{(nsr_1 + nsr_2)^{1/2}}$$

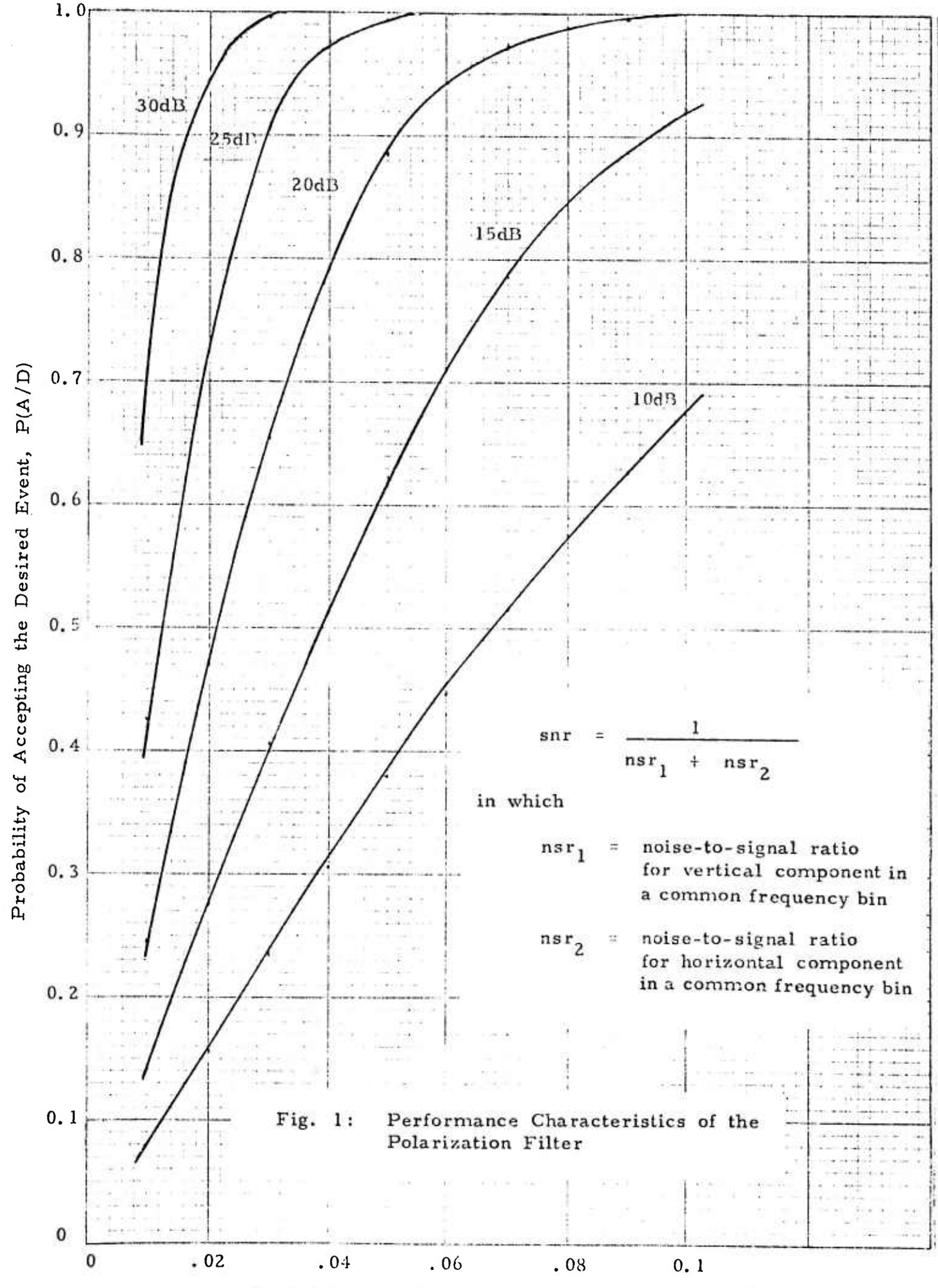

$$snr = \frac{1}{nsr_1 + nsr_2}$$

in which

nsr_1 = noise-to-signal ratio for vertical component in a common frequency bin

nsr_2 = noise-to-signal ratio for horizontal component in a common frequency bin

Fig. 1: Performance Characteristics of the Polarization Filter

and

$$P(A/D) = \sqrt{2\pi}\ \frac{P(A/I)}{(nsr_1 + nsr_2)^{1/2}}$$

Thus, to simultaneously have a high acceptance of the desired signal and a low acceptance of the interference requires

$$P(A/D) \approx 1$$

and

$$P(A/I) \approx \frac{(nsr_1 + nsr_2)^{1/2}}{\sqrt{2\pi}} << 0$$

For a reasonable level of accepting interference of ten percent,

$$(nsr_1 + nsr_2)^{1/2} = 0.10\sqrt{2\pi}$$
$$= 0.251$$

or

$$(nsr_1 + nsr_2) = 0.063$$
$$10\log(nsr_1 + nsr_2) = -12 \text{ dB}$$

Thus, the ratio of the desired signal to the background noise (in the frequency bin which has the desired signal) should be 12 to 15 dB or better for good performance. Since there are about a half-dozen frequency bands over the frequency range of interest, the wideband snr must be about 4 to 7 dB for good performance. If the reasonable level of accepting interference were set at five percent

$$(nsr_1 + nsr_2)^{1/2} = 0.05\sqrt{2\pi}$$
$$= 0.126$$

Then

$$(nsr_1 + nsr_2) = 0.016$$

$$10 \log (nsr_1 + nsr_2) = -18 \text{ dB}$$

The requirement on the ratio of the desired signal to background noise level would then be 18 to 21 dB. The corresponding wide-band snr should then be 10 to 13 dB for good performance.

The remaining point is to note that, for the level of accepting interference of ten percent, the window size is given by

$$P(A/I) = \Delta/\pi = 0.10$$

or the window is $\pm$ 18°. Thus, a ten percent interference acceptance level corresponds to the phase window of $\pm$ 20° which was used by Choy and McCamy. Note also that a $P(A/I)$ of 10 percent, on a per frequency bin basis, means for six bins no interference will be passed with a probability of $(0.9)^6$ or only fifty percent.

This means that, with a desired signal to background noise level of 4 to 7 dB, the Polarization Filter would operate satisfactorily against high interference levels about half the time. The filter function, however, should be more rectangular than that used by Choy and McCamy and with a window of $\pm$ 20°. To improve the level of satisfactory performance to about seventy-five percent of the time, the desired signal to background noise level would have to be 10 to 13 dB, and the filter function more rectangular and with a window of $\pm$ 10 degrees.

3.0 Azimuthal Filter

The Azimuthal Filter of Choy and McCamy is designed to separate Love waves from interfering waves. Love waves are horizontally polarized transverse waves i.e., the particle motion is perpendicular to the direction of propagation and exists only in the horizontal plane. The basis of the sorting procedure is to determine the apparent azimuth direction from the horizontal components and to pass only those waves whose apparent azimuth direction is close to the azimuth of the desired event. Filters of this type have been described by Sax and Mims (1965) and Simons (1968). Corresponding counterparts are used in radio direction finding and underwater sound systems.

The processing system is very similar to that of the Polarization Filter. The N - S component and the E - W component of the seismometers are Fourier transformed. For each frequency bin, an apparent azimuth is calculated

$$\hat{\theta}(\omega) = \tan^{-1} \frac{|X_{EW}(j\omega)|}{|X_{NS}(j\omega)|}$$

$X_{EW}(j\omega)$ is the E - W component in the frequency bin ω

$X_{NS}(j\omega)$ is the N - S component in the frequency bin ω.

The difference between the apparent azimuth, $\hat{\theta}$, and the azimuth of the desired event, $\bar{\theta}$, (or the azimuth being tested)

$$\theta(\omega) = \hat{\theta}(\omega) - \bar{\theta}(\omega)$$

determines whether or not the frequency components are passed. When

$$\theta(\omega) = \pm 90^{\circ} \pm \Delta$$

the Love wave is passed. Otherwise the frequency component is attenuated or blocked.

Choy and McCamy actually used the filter function

$$F(\omega) = \sin^{2N} \theta(\omega)$$

as the blocking function. As analyzed for the Polarization Filter, the exact filter function is not too critical, although one could optimize the function form for particular levels of desired signal, interference, and noise. The filter function essentially operates by passing all signals whose azimuths are within some $\pm \Delta$ of the expected azimuth. The relationship between the exponent, N, of the cosine power law filter and Δ is the same as that given in Section 2.2.1.

As with the Polarization Filter, the filter output is calculated by multiplying each Fourier component of the signal by the filter function. The frequency-time bin representations of the passed signal are then transformed into the time domain and smoothed to give the

estimated Love wave output for signals coming from the desired azimuth.

The limitations on this filter are similar to those of the Polarization Filter.

1. A high signal-to-background noise level is required,

2. The filter sorts rather than filters, so that the the desired signal and the interference should not occupy the same frequency bins at the same time.

3.1 Suggested Improvements in the Azimuthal Filter

The Ellipticity Filter is the suggested improvement of the Azimuthal Filter since it combines both the features of the Polarization Filter and the Azimuthal Filter as well as other decided advantages. More modest improvements can be made depending on the specific multipath components present.

3.1.1 Love-Love Wave Mixed Events

The Azimuthal Filter, as configured, works as expected against Love-Love wave mixed events. The system will filter Love waves from Love waves having a different azimuth. Confusion will result only if the mixed event is due to Love waves coming from the same azimuth or from directions 180^{o} apart. A simple improvement is to test amplitude as well as azimuth so that background noise levels in those frequency-time bins which are void of either Love wave components are not confused with the Love wave components.

3.1.2 Love-Rayleigh Wave Mixed Events

For Love-Rayleigh wave mixed events, the Love wave will be properly selected unless the Rayleigh wave occupies the same frequency-time bins as the Love wave or the Rayleigh wave coming from an azimuth which is normal to the expected Love wave azimuth.

In this latter case, examination of the frequency of the vertical component of the Rayleigh wave will serve to indicate which is the Love wave and which is the Rayleigh wave.

3.1.3 Rayleigh-Rayleigh Wave Mixed Events

If the apparent direction of the composite Rayleigh-Rayleigh wave mixed event is normal to the expected Love wave direction, the system will confuse the two. The obvious solution is to use the vertical component to determine the presence of two Rayleigh waves.

3.2 Performance Evaluation of the Azimuthal Filter

The performance evaluation of the Azimuthal Filter is similar to that of the Polarization Filter. The main difference is that the evaluation of azimuth cannot be done to the proper quadrant, whereas the evaluation of the polarization angle can be done to the proper quadrant. The result is that an acceptance angle of $\pm \Delta$ for the Azimuthal Filter means that interference will be effective over four regions as shown in Figure 2. For a reasonable Δ of 20^{o} (see Section 2.2 of the Polarization Filter analysis) this means that there is an 80^{o} range over which Love wave interference is serious and an 80^{o} range over which Rayleigh wave interference can be serious when the interference is in the same frequency-time bin as the desired signal. Clearly, the advantage of the Azimuthal Filter is similar to that of the Polarization Filter -- namely, that the filter shows when the desired signal alone occupies a frequency-time bin and when the desired signal is contaminated by an interference in the same frequency-time bin. Neither filters against this interference condition, they merely indicate its presence. The Ellipticity Filter, on the other hand, actually filters against these frequency-time bin overlapping events.

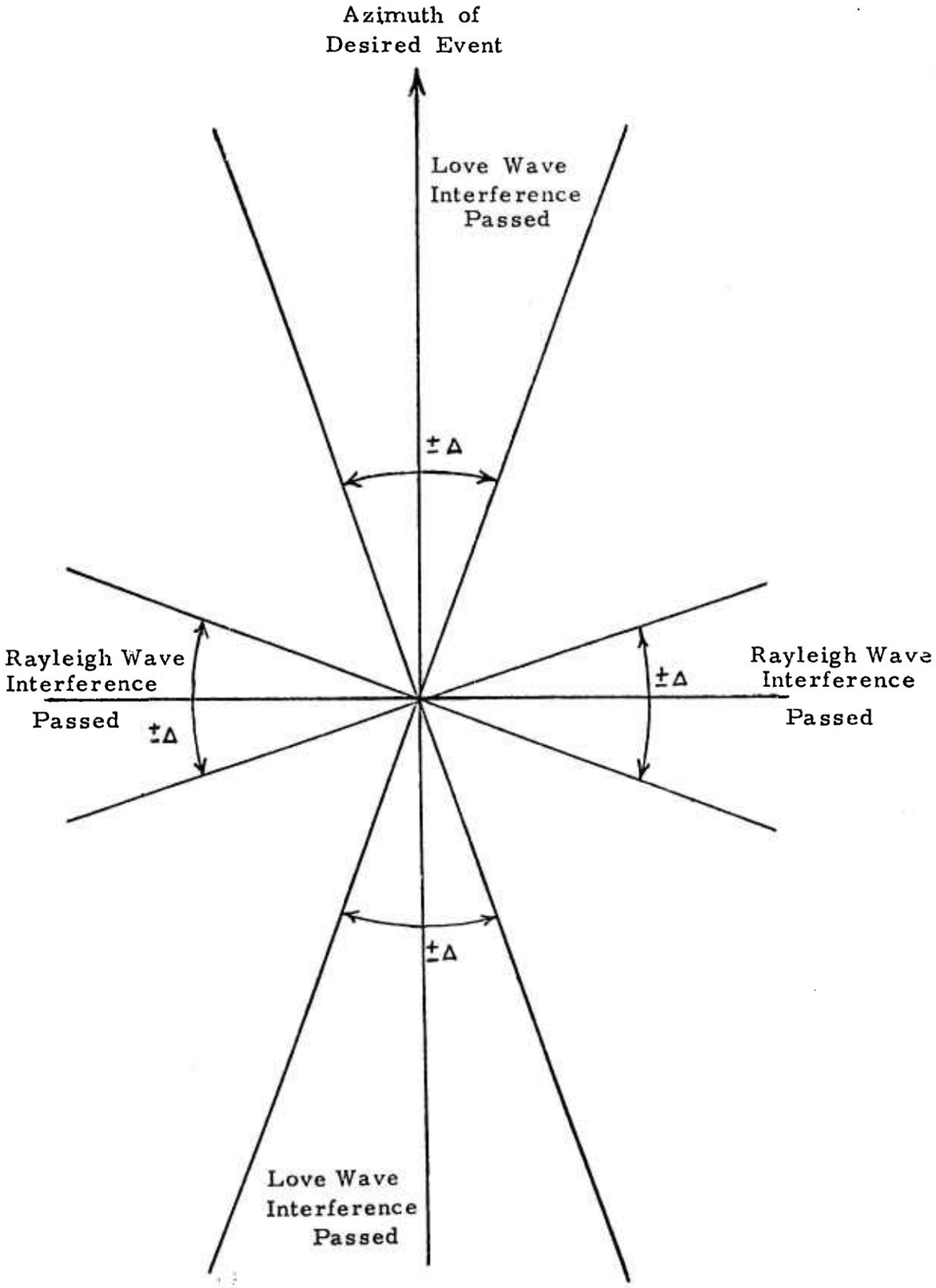

Fig. 2: Directions from which Interference is Passed by the Azimuthal Filter

SECTION II

MEASUREMENT OF SEISMOMETER MAGNIFICATION AND ELLIPTICITY AT A VLP STATION

As a possible solution to the mixed event problem in nuclear seismic discrimination, OAS has developed a filter termed the "ellipticity" filter which has the superposed Rayleigh and Love waves. Briefly, the ellipticity filter processes the output signals of a three-component seismometer station, using the value of ellipticity at the station to produce the complex amplitudes and azimuths of the superposed surface waves.

In order to use this filter, both the station calibration and ellipticity must be known. In this report, the calibration was determined for the Kongsberg VLP station during March 1972. With this calibration and three (3) earthquake seismograms, the value of station ellipticity was estimated. The rms error is less than 6% for periods from 21 to 64 seconds.

1.0 Introduction

As a possible solution to the mixed event problem in nuclear seismic discrimination, OAS has developed a filter termed the "ellipticity" filter which has the capability of separating sets of superposed Rayleigh and Love waves[11, 12]. Briefly, the ellipticity filter processes the output signals of a three component seismometer station using the value of ellipticity at the station to produce the complex amplitudes and azimuths of the superposed surface waves.

In order to use this filter, both the station calibration and ellipticity must be known. In this report, the calibration is determined for the Kongsberg VLP station during March 1972. With this calibration and the earthquake seismograms, the value of station ellipticity is estimated. The rms error is less than 6% for periods from 2 to 64 seconds.

Another approach to the determination of ellipticity could have been a theoretical calculation based on the known crustal structure at Kongsberg, Norway[14]. However, this approach was not implemented because the ellipticity measurement program allowed the evaluation of the concept of ellipticity on a group of events which were not highly selected, and in addition, permitted

a verification of the calibration method. Results of the calibration and ellipticity measurement indicate that, with slightly better instrumentation than available at the time, the actual separation of mixed events could be achieved.

The calibration was a simple, but tedious procedure. The Kongsberg station was selected because of its proximity to nuclear testing sites and because of the availability of digital data tapes. The rectangular pulses supplied daily to the system were used for calibration. Calibration was done by a complex amplitude fit in the frequency domain. Since it could not be determined whether the variation in the spectrum of the pulses was due to change in the seismometer parameters or to noise, four different calibration procedures were evaluated:

1. Fitting the daily response to a triple tuned model,
2. Fitting the average daily response to a triple tuned model,
3. Fitting the daily response by parabolic curve fitting,
4. Fitting the average daily response by parabolic curve fitting.

The evaluation involved the use of each calibration to determine station ellipticity from six events. The criterion for acceptance of a

procedure was the most consistent ellipticity evaluated. In the actual estimation of ellipticity, only events which had azimuths close to a cardinal direction were used. For these events, calibration errors cause only a scaling error in the estimation and not an error in the Rayleigh-Love wave separation process.

By the fitting of a 15 day average of the Fourier transforms of pulse to a triple-tuned seismometer response model, the best values (Table II) for the magnitude of the complex ellipticity were obtained. However, the best values for the angle of ellipticity were obtained by parabolic curve fitting of both the amplitude and phase to the 15 day average of the Fourier transforms. The results are shown in Table III.

Section 2 contains a brief review of the VLP System. In Section 3, a detailed explanation of the four calibration procedures appears. Section 4 presents the analysis of the ellipticity calculation for six earthquakes.

TABLE II: ELLIPTICITY MAGNITUDE FOR AVERAGE TRIPLE TUNED CALIBRATION MODEL

Period	Magnitude
64.0	1.72 ± .04
51.2	1.15 ± .03
42.7	1.16 ± .04
36.6	1.11 ± .06
32.0	1.07 ± .05
28.4	1.05 ± .05
25.6	1.06 ± .02
23.3	1.08 ± .06
21.3	1.01 ± .02
19.7	.873 ± .33

TABLE III: ELLIPTICITY ANGLE FOR PARABOLIC CURVE FITTING CALIBRATION METHODS

	FROM DAILY CALIBRATION		FROM AVERAGE CALIBRATION	
Period (sec)	Mean (degrees)	Standard Deviation (degrees)	Mean (degrees)	Standard Deviation (degrees)
64	89.8	5.3	96.6	5.3
51.2	87.0	6.7	91.3	5.1
42.6	83.5	15.3	91.8	11.6
36.6	89.5	27.4	93.3	13.2

2.0 System Description

The high gain, long period station developed by Lamont-Doherty Geological Observatory consists of three seismometers, one vertical and two horizontal, mounted at right angles to each other. Figure 3 shows a block diagram of the station[5]. Each seismometer has two velocity transducers, a displacement transducer, a primary calibration coil, and a secondary calibration coil. In normal station usage, only the primary coil is used for calibration.

For the high gain velocity channel, a velocity transducer is connected to a galvanometer with an attached mirror. After the position of the light beam reflected by this mirror is sensed with a pair of phototubes, the resulting signal is amplified and filtered. After the signal is digitized at a rate of 512 samples per second, it is averaged for one second and then stored on magnetic tape. In addition, it is recorded photographically on a drum recorder. For the low gain velocity channel, the output of the other velocity transducer is recorded directly on a photographic drum with a recording galvanometer.

In the displacement channel, a variable capacitance transducer together with an oscillator and discriminator are used to sense the

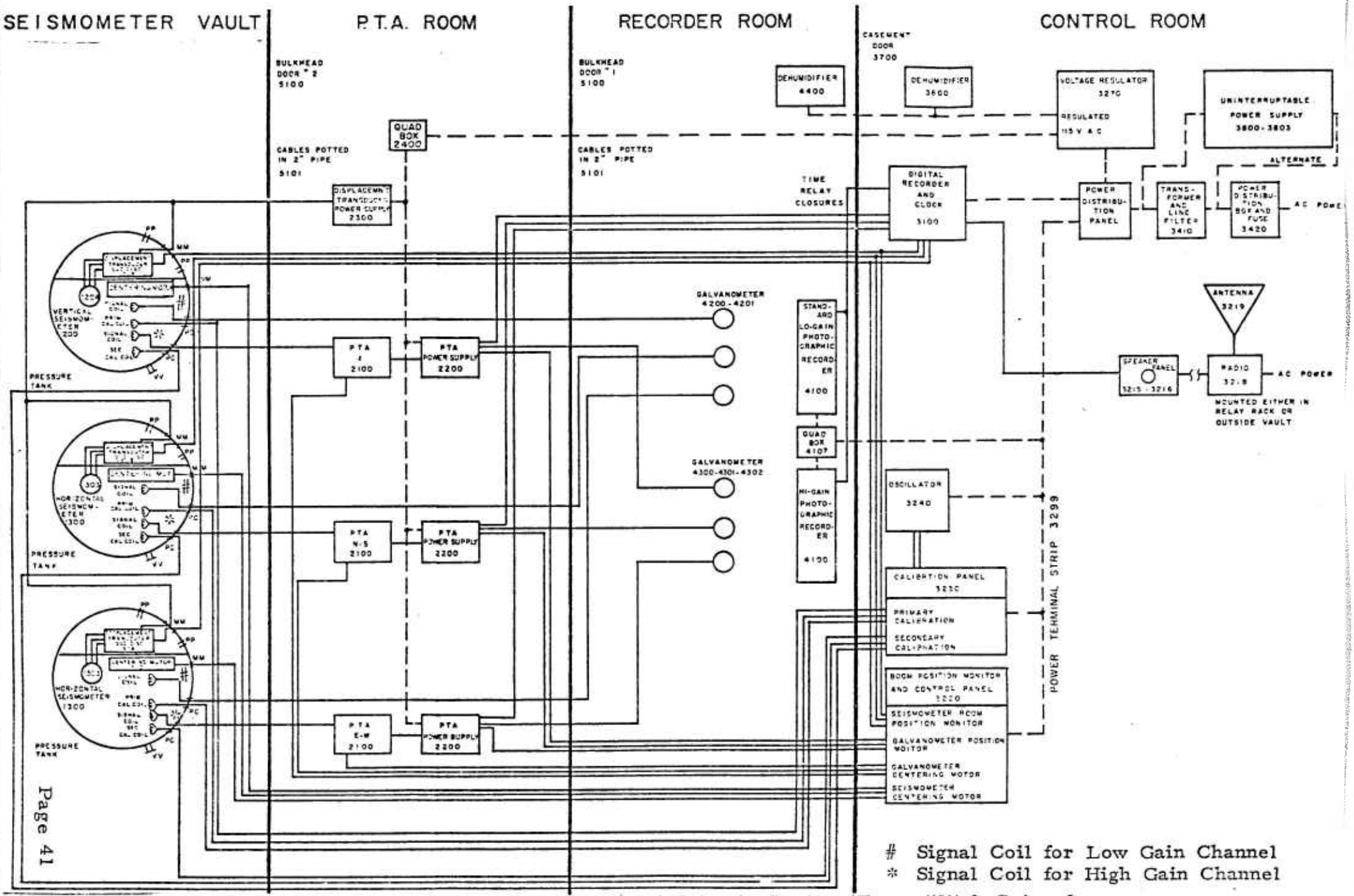

\# Signal Coil for Low Gain Channel
* Signal Coil for High Gain Channel

Fig. 3 : High Gain, Broad-Band Long Period Seismic Station (From "High-Gain, Long Period Seismograph Instrumentation," Volume 1, 1971)

position of the seismometer boom. The signal is then low pass filtered, digitized, and averaged. The displacement data is recorded on magnetic tape once every five seconds. In addition to giving an indication of boom position, the displacement channel monitors earth motion from a period of about 10 seconds to D. C.

3.0 Calibration

In order to calculate the station ellipticity from the digitized high gain velocity outputs of the three component seismometer, the instrumental response of the seismometer must first be removed from the signals. Let $X(t)$, $y(t)$, and $z(t)$ be the E/W, N/S, and vertical component signals expressed in digital counts. Assume that a Fourier transform of these signals has been taken for some desired window and are expressed as $X_i(jw)$, $Y_i(jw)$, and $Z_i(jw)$. Then the Fourier transform of the actual ground motions $X_g(jw)$, $Y_g(jw)$, and $Z_g(jw)$ may be expressed as

$$X_g(jw) = \frac{X_i(jw)}{M_x(jw)}$$

$$Y_g(jw) = \frac{Y_i(jw)}{M_y(jw)}$$

$$Z_g(jw) = \frac{Y_i(jw)}{M_z(jw)}$$

where $M_x(jw)$, $M_y(jw)$, and $M_z(jw)$ are the transfer functions of the component seismometers expressed in counts/micron. The transfer function is also called the magnification of the seismometer.

Since the Fourier transforms of the digitized outputs of the seismometers are expressed in counts, the transforms of the calculated ground motions will be microns.

The transfer function of a component seismometer is determined by passing a known current through its primary calibration coil and dividing the Fourier transform of its output by the transform of the known input signal. Corresponding to a force applied to the seismometer, the current causes a relative acceleration of the seismometer in the same manner that earth motion does. Before this method can be used at a station, the electromechanical constant, G, for the coil must first be determined. A variation of the standard weight lift method is used. In this method, a weight is attached to the seismometer. This weight causes a static deflection of the seismometer. A D.C. current is then sent through the coil and its magnitude is adjusted so that the seismometer returns to its initial position. The value of G may then be determined from the formula

$$G = \frac{\text{applied force in newtons}}{\text{restoring current in amperes}}$$

One known signal input for calibration is a set of sine waves with periods of 30, 40, 70, and 100 seconds. However, for the month selected, no sine wave calibration was available in Kongsberg. In 1972, the time between sine wave calibrations

at the station was greater than six (6) months. Inspection of Alberquerque Seismological Center records showed calibration changes of about 10% a month. Thus, sine wave calibrations could not be used even if they were present.

In addition to the sine waves, rectangular pulses of current are applied to calibration coils. At Kongsberg, calibrations pulses of 4μa and 50μa are applied simultaneously each day to all three seismometers. Examination of the plotted digital data shows that the pulses last for 240 seconds. Ideally, the large 50μa calibration pulse should be used to minimize the effect of noise on the calibration. However, the output shows an asymmetry because the large pulse makes the high gain velocity channel act in its non-linear region. Figure 4 shows an asymmetry of 43% into the y channel. Thus, the small pulses were used. In order to get frequency domain information from the pulse, a DFT transform with a window length of 480 seconds is used. This length window, in addition to letting the transient response of the system to go to zero, concentrates all of the signal energy in the odd harmonics of the DFT and gives maximum noise immunity.

3.1 Derivation of Calibration Equation

To use the pulses described in Section 3.0 as a calibration signal, the relation between the amplitude of the pulse and the transfer function must be derived. Since a current corresponds to

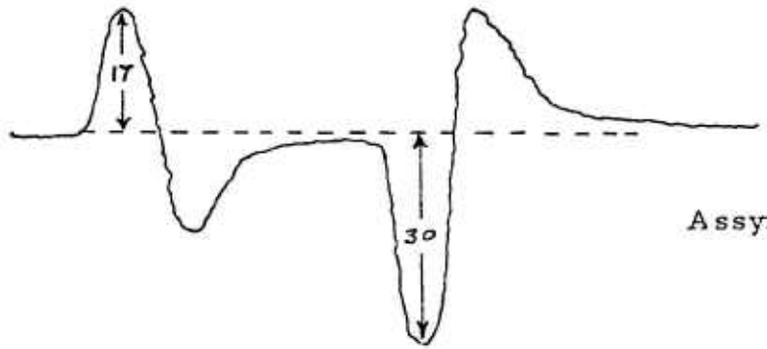

$$\text{Assymmetry} = \frac{30 - 17}{30} \times 100\%$$

$$= 43\ \%$$

Fig. 4: Asymmetric Calibration Pulse, Y Channel, Day 67

a force applied to the seismometer

$$\ddot{Y} = \frac{Gi}{m_e}$$

where

$\ddot{Y}$ = seismometer frame acceleration due to earth motion

G = motor constant of calibration coil

i = current in calibration coil

m_e = effective mass of seismometer.

Because the force generated by the coil is not applied at the center of mass of the seismometer, the effective seismometer mass is related to the true mass, M, by

$$m_e = \frac{M r_{cm}}{r_c}$$

where

r_{cm} = distance from the hinge of the pendulum to its center of mass

r_c = distance from hinge to center of coil

Therefore,

$$\ddot{Y} = \frac{G i r_c}{M r_{cm}}$$

Taking the Fourier transform of the equation

$$Y(jw) = \frac{GI(jw)r_c}{M r_{cm} w^2}$$

where

$Y(jw)$ is the Fourier transform of the displacement amplitude of earth vibration

$I(jw)$ is the Fourier transform of the input current.

The transfer function or dynamic magnification, $M(jw)$, of the seismometer system is then given by

$$M(jw) = \frac{\text{Fourier transform of Digital Record Amplitude}}{\text{Fourier transform of the displacement amplitude}}$$

$$M(jw) = \frac{Y_r(jw)}{Y(jw)}$$

Thus

$$M(jw) = -\frac{Y_r(jw) w^2 M r_{cm}}{GI(jw)}$$

All that remains to be calculated is $I(jw)$. Assume that

$$i(t) = \begin{matrix} I_{cal} & 0 < t \leq T \\ 0 & t > 0 \end{matrix}$$

Then the Fourier transform of the input is

$$I(jw) = \int_{-\infty}^{\infty} i(t) e^{-jwt} dt$$

Integration gives

$$I(jw) = \frac{2 I_{cal}\, e^{-j\frac{wT}{2}}}{w} \sin\left(\frac{wT}{2}\right)$$

Hence,

$$M(jw) = -\frac{Y_r(jw)\, w^3 M r_{cm} e^{-j\frac{wT}{2}}}{2\, G I_{cal} \sin\left(\frac{wT}{2}\right) r_c}$$

If a DFT of length 2T is used, then the equivalent formula is

$$M(jw_n) = -\frac{Y_r(jw_n)\, w_n^3 M r_{cm} e^{-j\frac{w_n T}{2}}}{2\, G I_{cal} \sin\left(w_n \frac{T}{2}\right) r_c}$$

where

$$w_n = \frac{2\pi n}{2T}$$

Simplifying yields

$$M(jw_n) = \frac{j\, Y_r(jw_n) w_n^3 M r_{cm}}{2 G I_{cal}\, r_c} \quad \text{for } n \text{ odd}$$

The expression is not defined for even harmonics because the amplitude of the input at even harmonic is zero.

The VLP seismometer has the following constants

	Vertical	Horizontal
M	13.2 kg	10.0 kg
r_{cm}	.230 meters	.227 meters
r_c	.378 meters	.378 meters

Using these constants, the magnifications $M_z(jw_n)$, $M_x(jw_n)$, and $M_y(jw_n)$ of the z, x, and y channels, respectively, may be reduced for odd n to

$$M_x(jw_n) = \frac{4.015\, j Y_{rx}(jw_n) w_n^3}{G I_{cal}}$$

$$M_y(jw_n) = \frac{3.003\, j Y_{ry}(jw_n) w_n^3}{G I_{cal}}$$

$$M_z(jw_n) = \frac{3.003\, j Y_{rz}(jw_n) w_n^3}{G I_{cal}}$$

where Y_{rx}, Y_{ry}, and Y_{rz} are the DFT transforms of the x, y, and z seismometer outputs (the length of the transform is twice the length of the pulse).

3.2 Averaging and Curve Fitting of Calibration

In order to obtain reliable estimates of the seismometer magnification from the small calibration pulses, averaging and frequency smoothing were applied to the harmonic data obtained from the magnification formulas in the preceding section. Figure 5 shows the actual measured values of magnification amplitude and fitted curves for three consecutive days. By just examining the curves, it is impossible to tell whether the 12% variation in the peaks of the curves should be attributed to an actual variation in the transfer function or just to a random variation caused by noise. Therefore, for the calculation of ellipticity, it was decided to do the calibration on both a daily basis and on an average of 15

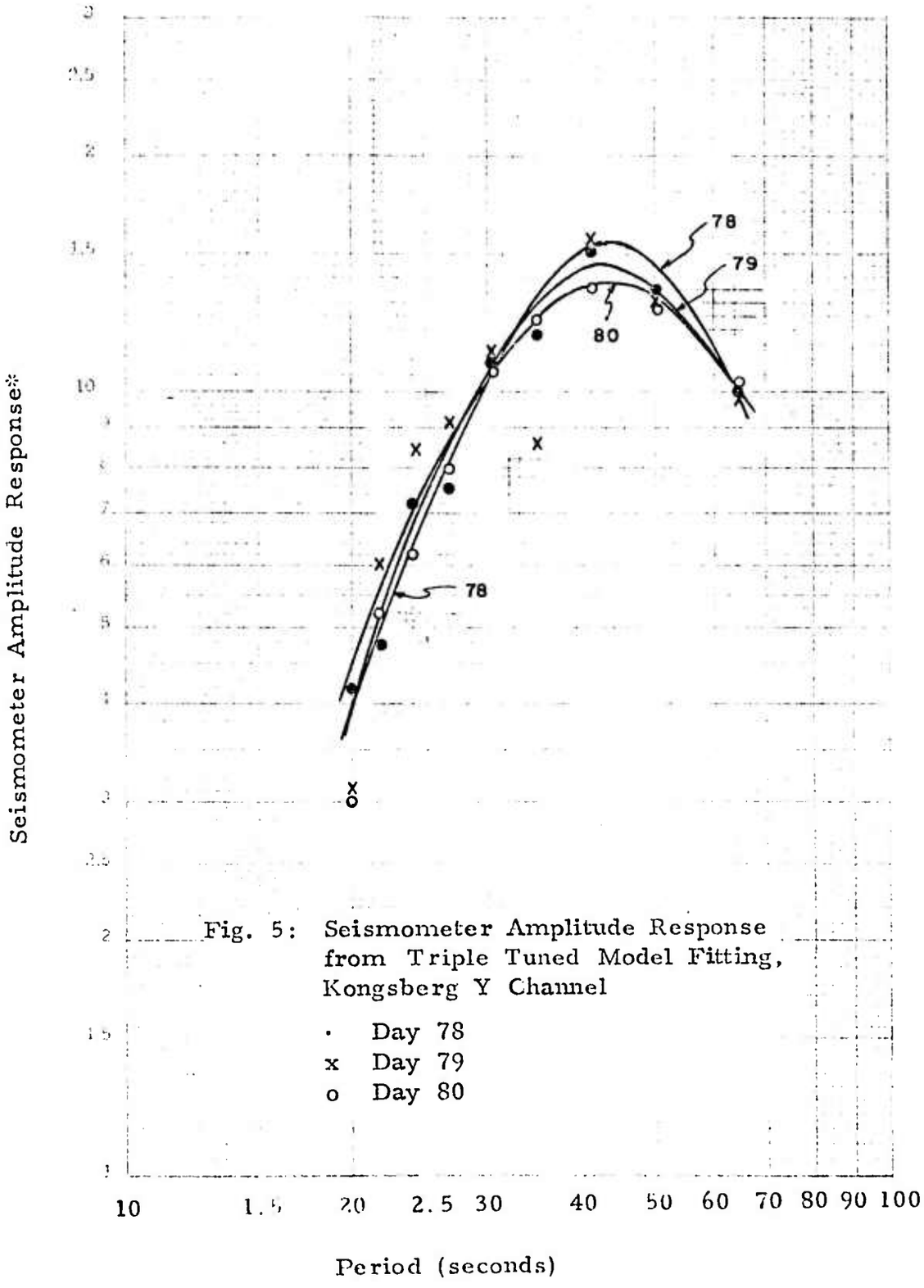

Fig. 5: Seismometer Amplitude Response from Triple Tuned Model Fitting, Kongsberg Y Channel

· Day 78
x Day 79
o Day 80

*The peak of the day 78 curve corresponds to 1224 counts/micron

days, so that variations of the instrument response, if they occurred, would not be averaged out. The best method would then be the one which resulted in the most consistent ellipticity calculation. As explained in the following paragraphs, two different curve fitting methods were used on both the daily and average calibrations.

One method of smoothing was to fit a triple tuned model to the amplitude of the magnification. From the parameters determined by the curve fit, the phase response was calculated. This method is explained in detail in Appendix A. Figures 6 and 7 show the application of this method to both daily and average calibrations. Since the phase response is determined from the amplitude response, the pulses do not have to be precisely aligned during the averaging process. The main disadvantage of this method is that even though it may give a reasonable fit to amplitude response, there may be systematic errors in the phase response. If the actual parametric form of the transfer function is not known and must be deduced from the data, then the amplitude response must be known very accurately in order to get the phase response from it.

In order to avoid the possible phase response problems and distortions introduced by the tuned circuit method, a second set of

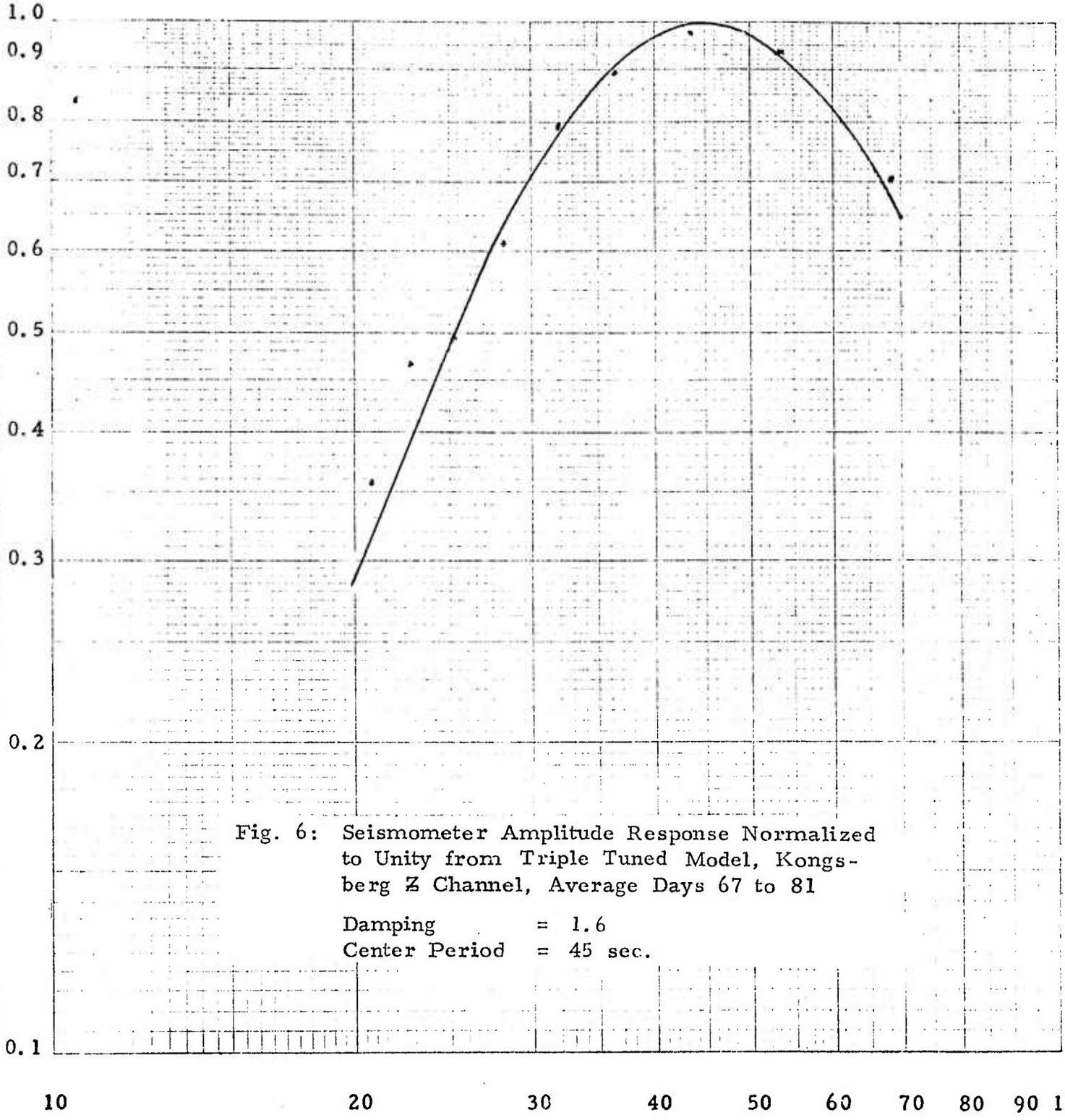

Fig. 6: Seismometer Amplitude Response Normalized to Unity from Triple Tuned Model, Kongsberg Z Channel, Average Days 67 to 81

Damping = 1.6
Center Period = 45 sec.

*Normalized Amplitude Response (1.0 corresponds to 1145 counts/micron)

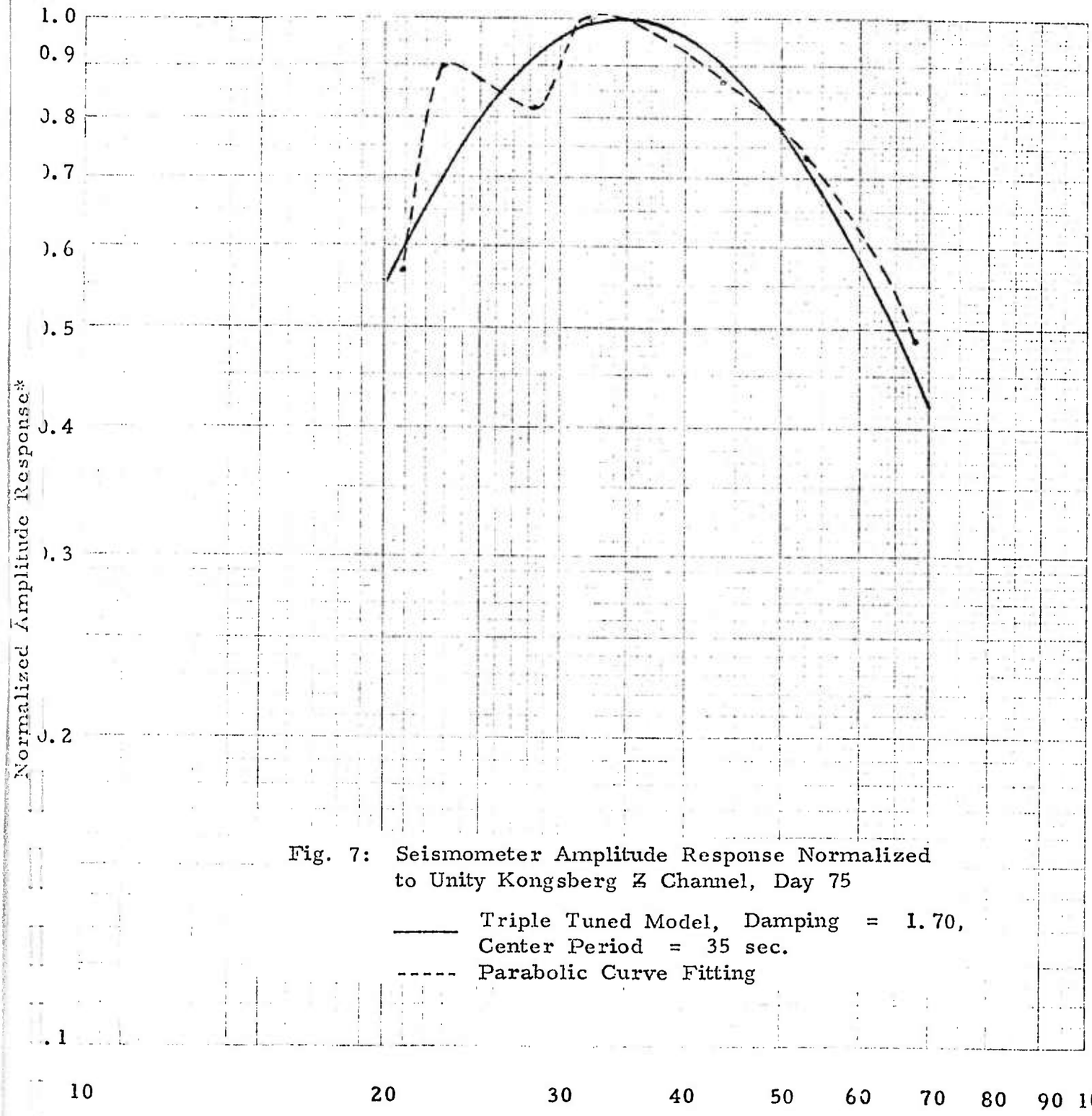

Fig. 7: Seismometer Amplitude Response Normalized to Unity Kongsberg Z Channel, Day 75

——— Triple Tuned Model, Damping = 1.70, Center Period = 35 sec.

----- Parabolic Curve Fitting

*Normalized Amplitude Response (1.0 corresponds to 858 counts/micron)

both daily and average calibrations were derived by just the free hand, parabolic curve fitting of both amplitude and phase of the seismometer magnification. Figures 7 and 8 show typical results of this method.

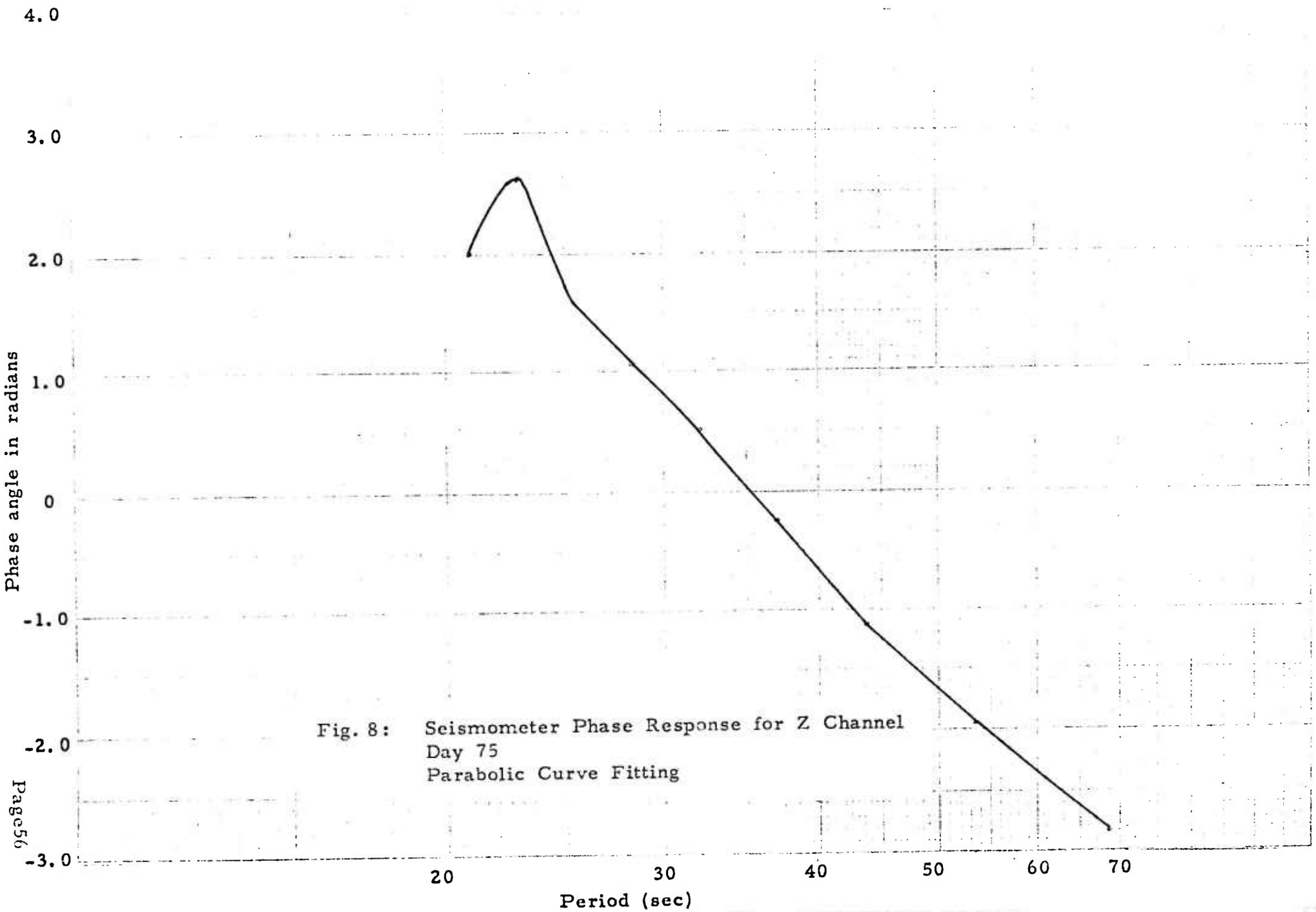

Fig. 8: Seismometer Phase Response for Z Channel
Day 75
Parabolic Curve Fitting

4.0 Measurement of Ellipticity

By the use of a filter similar to the Rayleigh-Love ellipticity filter described in the First Quarterly Report (OAS TR 74-232)[11], ellipticity measurements were made on six (6) earthquakes with four (4) different calibrations. Table IV contains a list of events. Three of the events were from the Honshu region and three from the Aleutians. Since the assumptions of this ellipticity filter are slightly different than the earlier one, a detailed derivation will now be given.

4.1 Description of Ellipticity Measurement Filter

Assume we have a three-component seismometer with the output signals $X(t)$, $Y(t)$, and $Z(t)$ and that the Fourier transform of these signals has been taken. The signals X, Y, and Z represent one of the Fourier components of the transformed signal and M_x, M_y, and M_z represent the complex magnification or transfer function at the frequency of the Fourier components of the signals.

Under these assumptions, a Rayleigh and Love wave coming from a single azimuth may be represented as

$$X/M_x = -ER\sin\theta - L\cos\theta \qquad (1)$$

$$X/M_y = -ER\cos\theta + L\sin\theta \qquad (2)$$

$$X/M_z = E \qquad (3)$$

TABLE IV: EVENT DATA

Location	O.A.S. Header	Azimuth (degrecs)	Distance (Kilometers)	Day of Ycar 1972	Origin Time (GMT)
Alcutians	Q005	8.57	7628	75	11:23
Alcutians	Q001	5.93	7693	80	07:45
Alcutians	Q012	3.96	7850	81	09:48
Honshu	Q003	39.74	8520	74	00:47
Honshu	Q008	35.54	8775	78	23:18
Honshu	Q009	36.08	8054	79	15:58

where

R is the complex amplitude of the Rayleigh wave

L is the complex amplitude of the Love wave

θ is the azimuth of both the Rayleigh and Love wave

E is the complex station ellipticity (ratio of horizontal to vertical)

Assuming that the Love and Rayleigh wave arrive by the great circle path (Second Quarterly Report, OAS TR 74-252), the azimuth of the event may be calculated from data supplied in the PDE. The above three complex equations represent six nonlinear equations in the unknown real and imaginary parts of E , R , and L . Thus we have six equations in six unknowns.

Substituting (3) into (1) and (2) gives

$$\left(\frac{X}{M_X}\right) = -E\left(\frac{Z}{M_Z}\right)\sin\theta - L\cos\theta \qquad (4)$$

$$\left(\frac{Y}{M_y}\right) = -E\left(\frac{Z}{M_Z}\right)\cos\theta + L\sin\theta \qquad (5)$$

Multiply (4) by $\sin\theta$ and (5) by $\cos\theta$, and then adding the resulting equations gives

$$\left(\frac{X}{M_X}\right)\sin\theta + \left(\frac{Y}{M_y}\right)\cos\theta = -2E\left(\frac{Z}{M_Z}\right)\left[\sin^2\theta + \cos^2\theta\right]$$

Solving for f and simplifying yields

$$E = \frac{-\left(\frac{X}{M_X}\right)\sin\theta - \left(\frac{Y}{M_y}\right)}{\left(\frac{Z}{M_Z}\right)} \qquad (6)$$

In a similar manner, the solution for the complex amplitude of the Love wave is

$$L = \frac{-\left(\frac{X}{M_x}\right)\cos\theta + \left(\frac{Y}{M_y}\right)\sin\theta}{\left(\frac{Z}{M_z}\right)}$$

The value of the complex amplitude of the Rayleigh wave is just given by

$$R = Z$$

4.2 Implementation of Filter

To obtain frequency domain information, a DFT with a 256 second cosine window was used. As explained in Appendix B, this window prevents leakage of the signal energy among the harmonics of the transform. The window was moved across the events with shifts of 15 seconds. For each of the harmonics from 64 to 19.6 seconds, the values of E , R , and L were calculated for every position of the window. The value of ellipticity chosen corresponded to that calculated for the peak amplitude arrival time of the Rayleigh waves. This procedure minimized the effect of interfering signals.

4.3 Results

For each of the four methods of calibration outlined in Section 3.2, the values of ellipticity for the six events were

calculated as outlined in the last section. Figures 9 to 12 show ellipticity magnitude and Figures 14 to 17 show ellipticity angle for each of the calibration procedures.

Even though the spread in azimuths of the Aleutian earthquakes is slightly larger than that for the Honshu events, the ellipticity magnitudes are much more consistent for the Aleutian than for the Honshu earthquakes. The explanation is that the Aleutian earthquakes with azimuths from 3.7° to 8.6° have Rayleigh waves which come in almost entirely on the N/S axis. For this case, if the calibration is incorrect, only a scaling error occurs in the ellipticity and the consistency of the ellipticity is not degraded. However, the Honshu events have azimuths from 35.5° to 39.7°. Thus, each axis receives a substantial fraction of the Rayleigh waves energy. In this case, in addition to scaling errors, errors occur because the Rayleigh and Love waves are not separated properly. An error in the ratio of the x to y seismometer calibration looks like an error in the azimuth of earthquakes. Therefore, the best estimation of ellipticity magnitude will come from the use of only Aleutian events. However, the scatter of ellipticity values for the six events in Figure 10 gives an indication of the performance of ellipticity filters.

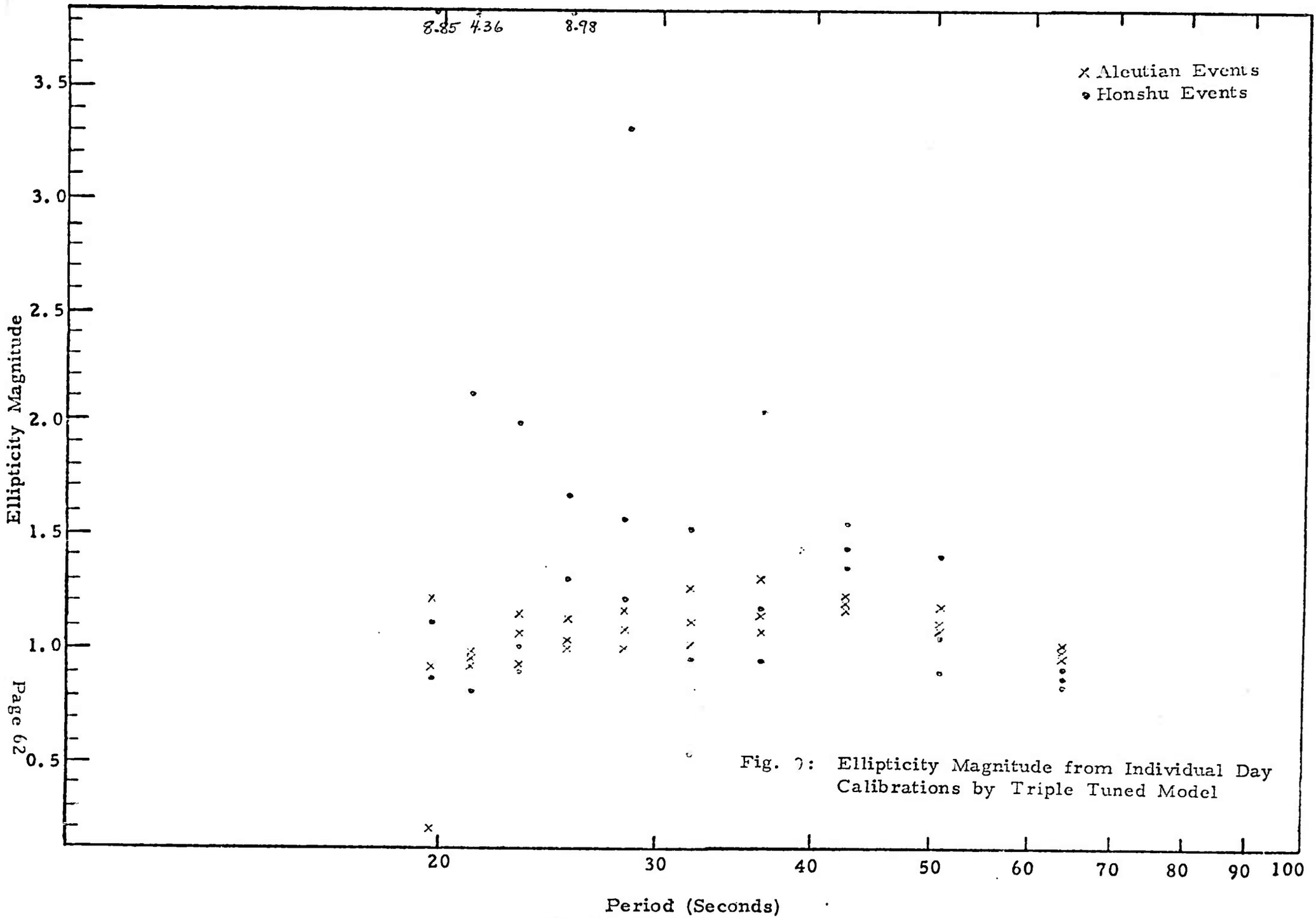

Fig. 9: Ellipticity Magnitude from Individual Day Calibrations by Triple Tuned Model

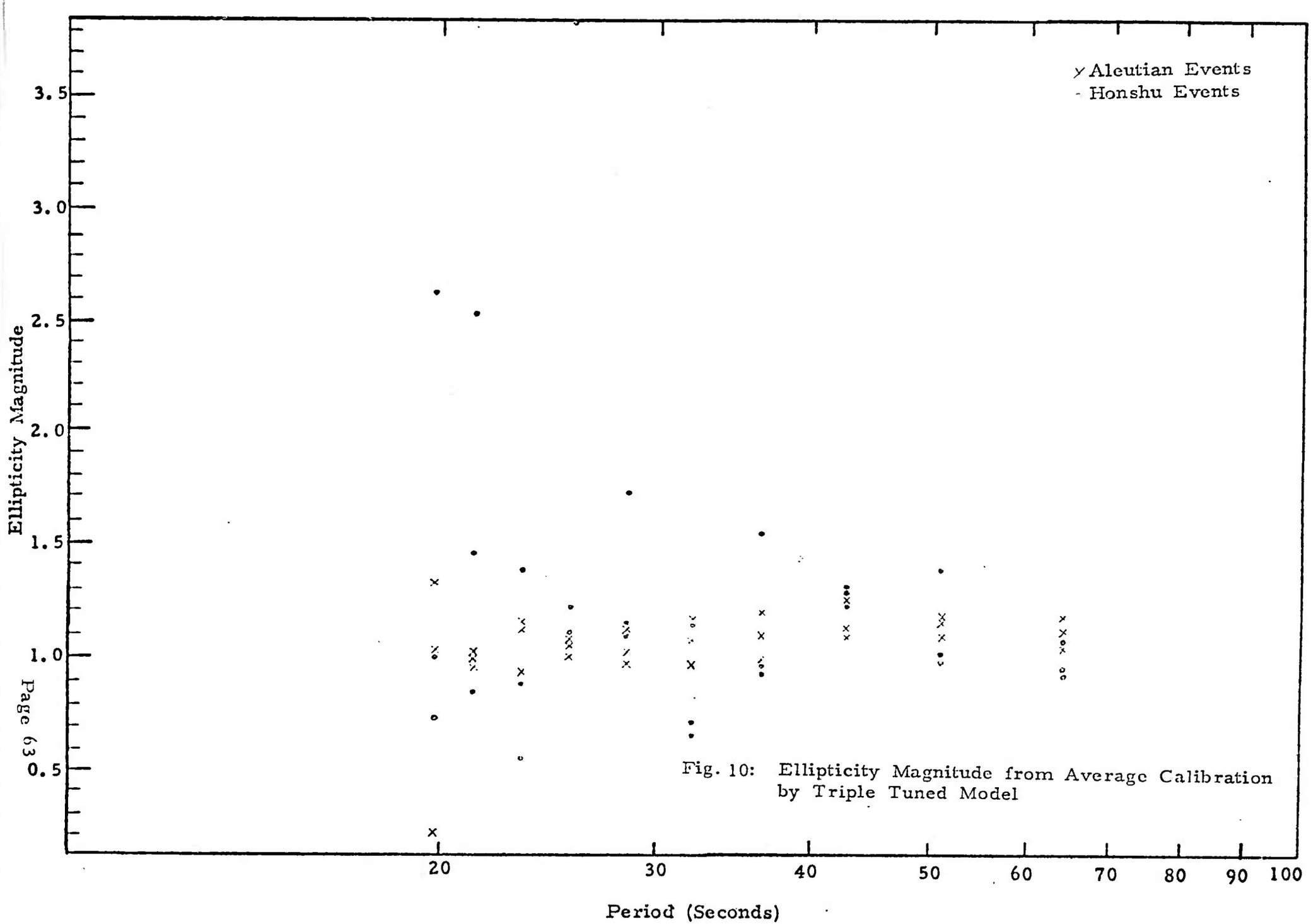

Fig. 10: Ellipticity Magnitude from Average Calibration by Triple Tuned Model

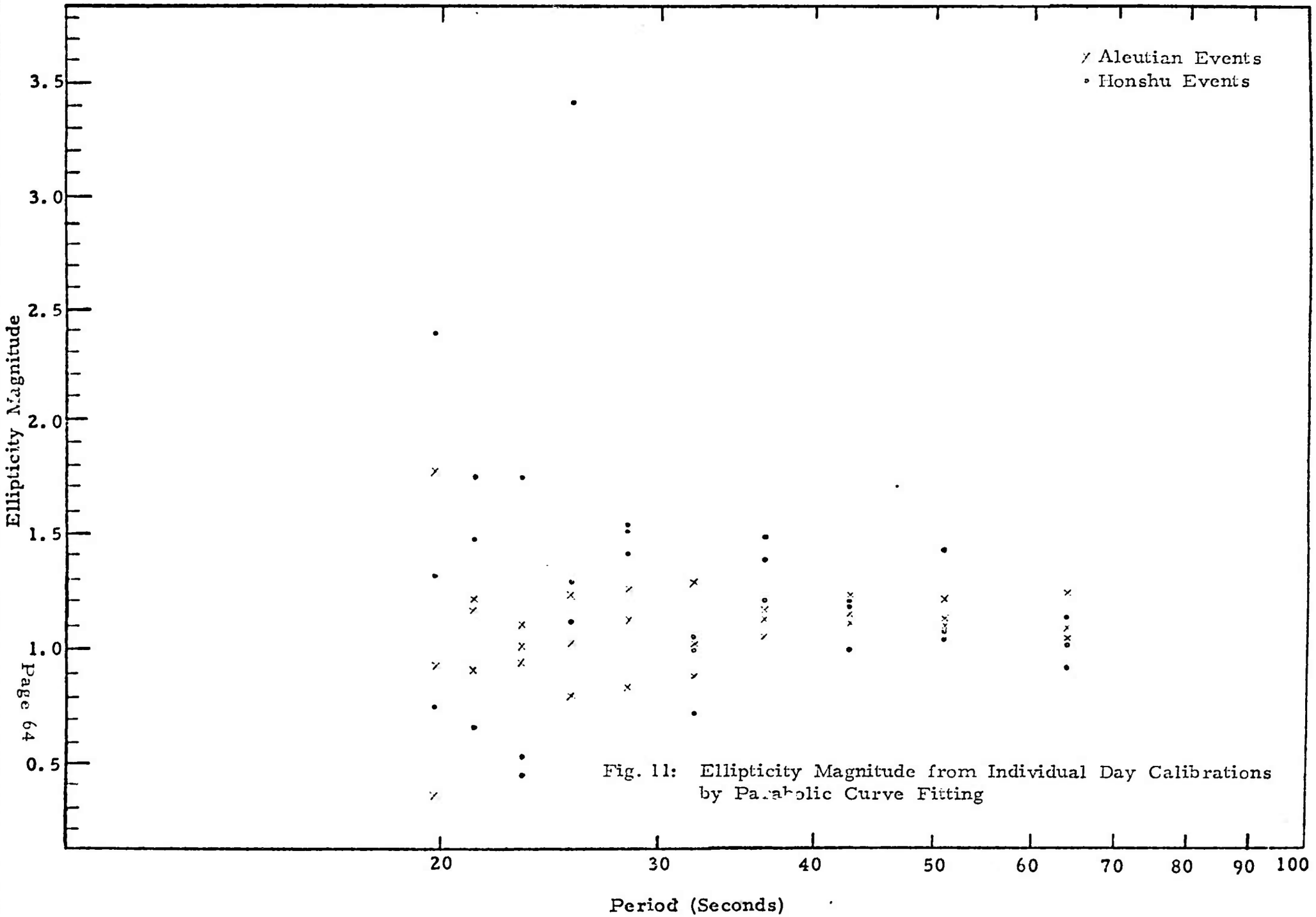

Fig. 11: Ellipticity Magnitude from Individual Day Calibrations by Parabolic Curve Fitting

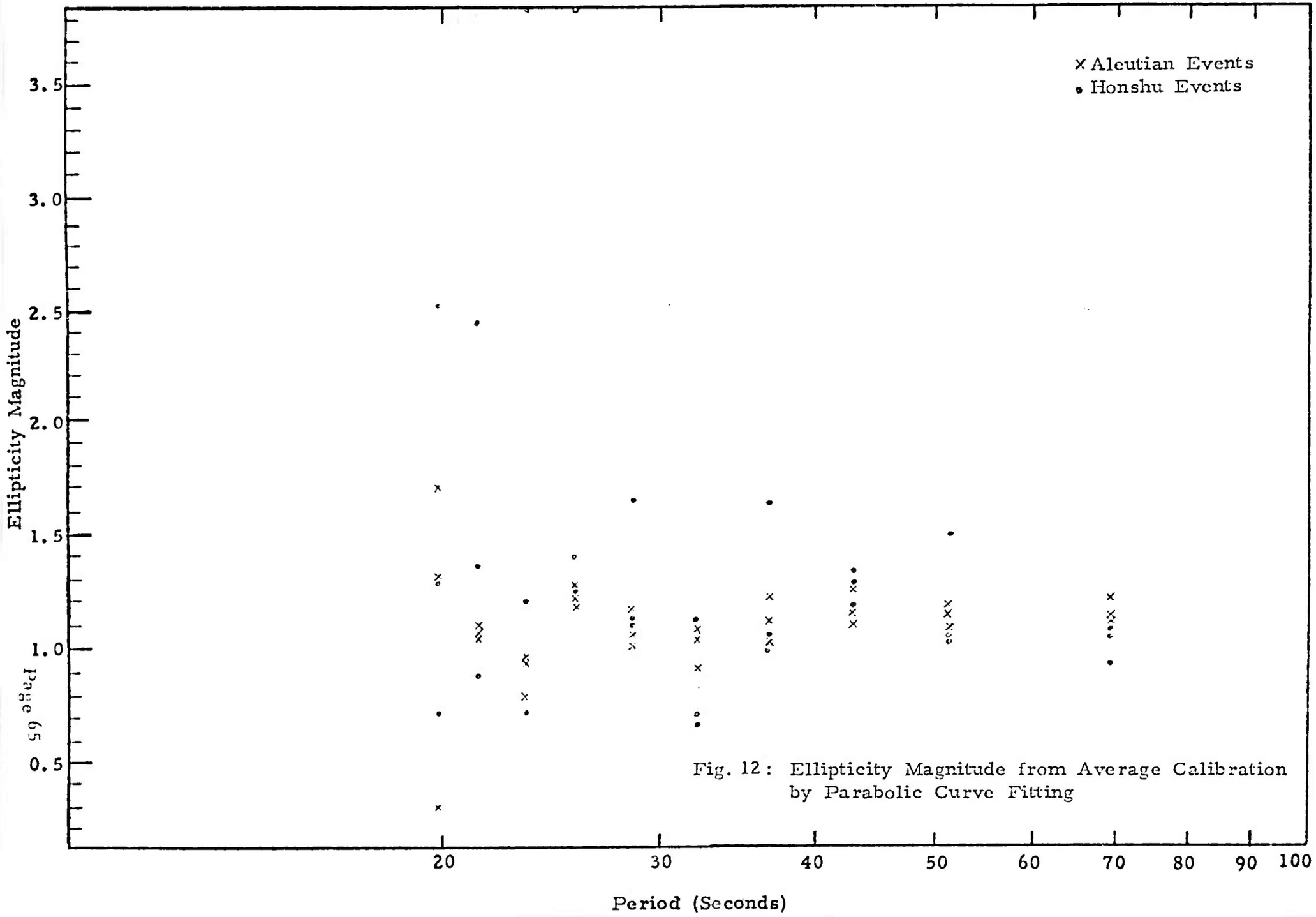

Fig. 12: Ellipticity Magnitude from Average Calibration by Parabolic Curve Fitting

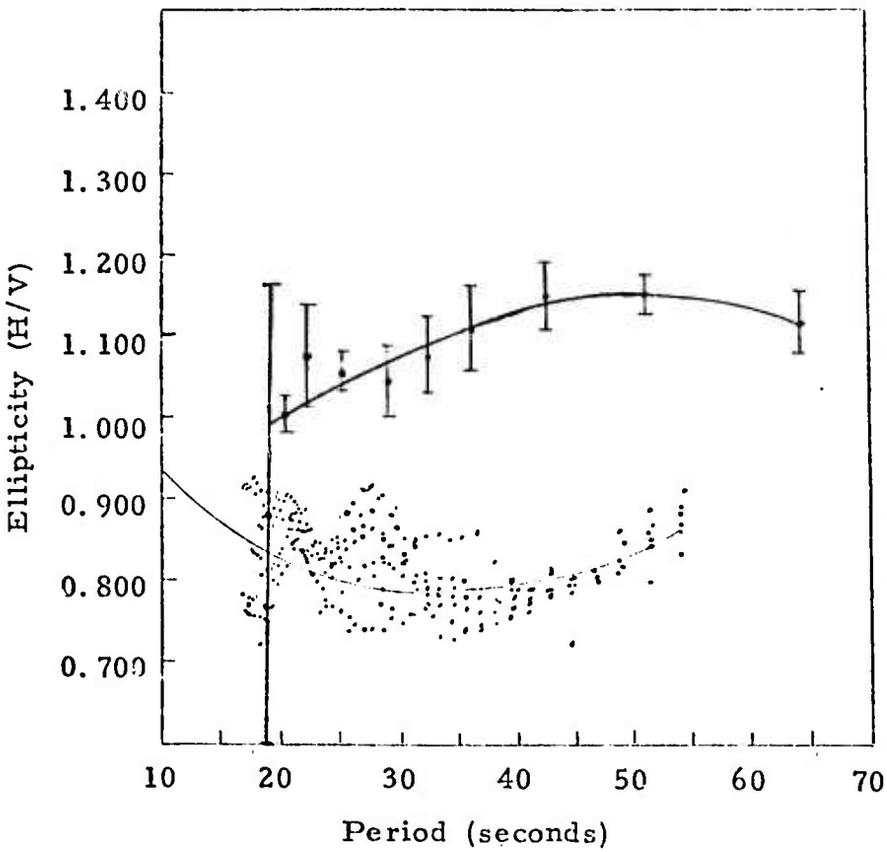

Fig. 13: Measured Ellipticities

I OAS for Kongsberg
. Boore and Toksöz (1969) for LASA
(From Reference 14)

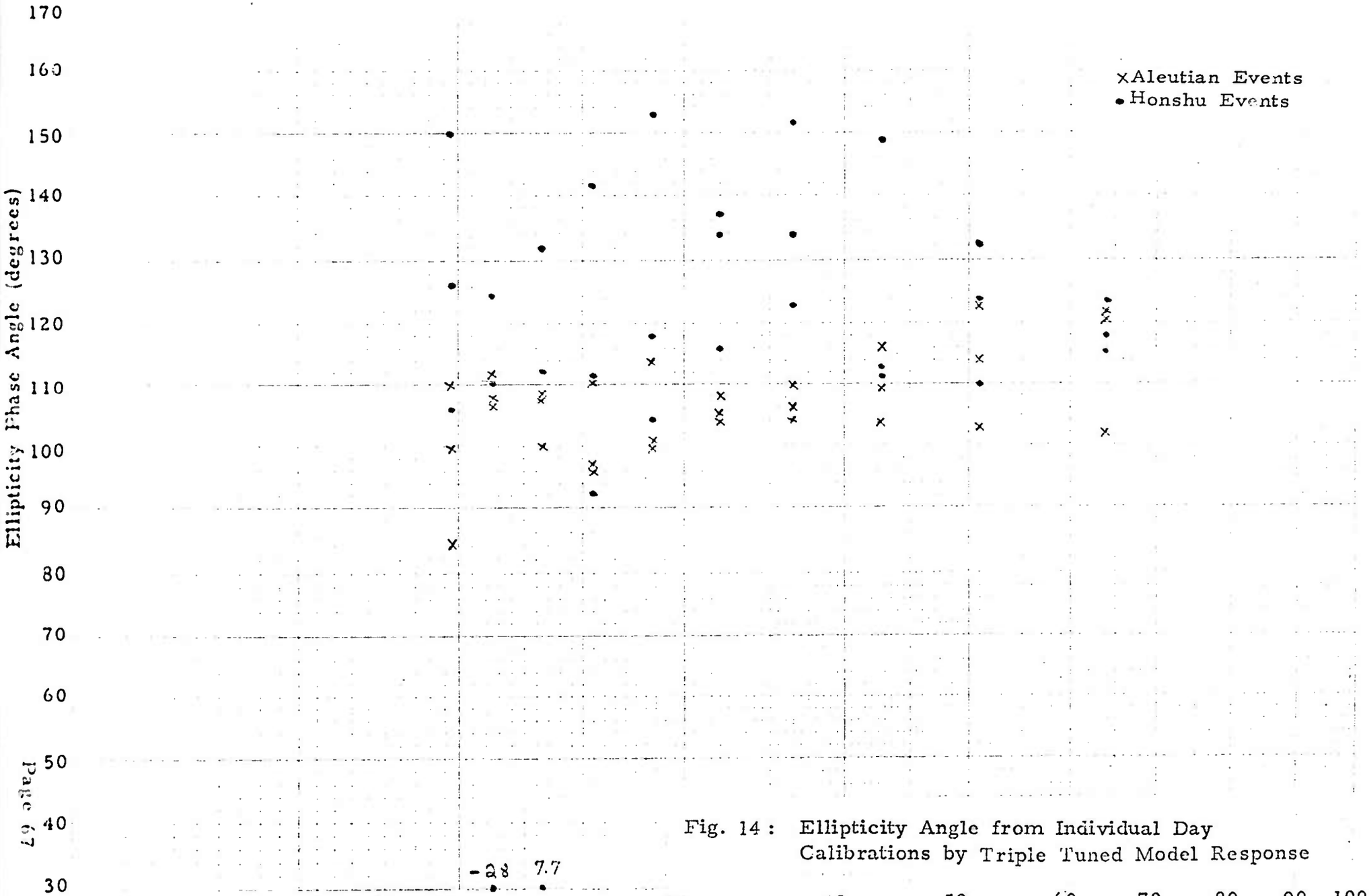

Fig. 14 : Ellipticity Angle from Individual Day Calibrations by Triple Tuned Model Response

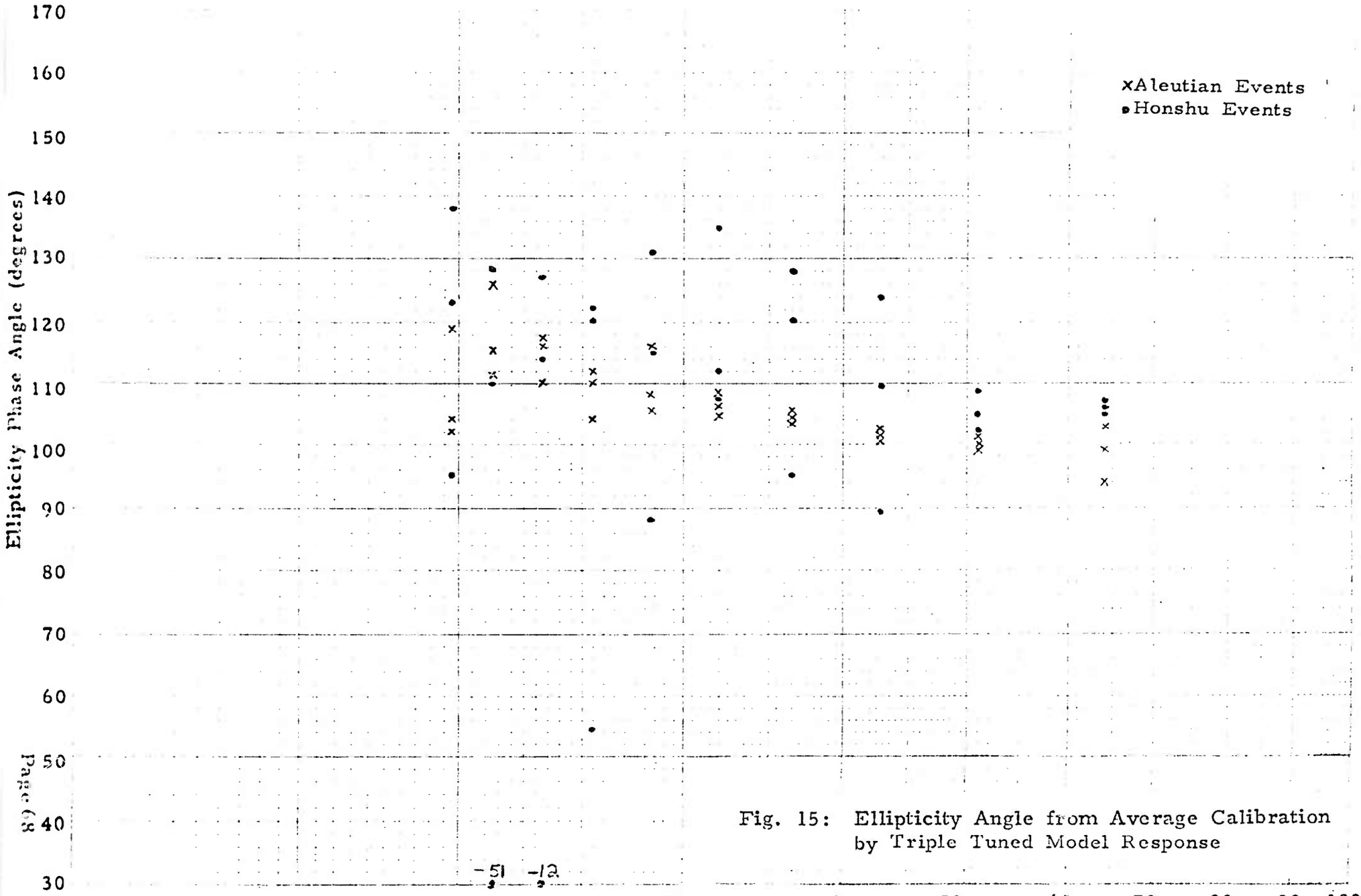

Fig. 15: Ellipticity Angle from Average Calibration by Triple Tuned Model Response

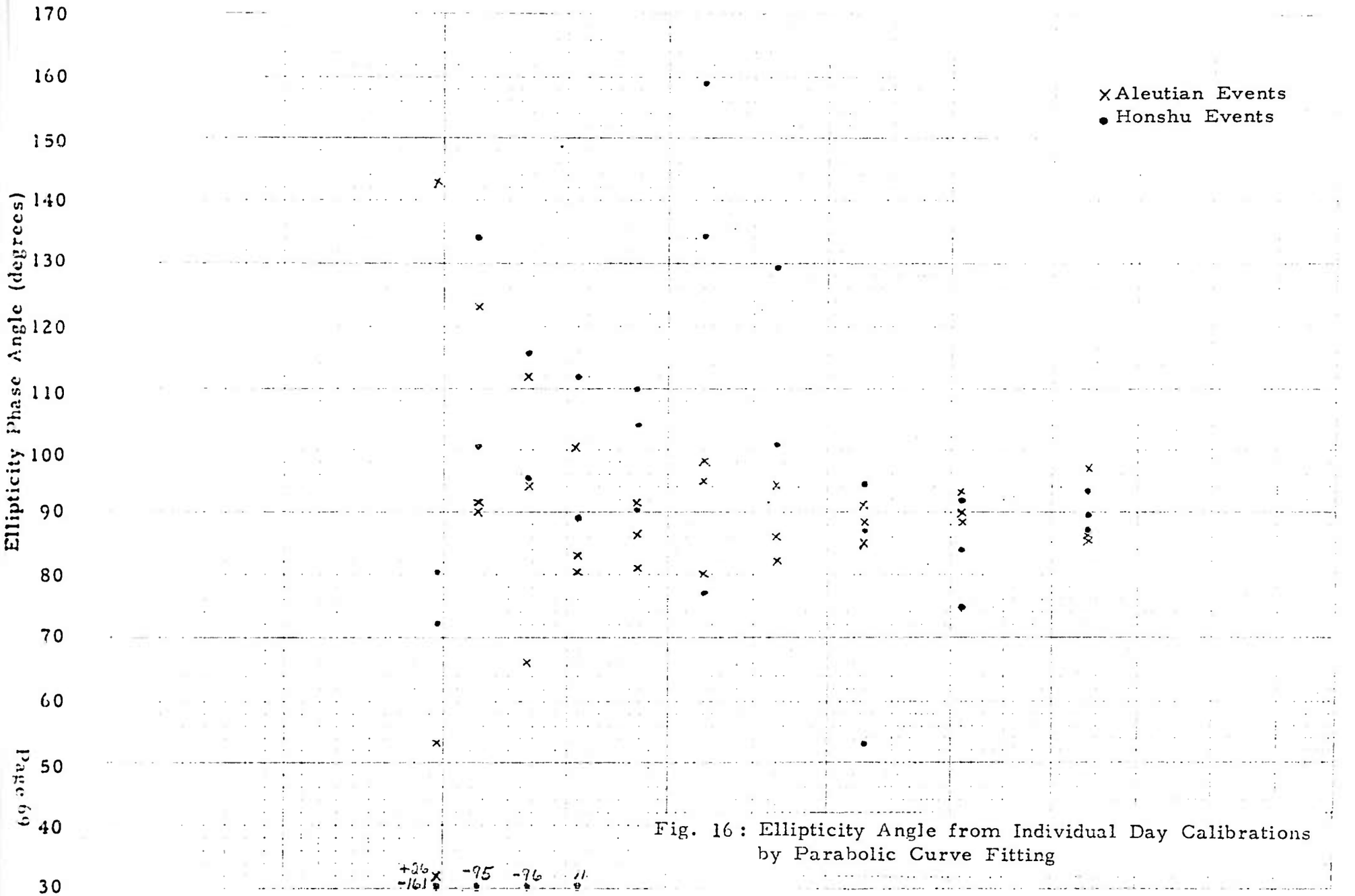

Fig. 16 : Ellipticity Angle from Individual Day Calibrations by Parabolic Curve Fitting

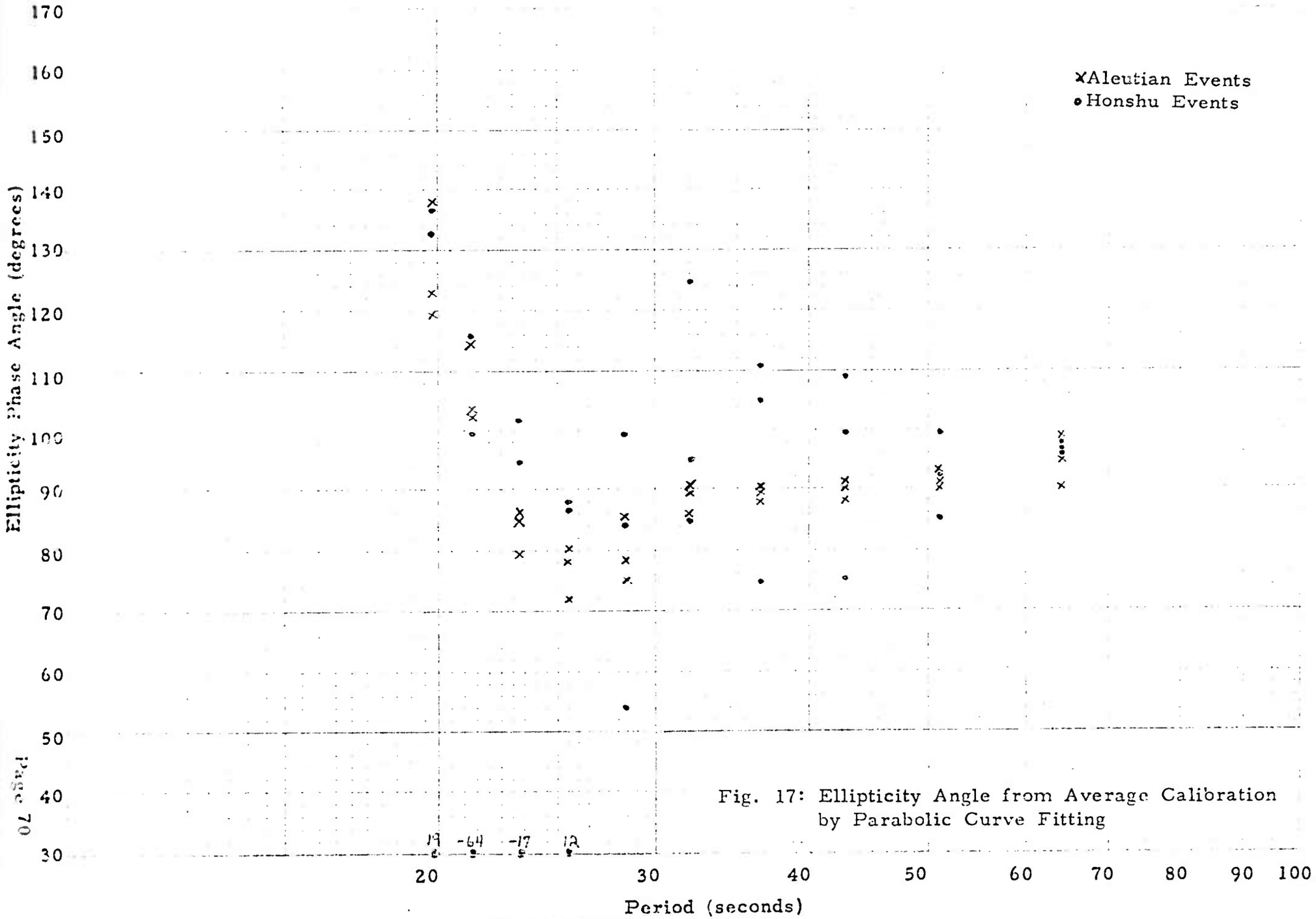

Fig. 17: Ellipticity Angle from Average Calibration by Parabolic Curve Fitting

The most consistent values of ellipticity magnitude (Figure 10) come from the average triple tuned model calibration. Table II shows the estimation of ellipticity based on this calibration procedure and the three Aleutian events. For periods from 21 to 64 seconds, the rms error is less than 6%. Figure 13 shows a comparison of our results with those of Boore and Toksöz (1969). The difference in the results is understandable since their ellipticity is for the Montana LASA station and ours is for the Kongsberg VLP station.

The ellipticity magnitude and angle is more consistent for the longer periods than for the shorter ones. The explanation for this is twofold. First, the effect of multipath is less for the longer periods than for the shorter ones. At the long periods, there is very little lateral refraction of the Rayleigh and Love waves off the ocean continent boundaries. The earthquake azimuths are very close to their great circle values. Second, the calibration signals had more energy at the longer periods than at the shorter ones. The increase in energy improved the estimation of the long period calibrations.

For a perfectly elastic layered medium, the theoretical value of ellipticity is 90°. Even in the case of extreme anelasticity, the variation from 90° is only a few degrees as determined by Boore and Toksöz (1969). The mean of the ellipticity angles shown in Figure 14 is 110° and that in Figure 15 is 115°. From those figures, it is evident that although the fitting of the tuned circuit

filter gives a reasonable approximation to the amplitude response of the system, it introduces phase bias errors of from 10^{o} to 15^{o}. If this type of calibration were used in ellipticity filters for mixed seismic signals, similar types of errors would occur.

The best values of ellipticity angles comes from the parabolic curve fitting calibration. Figures 16 and 17 show only a few degrees of mean error for all but the shortest periods. Table III shows the mean and standard derivation of the ellipticity angle for periods from 36.6 to 64 seconds. In general for the four longest periods shown in the table, the fitting to the average response is slightly better than that to the daily response. However, for the very short periods, the average method has a systematic biasing error.

SECTION III

THE ELEMENTARY RAYLEIGH-LOVE WAVE ELLIPTICITY FILTER

The Elementary Rayleigh-Love Wave Ellipticity Filter is one of the simplest Ellipticity Filters. The filter operates by taking the outputs of a three-axis seismometer station and generating a Rayleigh-Love wave decomposition based on the individual frequency-time bin data. This filter has been described previously, but not in full detail which is given here [11].

1.0 Introduction

The Elementary Rayleigh-Love Wave Ellipticity Filter is functionally shown in Figure 18. The basis of the decomposition is that the observed signal is comprised of, at most, a single Rayleigh and a single Love Wave component. No allowance is made for the background noise nor is any attempt made to acquire the potential processing gain due to averaging over the frequency-time bins. This filter is simply a logical extension of the Polarization and Azimuthal Filters with the important addition of the ellipticity constraint.

1. The inputs from the seismometers are the three-axis time waveforms $x(t)$, $y(t)$, and $z(t)$ corresponding to the E-W, N-S, and vertical instruments.

2. The signals are sampled and digitized and the descrete Fourier transform taken. A time aperture of about 200 seconds is used in taking the DFT. As discussed elsewhere[5], this duration is adequate for signal periods of as long as 60 seconds if a Cosine Fader is used. The frequency components of the Rayleigh and Love waves present are expected to be constant over this duration and to have almost constant azimuth[2].

3. The relationships for the component splitting at each frequency are

$$X(j\omega) = - E(j\omega)\, R(j\omega) \sin\theta_1 - L(j\omega) \cos\theta_2$$

$$Y(j\omega) = - E(j\omega)\, R(j\omega) \cos\theta_1 + L(j\omega) \sin\theta_2$$

$$Z(j\omega) = R(j\omega)$$

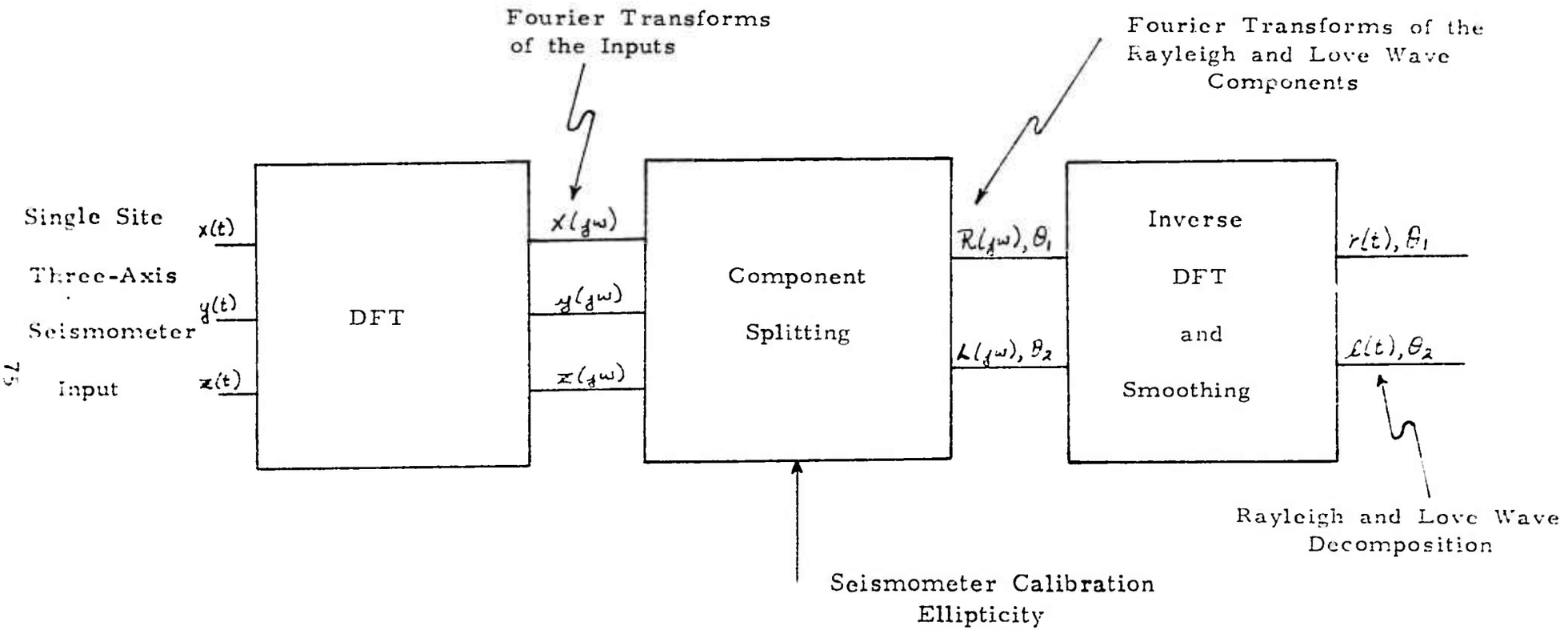

Fig. 18: The Elementary Rayleigh-Love Wave Ellipticity Filter in the Fourier Transform Domain

in which

$X(j\omega)$, $Y(j\omega)$, $Z(j\omega)$	are the complex Fourier Transforms of the seismometer signals,
$E(j\omega)$	is the ellipticity, defined as the ratio of the horizontal to the vertical motion,
$R(j\omega)$	is the complex amplitude of the Rayleigh event,
$L(j\omega)$	is the complex amplitude of the Love event,
θ_1, θ_2	are the azimuths of the Rayleigh and Love events.

4. The solution of these equations gives $L(j\omega)$, θ_1, and θ_2. Note that $R(j\omega)$ is known because it corresponds to the output of the vertical seismometer.

5. The Love wave frequency components can be assembled together and the inverse DFT taken. This will give the actual time waveform, $\ell(t)$. The horizontal Rayleigh Wave component can be similarly determined.

A similar filter can be constructed in the time domain using the analytic function. However, there appears to be little advantage in doing this because

1. A double DFT is required to give the analytic function.

2. The ellipticity is usually specified in the frequency domain.

The instrumentation of the Ellipticity Filter in the analytic function (time) domain is shown in Figure 19. The resulting equations would be a set of equations

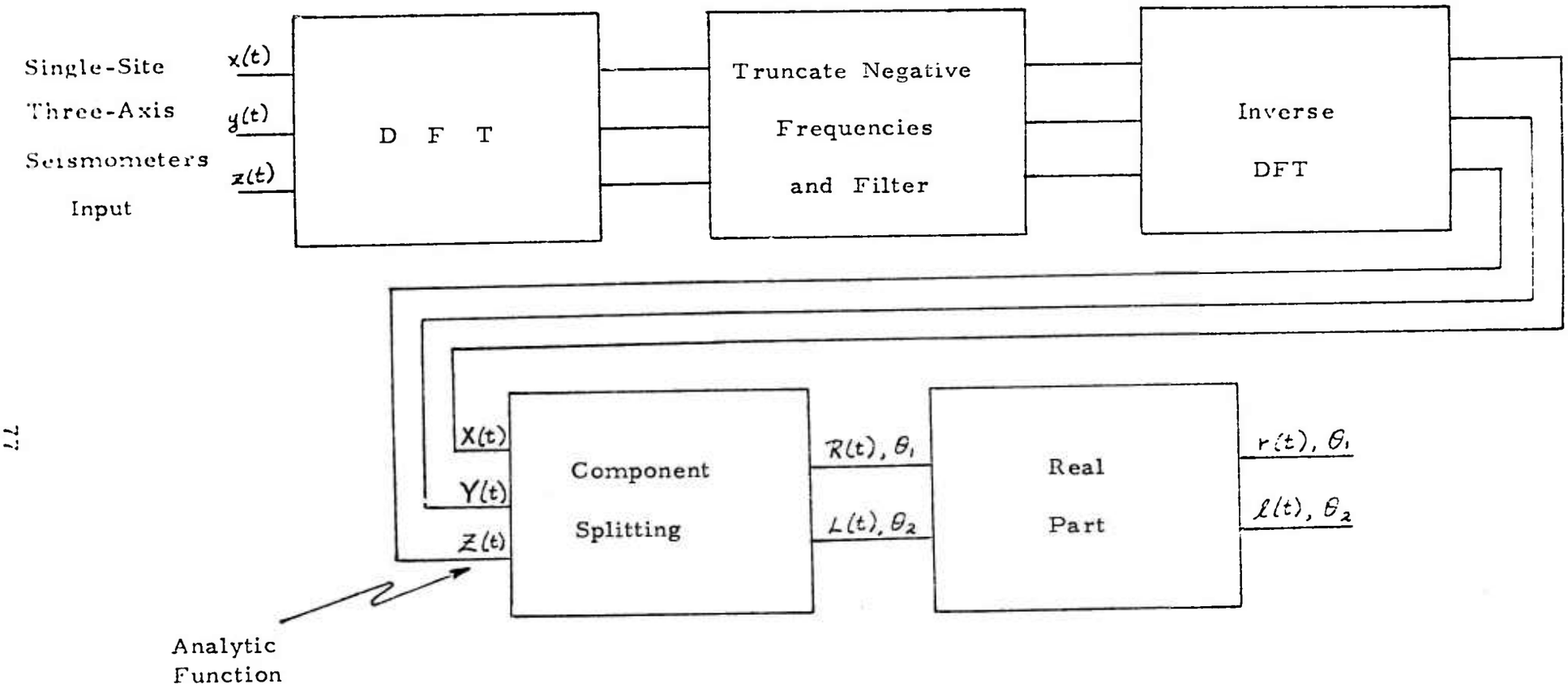

Fig. 19: The Elementary Rayleigh-Love Wave Ellipticity Filter in the Analytic Function or Time Domain

$$X(t) = -E(t)\ R(t) \sin\theta_1 - L(t) \cos\theta_2$$

$$Y(t) = -E(t)\ R(t) \cos\theta_1 + L(t) \sin\theta_2$$

$$Z(t) = R(t)$$

similar to that of the filter in the frequency domain, but $E(t)$ is harder to define. For this reason, the analytic function approach will not be pursued further here.

2.0 Ambiguities

As expected, this elementary decomposition can have ambiguities, but in actual operation these ambiguities can be removed, for the most part, by using additional constraints such as

1. Knowledge of the azimuth of one component,
2. Behavior of the reconstructed wave which should have the required dispersion properties.

The potential ambiguities are shown in Figure 20. The true azimuth of the Love Wave is always obtained as well as the true amplitude of the Rayleigh Wave. However, there is a spurious Love wave and a spurious Rayleigh wave which can be present in the solution. The corresponding amplitudes are tabulated below.

Condition		Rayleigh Wave Amplitude	Love Wave Amplitude
Rayleigh	Love		
True	True	R	L
Spurious	True	R	$L + 2ER \sin c$
True	Spurious	R	$-L$
Spurious	True	R	$-L - 2ER \sin c$

As noted above, these spurious waves can be eliminated when the azimuth of the Rayleigh or Love wave is known. Indeed, given

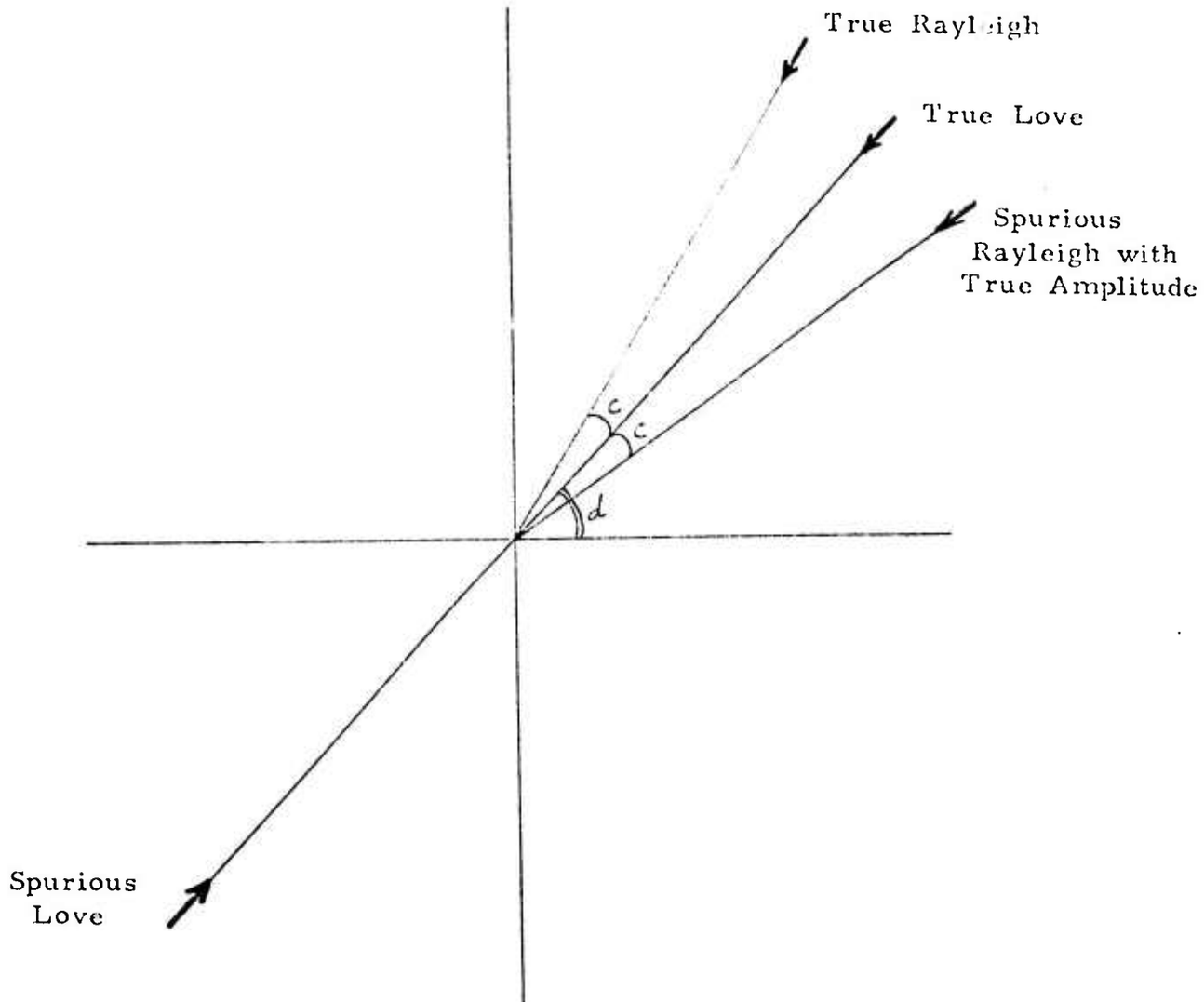

Fig. 20: Pattern of the Azimuth Ambiguity

either of these azimuths, a simple set of equations can be written to obtain the non-ambiguous solution.

2.1 Derivation of the Ambiguity Conditions

In the "noise-free" situation, the three basic observables are the transformed seismometer outputs, X , Y , Z . These are three complex numbers, one for each axis of the three-axis instrument, in either the time domain at some instant of time (analytic function) or in the frequency domain at some designated frequency (Descrete Fourier Transform).

The basic relations in either the time or the frequency domain are are:

$$X = -ER \sin\theta_1 - L \cos\theta_2 \qquad (1)$$

$$Y = -ER \cos\theta_1 + L \sin\theta_2 \qquad (2)$$

$$Z = R \qquad (3)$$

in which

R is the complex Rayleigh wave amplitude

L is the complex Love wave amplitude

θ_1 is the azimuth of the Rayleigh wave

θ_2 is the azimuth of the Love wave

E is the Complex Ellipticity as the ratio of the horizontal to the vertical motion for the Rayleigh wave.

If one sets

$$\theta_1 = \frac{3\pi}{2} - \alpha_1$$

$$\theta_2 = \pi - \alpha_2$$

these have the symmetrical form

$$X = ER \cos\alpha_1 + L \cos\alpha_2$$
$$Y = ER \sin\alpha_1 + L \sin\alpha_2$$

Then, designating real and imaginary parts by the subscripts r and i respectively

$$X_r = (ER)_r \cos\alpha_1 + L_r \cos\alpha_2$$
$$X_i = (ER)_i \cos\alpha_1 + L_i \cos\alpha_2$$

$$y_r = (ER)_r \sin\alpha_1 + L_r \sin\alpha_2$$
$$y_i = (ER)_i \sin\alpha_1 + L_i \sin\alpha_2$$

The complex rotation can than be used

$$u = x_r + j y_r = (ER)_r e^{j\alpha_1} + L_r e^{j\alpha_2} \quad (4)$$

$$v = x_i + j y_i = (ER)_i e^{j\alpha_1} + L_i e^{j\alpha_2} \quad (5)$$

in which u and v are complex numbers, but $(ER)_r$, (ER_i), L_r L_i are not.

Then

$$\frac{u}{(ER)_r} = e^{j\alpha_1} + \frac{L_r}{(ER)_r} e^{j\alpha_2}$$

$$\frac{v}{(ER)_i} = e^{j\alpha_1} + \frac{L_i}{(ER)_i} e^{j\alpha_2}$$

$$\left[\frac{u}{(ER)_r} - \frac{v}{(ER)_i}\right] = \left[\frac{L_r}{(ER)_r} - \frac{L_i}{(ER)_i}\right] e^{j\alpha_2}$$

Thus, the phase of $\left[\frac{u}{(ER)_r} - \frac{v}{(ER)_i}\right]$ is α_2, while the magnitude is $\left[\frac{L_r}{(ER)_r} - \frac{L_i}{(ER)_i}\right]$.

There is thus a π ambiguity in α_2 for which the sign of the amplitude of the Love wave reverses.

The azimuth of the Love wave, α_2 or θ_2, cannot be solved for if

$$\left[\frac{u}{(ER)_r} - \frac{v}{(ER)_i}\right] = \left[\frac{L_r}{(ER)_r} - \frac{L_i}{(ER)_i}\right] = 0$$

This situation occurs when

1) The Love wave amplitude is zero.

   In this case, the solution is meaningless anyway.

2) The Rayleigh wave amplitude is zero

   In this case, the vertical seismometer output is zero and a simpler set of equations can be used.

3) The Love wave component (L) is in phase with the horizontal Rayleigh wave component (ER).

   In this case, the proportionality constant (real)

$$L = K(ER)$$

   has a locus of solutions

$$\frac{K\cos\alpha_1 + \cos\alpha_2}{K\sin\alpha_1 + \sin\alpha_2} = \frac{X}{Y}$$

In the "noise-free" situation, these conditions can be separately tested for without difficulty.

With α_2 known, the expression can be written as

$$\mu\, e^{-j\alpha_2} = (ER)_r\, e^{j(\alpha_1-\alpha_2)} + L_r$$

$$v\, e^{-j\alpha_2} = (ER)_i\, e^{j(\alpha_1-\alpha_2)} + L_i$$

These are triangle relations since each expression involves only three vectors.

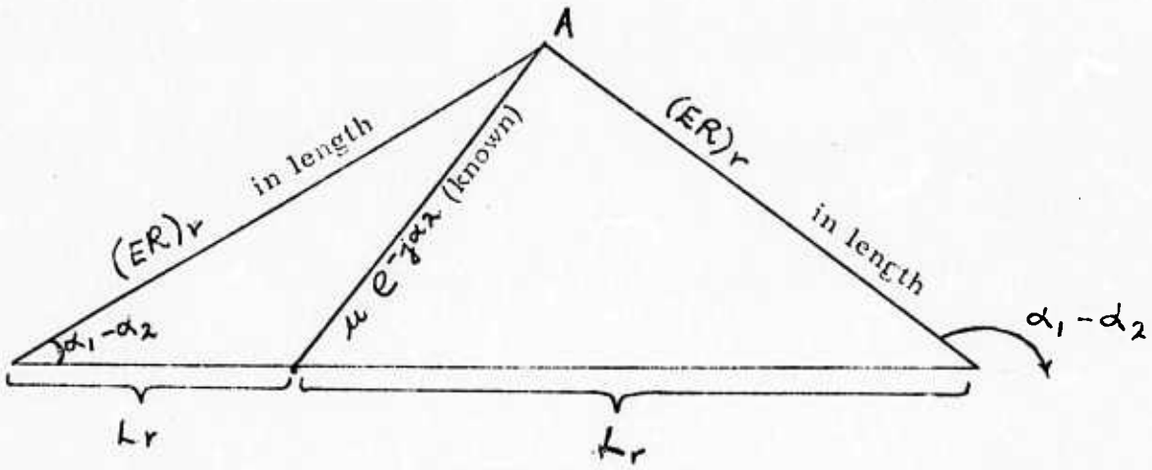

As shown above, there are two solutions which could be found geometrically by erecting $\mu e^{-j\alpha_2}$ and then drawing a circle whose center is A and radius $(ER)_r$.

One of the simplist relations which can be used is

$$\sin(\alpha_1-\alpha_2) = \mathrm{Im}\left\{\frac{\mu\, e^{-j\alpha_2}}{(ER)_r}\right\}$$

If $\alpha_1-\alpha_2 = b$ is a solution, $\pi - b$ is also a solution

There are thus four solutions

$$\alpha_2 = a \;, \quad \alpha_1 - \alpha_2 = b \;, \quad \alpha_1 = \alpha_2 + b$$

$$\alpha_2 = \pi + a \;, \quad \alpha_1 - \alpha_2 = \pi - b \;, \quad \alpha_1 = \pi - b + \alpha_2$$

when written out are

$$\alpha_1 = a + b \qquad \alpha_1 = a + b + \pi$$
$$\alpha_2 = a \qquad \alpha_2 = a + \pi$$

$$\alpha_1 = a - b + \pi \qquad \alpha_1 = a - b$$
$$\alpha_2 = a \qquad \alpha_2 = a + \pi$$

In terms of the original angles

$$\theta_1 = \frac{3\pi}{2} - \alpha_1$$

$$\theta_2 = \pi - \alpha_2$$

the solutional forms are

$$\theta_1 = \frac{3\pi}{2} - a - b \qquad \theta_1 = \frac{\pi}{2} - a - b$$
$$\theta_2 = \pi - a \qquad \theta_2 = -a$$

$$\theta_1 = \frac{\pi}{2} - a + b \qquad \theta_1 = \frac{3\pi}{2} - a + b$$
$$\theta_2 = \pi - a \qquad \theta_2 = -a$$

Let

$$c = \frac{\pi}{2} - b, \qquad b = \frac{\pi}{2} - c$$

$$d = \pi - a, \qquad a = \pi - d$$

then

$$\theta_1 = d + c \qquad \theta_1 = d + c$$

$$\theta_2 = d \qquad \theta_2 = d + \pi$$

$$\theta_1 - \theta_2 = c \qquad \theta_1 - \theta_2 = c - \pi = \pi + c$$

$$\theta_1 = d - c \qquad \theta_1 = d - c$$

$$\theta_2 = d \qquad \theta_2 = d + \pi$$

$$\theta_1 - \theta_2 = -c \qquad \theta_1 - \theta_2 = -c - \pi = \pi - c$$

are the solutional forms for the azimuths.

Note that if $\theta_2 - \theta_1 = c - d$ is a solution, $\theta_2 - \theta_1 = d - c$ is a solution.

It remains to write the solutions in terms of the original quantities.

(1) Relation for θ_2

$$\theta_2 = \pi - \alpha_2$$

α_2 is the phase of $\left[\frac{u}{(ER)_r} - \frac{v}{(ER)_i}\right] \begin{matrix} +\pi \\ +0 \end{matrix}$

$\therefore$ θ_2 is the negative of the phase of $\left[\frac{u}{(ER)_r} - \frac{v}{(ER)_i}\right] \begin{matrix} +\pi \\ +0 \end{matrix}$

$$\left[\frac{u}{(ER)_r} - \frac{v}{(ER)_i}\right] = \left[\frac{(x_r + j y_r)}{(ER)_r} - \frac{(x_i + j y_i)}{(ER)_i}\right]$$

$$= \left[\frac{x_r}{(ER)_r} - \frac{x_i}{(ER)_i}\right] + j\left[\frac{y_r}{(ER)_r} - \frac{y_i}{(ER)_i}\right]$$

$$\therefore \theta_2 = -\tan^{-1}\left[\frac{\frac{y_r}{(ER)_r} - \frac{y_i}{(ER)_i}}{\frac{x_r}{(ER)_r} - \frac{x_i}{(ER)_i}}\right]$$

Quadrent selector is done by the signs of the numerator and denominator.

Both θ_2 and $\theta_2 + \pi$ are solutions.

(2) Relation for $\theta_1 - \theta_2$

The relation will be used

$$\sin(\alpha_1 - \alpha_2) = \frac{\mathrm{Im}(u\, e^{-j\alpha_2})}{(ER)_r}$$

$$\alpha_1 = \frac{3\pi}{2} - \theta_1$$

$$\alpha_2 = \pi - \theta_2$$

$$\alpha_1 - \alpha_2 = \frac{\pi}{2} - (\theta_1 - \theta_2)$$

$$\sin(\alpha_1 - \alpha_2) = \sin\left[\frac{\pi}{2} - (\theta_1 - \theta_2)\right] = \cos(\theta_1 - \theta_2)$$

Hence

$$\cos(\theta_1 - \theta_2) = \frac{\mathrm{Im}\left[(x_r + j y_r)(\cos\alpha_2 - j\sin\alpha_2)\right]}{(ER)_r}$$

$$= \frac{-y_r \cos\theta_2 - x_r \sin\theta_2}{(ER)_r}$$

If $\theta_1 - \theta_2 = d - c$ is a solution, then $\theta_1 - \theta_2 = c - d$ is a solution.

(3) Relation for L

The corresponding equations for L_r and L_i can be found by pairing the equations (1), (2) and (3), (4).

$$X_r \cos\alpha_2 = (ER)_r \cos\alpha_1 \cos\alpha_2 + L_r \cos^2\alpha_2$$
$$y_r \sin\alpha_2 = (ER)_r \sin\alpha_1 \sin\alpha_2 + L_r \sin^2\alpha_2$$

$$X_r \cos\alpha_2 + y_r \sin\alpha_2 = (ER)_r \cos(\alpha_1 - \alpha_2) + L_r$$

or

$$L_r = X_r \cos\alpha_2 + y_r \sin\alpha_2 - (ER)_r \cos(\alpha_1 - \alpha_2)$$

Since $\alpha_1 = \frac{3\pi}{2} - \theta_1$ $\qquad \alpha_1 - \alpha_2 = \frac{\pi}{2} - (\theta_1 - \theta_2)$

$\alpha_2 = \pi - \theta_2$

$$L_r = -X_r \cos\theta_2 + y_r \sin\theta_2 - (ER)_r \sin(\theta_1 - \theta_2)$$

In a similar manner,

$$X_i \cos\alpha_2 = (ER)_i \cos\alpha_1 \cos\alpha_2 + L_i \cos^2\alpha_2$$

$$y_i \sin\alpha_2 = (ER)_i \sin\alpha_1 \sin\alpha_2 + L_i \sin^2\alpha_2$$

$$X_i \cos\alpha_2 + y_i \sin\alpha_2 = (ER)_i \cos(\alpha_1 - \alpha_2) + L_i \tag{7}$$

$$L_i = X_i \cos\alpha_2 + y_i \sin\alpha_2 - (ER)_i \cos(\alpha_1 - \alpha_2)$$

or

$$L_i = -X_i \cos\theta_2 + y_i \sin\theta_2 - (ER)_i \sin(\theta_1 - \theta_2)$$

The final relations for L_r and L_i show that if L is the solution for $\theta_1 = c$, $\theta_2 = d$, then $-L$ is <u>not</u> the solution for $\theta_1 = c + \pi$, $\theta_2 = d + \pi$ because although θ_1 and θ_2 change by π , the difference does not. The two relations for L_r and L_i given above can be summarized as follows:

$$L = -X \cos\theta_2 + Y \sin\theta_2 - (ER) \sin(\theta_1 - \theta_2)$$

(4) The pattern of the solution can be described as follows:

For

$\theta_1 = \alpha + C$ (true Rayleigh) $L = -x \cos\alpha + y \sin\alpha - ER \sin C$

$\theta_2 = \alpha$ (true Love) This is taken as the true relation

$\theta_1 - \theta_2 = C$ and will be designated as L_t.

$$\therefore \quad L = L_t$$

For

$\theta_1 = \alpha - C$ (Spurious Rayleigh)

$\theta_2 = \alpha$ (True Love)

$\theta_1 - \theta_2 = -C$

$$L = x \cos\alpha + y \sin\alpha + ER \sin C$$
$$= L_t + 2ER \sin C$$

For

$\theta_1 = \alpha + C$ (True Rayleigh)

$\theta_2 = \alpha + \pi$ (Spurious Love)

$\theta_1 - \theta_2 = C$

$$L = + x \cos\alpha - y \sin\alpha + ER \sin C$$
$$= -L_t$$

For

$\theta_1 = \alpha - C$ (Spurious Rayleigh)

$\theta_2 = \alpha + \pi$ (Spurious Love)

$\theta_1 - \theta_2 = -C - \pi$

$$L = x \cos\alpha - y \sin\alpha - ER \sin C$$
$$L = L_t - 2ER \sin C$$

Numerical Example

Select $ER = 1 + j$

$L = 1 + 2j$

$\theta_1 = 20^\circ$

$\theta_2 = 30^\circ$

Then $X = -ER \sin\theta_1 - L \cos\theta_2$

$= (-\sin 20^\circ - \cos 30^\circ) + j(-\sin 20^\circ - 2\cos 30^\circ)$

$= -1.2080 - j\,2.0741$

$Y = -ER \cos\theta_1 + L \sin\theta_2$

$= (-\cos 20^\circ + \sin 30^\circ) + j(-\cos 20^\circ + 2\cos 30^\circ)$

$= -0.4397 + j\,0.0603$

$$\theta_2 = -\tan^{-1}\left[\frac{\frac{Y_r}{(ER)_r} - \frac{Y_i}{(ER)_i}}{\frac{X_r}{(ER)_r} - \frac{X_i}{(ER)_i}}\right]$$

$$= -\tan^{-1}\left[\frac{-0.4397 - 0.0603}{-1.2080 + 2.0741}\right]$$

$= -\tan^{-1}(-0.5773)$ Fourth Quadrant

$\therefore \theta_2 = 30^\circ$ and 210°

$$\cos(\theta_1 - \theta_2) = -\frac{y_r \cos\theta_2 - x_r \sin\theta_2}{(ER)_r}$$

For $\theta_2 = 30^\circ$

$$\cos(\theta_1 - \theta_2) = 0.4397 \cos 30^\circ + 1.2080 \sin 30^\circ$$

$$= 0.9848$$

$$\therefore \theta_1 - \theta_2 = 10.00^\circ \quad , \quad \theta_1 = \theta_2 \pm 10^\circ$$

and -10.00°

For $\theta_2 = 210^\circ$, $(180^\circ + 30^\circ)$

$$\theta_1 - \theta_2 = 170^\circ \qquad \theta_1 = \theta_2 \pm 170^\circ$$

and -170°

$\therefore$ $\theta_1 = 20^\circ$ $\qquad$ $\theta_1 = 40^\circ$

$\theta_2 = 30^\circ$ $\qquad$ $\theta_2 = 30^\circ$

$\theta_1 - \theta_2 = -10^\circ$ $\qquad$ $\theta_1 - \theta_2 = +10^\circ$

$\theta_1 = 40^\circ$ $\qquad$ $\theta_1 = 20^\circ$

$\theta_2 = 210^\circ$ $\qquad$ $\theta_2 = 210^\circ$

$\theta_1 - \theta_2 = -170^\circ$ $\qquad$ $\theta_1 - \theta_2 = -190^\circ$

The Rayleigh component is at 20° (true angle) or 40° (spurious angle).

The Love component is at 30° (true angle) or 210° (180° off).

$$L_r = -X_r \cos\theta_2 + y_r \sin\theta_2 - (ER)_r \sin(\theta_1 - \theta_2)$$
$$L_i = -X_i \cos\theta_2 + y_i \sin\theta_2 - (ER)_i \sin(\theta_1 - \theta_2)$$

$\theta_1 = 20^\circ$
$\theta_2 = 30^\circ$
$\theta_1 - \theta_2 = -10^\circ$

$L_r = 1.2080 \cos 30^\circ - 0.4397 \sin 30^\circ - \sin(-10^\circ)$
$= 1.0000$

$L_i = 2.0741 \cos 30^\circ + 0.0603 \sin 30^\circ - \sin(-10^\circ)$

$\theta_1 = 40^\circ$
$\theta_2 = 30^\circ$
$\theta_1 - \theta_2 = +10^\circ$

$L_r = 1.000 - 2 \sin 10^\circ = 0.6527$
$L_r = 2.000 - 2 \sin 10^\circ = 1.6527$

$\theta_1 = 40^\circ$ $L_r = -0.6527$
$\theta_2 = 210^\circ = 180^\circ + 30^\circ$ $L_r = -1.6527$
$\theta_1 - \theta_2 = -170^\circ = 180^\circ + 10^\circ$

$\theta_1 = 20^\circ$ $L_r = -1.0000$
$\theta_2 = 210^\circ = 180^\circ + 30^\circ$ $L_r = -2.000$
$\theta_1 - \theta_2 = -190^\circ = +180^\circ - 10^\circ$

Condition		θ_1	θ_2	ER	L
Rayleigh	Love				
True	True	20°	30°	$1+j$	$1+j2$
Spurious	True	40°	30°	$1+j$	$0.6527+j1.6527$
True	Spurious	20°	210°	$1+j$	$-1-j2$
Spurious	Spurious	40°	210°	$1+j$	$-0.6527-j1.6527$

As a check

$\theta_1 = 20^\circ$ $\quad X = (-\sin 20^\circ - \cos 30^\circ) + j(-\sin 20^\circ - 2\cos 30^\circ)$

$\theta_2 = 30^\circ$ $\quad = -1.2080 - j2.0741$

$ER = 1+j$ $\quad Y = (-\cos 20^\circ + \sin 30^\circ) + j(-\cos 20^\circ + 2\sin 30^\circ)$

$L = 1+2j$ $\quad = -0.4397 + j0.0603$

$\theta_1 = 40^\circ$ $\quad X = (-\sin 40^\circ - 0.6527\cos 30^\circ) + j(-\sin 40^\circ - 1.6527\cos 30^\circ)$

$\theta_2 = 30^\circ$ $\quad = -1.2080 - j2.0741$

$ER = 1+j$ $\quad Y = (-\cos 40^\circ + .6527\sin 30^\circ) + j(-\cos 40^\circ + 1.6527\sin 30^\circ)$

$L = 0.6527 + j1.6527$ $\quad = -0.4397 + j0.0603$

$\theta_1 = 20^\circ$ $\quad X = (-\sin 20^\circ + \cos 210^\circ) + j(-\sin 20^\circ + 2\cos 210^\circ)$

$\theta_2 = 210^\circ$ $\quad = -1.2080 - j2.0741$

$ER = 1+j$ $\quad Y = (-\cos 20^\circ - j\sin 210^\circ) + j(-\cos 20^\circ - 2\sin 210^\circ)$

$L = -1-2j$ $\quad = -0.4397 + j0.0603$

$\theta_1 = 40^\circ$ $\quad X = (-\sin 40^\circ + 0.6527 \cos 210^\circ) + j(-\sin 40 + 1.6527 \cos 210)$

$\theta_2 = 210^\circ$ $\quad = -1.2080 - j\,2.0741$

$ER = 1 + j$ $\quad Y = (-\cos 40 - .6527 \sin 210^\circ) + j(-\cos 40 - 1.6527 \sin 210)$

$= -0.4397 + j\,0.0603$

$L = -.6527 - j\,1.6527$

SECTION IV

THE ELEMENTARY RAYLEIGH-RAYLEIGH WAVE ELLIPTICITY FILTER

The Elementary Rayleigh-Rayleigh Wave Ellipticity Filter is a simple Ellipticity Filter which is based on using the three-axis outputs of a seismometer station to generate a Rayleigh-Rayleigh wave decomposition. This filter has been previously described, but not in the full detail given here.

1.0 Introduction

The Elementary Rayleigh-Rayleigh Wave Ellipticity Filter is functionally similar to the Rayleigh-Love Wave Filter except modified decomposition equations are used. The formulation is best done in the frequency domain as described here. No allowance is made for background noise.

2.0 Performance When a Single Rayleigh Wave is Present

When a single Rayleigh Wave is present, the received signals are

$$X_o = \mathcal{R} \sin\theta$$
$$Y_o = \mathcal{R} \cos\theta$$
$$\mathcal{Z} = \mathcal{R}$$

The azimuth, θ, and the complex amplitude, $\mathcal{R}$, are uniquely obtainable from the observed signals

$$\mathcal{R} = \mathcal{Z}$$
$$\sin\theta = X_o / \mathcal{Z}$$
$$\cos\theta = Y_o / \mathcal{Z}$$

The presence of a single Rayleigh wave can be distinguished from two Rayleigh waves, although it may not always be distinguished from more than two Rayleigh waves. The test can be made by examining

$$T = X_o^2 + Y_o^2 - \mathcal{Z}^2$$

and, if $T = 0$, deciding that one Rayleigh wave is present.

The basis of this test is that, for two Rayleigh wave components, the observables are

$$X_o = R_1 \sin\theta_1 + R_2 \sin\theta_2$$

$$Y_o = R_1 \cos\theta_1 + R_2 \cos\theta_2$$

$$\mathcal{Z} = R_1 + R_2$$

$$T = X_o^2 + Y_o^2 - \mathcal{Z}^2$$

$$= 2R_1R_2\left[\sin\theta_1 \sin\theta_2 + \cos\theta_1 \cos\theta_2 - 1\right]$$

$$= 2R_1R_2\left[\cos(\theta_1 - \theta_2) - 1\right]$$

Hence, if $R_1 \neq 0$ or $R_2 \neq 0$, the test quantity, T, is zero if, and only if, $\theta_1 = \theta_2$.

3.0 Performance When Two Rayleigh Waves are Present

The direct method of decomposing two Rayleigh waves has been previously presented[1]. The main results are reviewed here with additional comments.

When two Rayleigh waves are present, the basic relations are

$$X_o = R_1 \sin\theta_1 + R_2 \sin\theta_2$$
$$Y_o = R_1 \cos\theta_1 + R_2 \cos\theta_2$$
$$Z = R_1 + R_2$$

in which the ellipticity factor, assumed known, is included within the observables X_o and Y_o. In terms of the real and imaginary parts, these equations become

$$X_{or} = R_{1r} \sin\theta_1 + R_{2r} \sin\theta_2$$
$$X_{oi} = R_{1i} \sin\theta_1 + R_{2i} \sin\theta_2$$

Multiplying the first equation by R_{1i} and the second by R_{1r} and subtracting gives

$$X_{or} R_{1i} - X_{oi} R_{1r} = (R_{2r} R_{1i} - R_{2i} R_{1r}) \sin\theta_2$$

Defining

$$P_1 = R_{1i} / R_{1r}$$

gives the compact form

$$(X_{oi} - P_1 X_{or}) = (R_{2i} - P_1 R_{2r}) \sin\theta_2$$

In a similar manner, the Y_o equations can be paired

$$Y_{or} = R_{1r}\cos\theta_1 + R_{2r}\cos\theta_2$$
$$Y_{oi} = R_{1i}\cos\theta_1 + R_{2i}\cos\theta_2$$

to give

$$(Y_{oi} - P_1 Y_{or}) = (R_{2i} - P_1 R_{2r})\cos\theta_2$$

The relations

$$Z = R_1 + R_2$$
$$Z_r = R_{1r} + R_{2r}$$
$$Z_i = R_{1i} + R_{2i}$$

can be used to reduce

$$R_{2i} - \frac{R_{1i} R_{2r}}{R_{1r}} = (Z_i - R_{1i}) - \frac{R_{1i}}{R_{1r}}(Z_r - R_{1r})$$

$$= Z_i - \frac{R_{1i}}{R_{1r}} Z_r$$

$$= Z_i - P_1 Z_r$$

Hence,

$$(X_{oi} - P_1 X_{or}) = (Z_i - P_1 Z_r) \sin\theta_2$$
$$(Y_{oi} - P_1 Y_{or}) = (Z_i - P_1 Z_r) \cos\theta_2$$

Squaring and adding then gives the quadratic form for P_1

$$a P_1^2 + b P_1 + c = 0$$

By a similar derivation, the same quadratic equation is obtained for P_2,

$$P_2 = P_{2i} / P_{2r}$$

Thus, P_1 and P_2 are the roots of the quadratic equation in which

$$a = X_{or}^2 + Y_{or}^2 - Z_{or}^2$$
$$b = 2[Z_{or} Z_{oi} - Y_{or} Y_{oi} - X_{or} X_{oi}]$$
$$c = X_{oi}^2 + Y_{oi}^2 - Z_{oi}^2$$

Note that

$$a = (R_{1r} \sin\theta_1 + R_{2r} \sin\theta_2)^2 + (R_{1r} \cos_1 + R_{2r} \cos\theta_2)^2 - (R_{1r} + R_{2r})^2$$
$$= 2 R_{1r} R_{2r} [\cos(\theta_1 - \theta_2) + 1]$$

$$b = 2[(R_{1r} + R_{2r})(R_{1i} + R_{2i}) - (R_{1r} \cos\theta_1 + R_{2r} \cos\theta_2)(R_{1i} \cos\theta_1 + R_{2i} \cos\theta_2$$
$$- (R_{1r} \sin\theta_1 + R_{2r} \sin\theta_2)(R_{1i} \sin\theta_1 + R_{2i} \sin\theta_2)$$

$$= 2\Big[R_{1r} R_{1i} (1 - \cos^2\theta_1 - \sin^2\theta_1)$$
$$R_{1r} R_{2i} (1 - \cos\theta_1 \cos\theta_2 - \sin\theta_1 \sin\theta_2)$$
$$R_{2r} R_{1i} (1 - \cos\theta_2 \cos\theta_1 - \sin\theta_2 \sin\theta_1)$$
$$R_{2r} R_{2i} (1 - \cos^2\theta_1 - \sin^2\theta_2)\Big]$$

$$= -2(R_{1r} R_{2i} + R_{2r} R_{1i})\big[\cos(\theta_1 - \theta_2) - 1\big]$$

$$c = 2 R_{1i} R_{2i} \big[\cos(\theta_1 - \theta_2) - 1\big]$$

Hence, if $\theta_1 = \theta_2$, $a = b = c$ is zero. This degenerate case can be avoided by first testing for

$$T = X_o^2 + Y_o^2 - Z_o^2$$

and, if $T = 0$, using the single Rayleigh decomposition.

With P_1 and P_2 solved for, θ_1 and θ_2 can be found from

$$\tan\theta_2 = \frac{x_{oi} - P_1 x_{or}}{y_{oi} - P_1 y_{or}}$$

and

$$\tan\theta_1 = \frac{x_{oi} - P_2 x_{or}}{y_{oi} - P_2 y_{or}}$$

These have a π ambiguity.

If $\theta_1 = \bar{\theta}_1$, then $\theta_1 = \bar{\theta}_1 + \pi$ is also a solution, and if $\theta_2 = \bar{\theta}_2$ then $\theta_2 = \bar{\theta}_2 + \pi$ is apparently a solution.

These ambiguities in azimuth can be resolved by using two of the three relations

$$\sin\theta_2 = \frac{Im\left(-X/E\right) - P_1 Re\left(-X/E\right)}{Im\left(Z\right) - P_1 Re\left(Z\right)}$$

$$\cos\theta_2 = \frac{Im\left(-Y/E\right) - P_1 Re\left(-Y/E\right)}{Im\left(Z\right) - P_1 Re\left(Z\right)}$$

$$\tan\theta_2 = \frac{Im\left(-X/E\right) - P_1 Re\left(-X/E\right)}{Im\left(-Y/E\right) - P_1 Re\left(-Y/E\right)}$$

or testing the quantities

$$A = X_{oi} - P_1 X_{or}$$

$$B = Z_{oi} - P_1 Z_{or}$$

$$C = Y_{oi} - P_1 Y_{or}$$

and assigning the quadrant by the rule

A	B	C	Sine	Cosine	Quadrant
+	+	+	+	+	I
+	+	-	+	-	II
+	-	+	-	-	III
+	-	-	-	+	IV
-	+	+	-	+	IV
-	+	-	-	-	III
-	-	+	+	-	II
-	-	-	+	+	I

The amplitude and phase of the Rayleigh components can be resolved as follows.

If now

$$R_1 = |R_1| e^{j\phi_1} = |R_1| \cos \phi_1 + j |R_1| \sin \phi_1 = R_{1r} + j R_{1i}$$

$$R_2 = |R_2| e^{j\phi_2} = |R_1| \cos \phi_2 + j |R_2| \sin \phi_2 = R_{2r} + j R_{2i}$$

it follows that

$$\tan \phi_1 = P_1$$

$$\tan \phi_2 = P_2$$

except that there is a π ambiguity so that if,

$$\phi_1 = \bar{\phi}_1 \,, \qquad \phi_1 = \bar{\phi}_1 + \pi \qquad \text{is a solution}$$

$$\phi_2 = \bar{\phi}_2 \,, \qquad \phi_2 = \bar{\phi}_2 + \pi \qquad \text{is a solution.}$$

To resolve these ambiguities, the magnitudes of $\mathcal{R}_1$ and $\mathcal{R}_2$ are solved for.

The magnitudes $\mathcal{R}_{1m}$ and $\mathcal{R}_{2m}$ can be found from

$$\mathcal{Z} = \mathcal{R}_1 + \mathcal{R}_2$$

$$= \mathcal{R}_{1m} e^{j\phi_1} + \mathcal{R}_{2m} e^{j\phi_2}$$

$$\mathcal{Z} e^{-j\phi_1} = \mathcal{R}_{1m} + \mathcal{R}_{2m} e^{j(\phi_1 - \phi_2)}$$

$$(\mathcal{Z}_r + j\mathcal{Z}_i)(\cos\phi_1 - j\sin\phi_1) = \mathcal{R}_{1m} + \mathcal{R}_{2m}\left[\cos(\phi_2 - \phi_1) + j\sin(\phi_2 - \phi_1)\right]$$

The imaginary parts of this equation give

$$\mathcal{Z}_i \cos\phi_1 - \mathcal{Z}_r \sin\phi_1 = \mathcal{R}_{2m} \sin(\phi_2 - \phi_1)$$

$$\therefore \quad \mathcal{R}_{2m} = \frac{\mathcal{Z}_i \cos\phi_1 - \mathcal{Z}_r \sin\phi_1}{\sin(\phi_2 - \phi_1)}$$

$$\mathcal{R}_{2m} = \frac{\mathcal{Z}_i - P_1 \mathcal{Z}_r}{\sin\phi_2 - P_1 \cos\phi_2}$$

If $\mathcal{R}_{2m}$ is to be positive, φ_2 must be chosen as $\bar{\varphi}_2$ or $\bar{\varphi}_2 + \pi$ to do so. This selection is unique.

Similarly

$$\mathcal{R}_{1m} = \frac{\mathcal{Z}_i - P_2 \mathcal{Z}_r}{\sin \varphi_1 - P_2 \cos \varphi_1}$$

requires the same selection between $\bar{\varphi}_1$ and $\bar{\varphi}_1 + \pi$.

What may not be apparent from this direct method is that the solution is ambiguous if

$$\mathcal{R}_{1i} / \mathcal{R}_{1r} = \mathcal{R}_{2i} / \mathcal{R}_{2r}$$

or

$$P_1 = P_2$$

Then

$$\mathcal{R}_1 = \mathcal{R}_{1m} e^{j\varphi_1} = \mathcal{R}_{1m} e^{j\varphi}$$

$$\mathcal{R}_2 = \mathcal{R}_{2m} e^{j\varphi_2} = \mathcal{R}_{2m} e^{j\varphi}$$

since

$$\varphi_1 = \varphi_2 = \varphi$$

Then,

$$X_0 = (\mathcal{R}_{1m} \sin \theta_1 + \mathcal{R}_{2m} \sin \theta_2) e^{j\varphi}$$

$$y_0 = (\mathcal{R}_{1m} \cos \theta_1 + \mathcal{R}_{2m} \cos \theta_2) e^{j\varphi}$$

$$\mathcal{Z} = (\mathcal{R}_{1m} + \mathcal{R}_{2m}) e^{j\varphi}$$

or all the observables have the same phase angle. While φ can be solved for, the equations are degenerate

$$X_{om} = R_{1m} \sin\theta_1 + R_{2m} \sin\theta_2$$

$$Y_{om} = R_{1m} \cos\theta_1 + R_{2m} \cos\theta_2$$

$$Z_{om} = R_{1m} + R_{2m}$$

There are three equations for four unknowns.

If $X_{om}^2 + Y_{om}^2 - Z_{om}^2$ is formed

$$X_{om}^2 + Y_{om}^2 - Z_{om}^2 = 2 R_{1m} R_{2m} \left[\cos(\theta_1 - \theta_2) - 1\right] \neq 0$$

and one can select any $\theta_1 - \theta_2$ as a solution.

This case is quite unique and, thus, not too likely to occur. To assure ourselves that there are no other ambiguous solutions, the indirect method, discussed in the next section, is used.

4.0 Performance When Two Rayleigh Waves are Present: Indirect Method

Additional insight into the uniqueness of the solution can be obtained by a somewhat different approach. The direct solution has a jump discontinuity as $\theta_1 \to \theta_2$. To avoid this, let

$$\mu = R_1 + R_2 \qquad R_1 = (\mu + v)/2$$

$$v = R_1 - R_2 \qquad R_2 = (\mu - v)/2$$

since these variables have no such discontinuities.

Then

$$\chi_o = \mu/2\,[\sin\theta_1 + \sin\theta_2] + v/2\,[\cos\theta_1 - \sin\theta_2]$$

$$\gamma_o = \mu/2\,[\cos\theta_1 + \cos\theta_2] + v/2\,[\cos\theta_1 - \cos\theta_2]$$

$$\mathcal{Z} = \mu$$

The basic relations

$$\sin\theta_1 + \sin\theta_2 = 2\sin\left(\frac{\theta_1+\theta_2}{2}\right)\cos\left(\frac{\theta_1-\theta_2}{2}\right)$$

$$\sin\theta_1 - \sin\theta_2 = 2\sin\left(\frac{\theta_1-\theta_2}{2}\right)\cos\left(\frac{\theta_1+\theta_2}{2}\right)$$

$$\cos\theta_1 + \cos\theta_2 = 2\cos\left(\frac{\theta_1+\theta_2}{2}\right)\cos\left(\frac{\theta_1-\theta_2}{2}\right)$$

$$\cos\theta_1 - \cos\theta_2 = -2\sin\left(\frac{\theta_1+\theta_2}{2}\right)\sin\left(\frac{\theta_1-\theta_2}{2}\right)$$

suggest another change in variable

$$\alpha = \frac{\theta_1 + \theta_2}{2}$$

$$\beta = \frac{\theta_1 - \theta_2}{2}$$

This gives the set of relations

$$X_o = Z \sin\alpha \cos\beta + V \cos\alpha \sin\beta$$

$$Y_o = Z \cos\alpha \cos\beta - V \sin\alpha \sin\beta$$

In terms of the real and imaginary parts

$$X_{or} = Z_r \sin\alpha \cos\beta + V_r \cos\alpha \sin\beta$$

$$Y_{or} = Z_r \cos\alpha \cos\beta - V_r \sin\alpha \sin\beta$$

$$X_{or} + j Y_{or} = Z_r \cos\beta (\sin\alpha + j\cos\alpha) + V_r \sin\beta (\cos\alpha - j\sin\alpha)$$

$$e^{-j\alpha} = \cos\alpha - j\sin\alpha$$

$$j e^{-j\alpha} = \sin\alpha + j\cos\alpha$$

$$\therefore X_{or} + j Y_{or} = Z_r \cos\beta\, j e^{-j\alpha} + V_r \sin\beta\, e^{-j\alpha}$$

In a similar fashion

$$X_{oi} + j y_{oi} = Z_i \cos\beta\, j e^{-j\alpha} + V_i \sin\beta\, e^{-j\alpha}$$

Then,

$$\left(\frac{X_{or} + j Y_{or}}{Z_r} - \frac{X_{oi} + j Y_{oi}}{Z_i} \right) = \left(\frac{V_r}{Z_r} - \frac{V_i}{Z_i} \right) \sin \beta \, e^{-j\alpha}$$

If

$$\frac{X_{or} + j Y_{or}}{Z_r} \neq \frac{X_{oi} + j Y_{oi}}{Z_i}, \quad \alpha \text{ or } \alpha + \pi \text{ is}$$

the phase of

$$\left(\frac{X_{or} + j Y_{or}}{Z_r} - \frac{X_{oi} + j Y_{oi}}{Z_i} \right)$$

Hence,

$$\tan \alpha = \frac{\frac{Y_{or}}{Z_r} - \frac{Y_{oi}}{Z_i}}{\frac{X_{or}}{Z_r} - \frac{X_{oi}}{Z_i}}$$

Once α is known, the other quantities v and β can be solved for.

The solution breaks down

1. If $\beta = 0$. This corresponds to $\theta_1 = \theta_2$ or the case in which only one Rayleigh wave is present

2. If

$$\frac{X_{or} + j Y_{or}}{Z_r} = \frac{X_{oi} + j Y_{oi}}{Z_i}.$$

In this case

$$V_r / Z_r = V_i / Z_i$$

This corresponds to

$$\frac{R_{1r} - R_{2r}}{R_{1r} + R_{2r}} = \frac{R_{1i} - R_{2i}}{R_{1i} + R_{2i}}$$

or

$$R_{1i}/R_{2i} = R_{1r}/R_{2r}$$

Physically, this corresponds to the two Rayleigh waves having the same phasing.

These are the only possible ambiguous cases that can be present.

Numerical Example

$$-ER_1 = 1 + 2j = 2.2361 \ @ \ 63.4349^\circ$$
$$-ER_2 = 3 + 4j = 5.0000 \ @ \ 53.1301^\circ$$
$$\theta_1 = 20^\circ$$
$$\theta_2 = 30^\circ$$
$$E = 1$$

$$X = (1 + 2j)\sin 20^\circ + (3 + 4j)\sin 30^\circ$$
$$= (\sin 20^\circ + 3\sin 30^\circ) + j(2\sin 20^\circ + 4\sin 30^\circ)$$
$$= 1.8420 + j\,2.6840$$

$$Y = (1 + 2j)\cos 20^\circ + (3 + 4j)\cos 30^\circ$$
$$= (\cos 20^\circ + 3\cos 30^\circ) + j(2\cos 20^\circ + 4\cos 30^\circ)$$
$$= 3.5378 + j\,5.3435$$

$$Z = 4 + 6j$$

$$a = (3.5378)^2 + (1.8420)^2 - (4)^2$$

$$= -0.09101$$

$$b = 2[(4)(6) - (3.5378)(5.3435) - (1.8400)(2.6840)]$$

$$= 0.30368$$

$$c = (5.3435)^2 + (2.6840)^2 - (6)^2$$

$$= -0.24315$$

$$aP^2 + bP + c = 0$$

has the solutions

$$P_1 = \begin{matrix} 2.002, \\ (2.000) \end{matrix} \qquad P_2 = \begin{matrix} 1.3339 \\ (1.3333) \end{matrix} \qquad \text{(checks)}$$

$$\theta_2 = \tan^{-1}\left[\frac{Im\left(-\frac{X}{E}\right) - P_1 Re\left(-\frac{X}{E}\right)}{Im\left(-\frac{Y}{E}\right) - P_1 Re\left(-\frac{Y}{E}\right)}\right]$$

$$= \tan^{-1}\left[\frac{-2.6840 + (2.002)(1.8420)}{-5.3435 + (2.002)(3.5378)}\right]$$

$$= \tan^{-1}\frac{+1.0000}{+1.7321}$$

$$= \tan^{-1} 0.57733$$

$$= 30^\circ \text{ and } 210^\circ$$

However,

$$A = 1.0000$$

$$B = 1.7321$$

$$C = Im\left(-\frac{Y}{E}\right) - P_1\, Re\left(-\frac{Y}{E}\right)$$

$$= -5.3435 - (2.002)(-3.5378)$$

$$= 1.7392$$

since A is +

B is + only 30.00° is the correct solution

C is +

$$\theta_1 = \tan^{-1}\left[\frac{(-2.6840) - (1.3333)(-1.8420)}{-5.3435 - (1.3333)(-3.5378)}\right]$$

$$= \tan^{-1}\frac{-0.22801}{-0.62645}$$

$$= \tan^{-1} 0.36397$$

$$= 20.00^\circ \text{ and } 200^\circ$$

However,

$$A = -0.22801$$

$$B = -0.62645$$

$$C = Im\left(-\frac{Y}{E}\right) - P_1\, Re\left(-\frac{Y}{E}\right)$$

$$= -5.3435 - (1.3333)(-3.5378)$$

$$= -0.6264$$

Since A is -

B is - only 20.00° is the correct solution

C is -

$$\text{amplitude } A_1 = \frac{\mathrm{Im}(z) - P_2\,\mathrm{Re}(z)}{\sin\phi_1 - P_2\cos\phi_1} \qquad \text{for } \phi = 63.434^\circ$$

$$= \frac{6 - (1.3333)(4)}{\sin 63.434^\circ - (1.3333)\cos 63.434^\circ}$$

$$= 2.2367 \text{ (checks)}$$

$$\text{amplitude } A_1 = \frac{6 - (1.3333)(4)}{\sin 243.434^\circ - (1.3333)\cos 243.434^\circ} \qquad \text{for } \phi = 243.434^\circ$$

$$= -2.2363 \text{ (checks)}$$

Sign of A_1 reverses so that this is one solution

$$A_1 = 2.2367 \angle 63.434^\circ \text{ (checks)}$$

$$\text{amplitude } A_2 = \frac{6 - 2.0000(4)}{\sin 53.130^\circ - (2.0000)\cos 53.130^\circ} \qquad \text{for } \phi = 53.130^\circ$$

$$= 5.0000$$

$$A_2 = 5.0000 \angle 53.130^\circ \text{ (checks)}$$

Hence, the unique and correct solution is

$$\theta_1 = 20^\circ$$

$$\theta_2 = 30^\circ$$

$$A_1 = 2.2361 \angle 63.4349^\circ$$

$$A_2 = 5.0000 \angle 53.1301^\circ$$

SECTION V

AN ELLIPTICITY FILTER CONFIGURATION BASED ON MINIMUM NOISE MAGNITUDE ESTIMATORS

It is sometimes desired to estimate the magnitude of an event from surface wave data, when the surface waves are partially masked either by the main surface wave arrivals or by the late-arriving Rayleigh wave coda of another seismic event, and when noise may also be present in the record. A minimum noise solution for magnitude is developed, based on an Ellipticity Filter processor in which a flexible three-component signal waveform is derived from surface wave data from previous signals from nearby epicenters. In the case of interfering Rayleigh and Love waves from a known epicenter, the solution for signal magnitude has been derived in closed form. In the case of interfering Rayleigh wave coda from unknown directions, the solution is obtained by a single-variable search. It is expected that these solutions are considerably more robust than those of the Elementary Ellipticity Filters predicated on low-noise data.

1.0 Introduction

The problem is to estimate the magnitude of an event, based on the Rayleigh and Love wave signal, when the event is mixed with the main surface wave or the late-arriving surface wave coda from another seismic event. The approach is to find that Ellipticity Filter decomposition of the signal and the interference which minimizes the residual noise in the records.

The method utilizes the assumption that the actual signal will differ deterministically from a "prototype" signal (empirically modelled from similar events from the same region) as a result of differing origin time, range, azimuth, and Rayleigh/Love energy ratio as well as magnitude. The method further assumes that the interference is either a combination of Love and Rayleigh waves arriving from the epicenter of the other seismic event, or that it is late-arriving coda consisting only of Rayleigh waves from unknown azimuths corresponding to various multipaths.

2.0 Derivation

The three observables are the outputs of the three x-axis seismometers. As before, the solution is obtained in the frequency domain. Thus,

X, Y, Z are the Fourier transforms of the time-domain observables corresponding to eastward, northward, and upward motion being positive.

The decomposition is based on the prototype waves being

R_p for the amplitude of the prototype Rayleigh Wave

L_p for the amplitude of the prototype Love Wave

R_I for the amplitude of the interfering Rayleigh Wave

L_I for the amplitude of the interfering Love Wave.

These quantities R_p, L_p, R_I, L_I, X, Y, and Z are all complex. The notation will be used that, if Q is complex, Q^* is the complex conjugate and

$$Q = q_r + i q_i$$

For the actual event, the azimuth associated with each wave is designated by θ_{rp}, θ_{lp}, θ_{rI}, and θ_{lI} respectively. The magnification of the prototype Rayleigh and Love waves are designated by M_{rp}, M_{lp}.

The noise is denoted by N_x , N_y , and N_z corresponding to the three-axes of the seismometer.

The range dependancy effects are taken care of by the inclusion of an $\exp(-j\Delta)$ factor in which

$$\Delta = \omega(\tau + \delta/v)$$

ω being the frequency of the Fourier transform bin,

τ being the delay in origin time,

δ being the increase in range from the prototype reference,

v being the phase velocity.

If no subscript appears on Δ , it is implied that Δ and V correspond to the wave type associated with the $\exp(-i\Delta)$ factor.

The decomposition equations are then

$$X = -E\left(M_{rp} R_p e^{-i\Delta} \sin\theta_{rp} + R_I \sin\theta_{rI}\right) - \left(M_{lp} L_p e^{-j\Delta} \cos\theta_{lp} + L_I \cos\theta_{lI}\right) + N_x$$

$$Y = -E\left(M_{rp} R_p e^{-i\Delta} \cos\theta_{rp} + R_I \cos\theta_{rI}\right) + \left(M_{lp} L_p e^{-j\Delta} \sin\theta_{lp} + L_I \sin\theta_{lI}\right) + N_y$$

$$Z = M_{rp} R_p e^{-i\Delta} + R_I + N_z$$

The decomposition is based on minimizing the noise sum expression

$$N^2 = W^2 N_Z N_Z^* + N_X N_X^* + N_Y N_Y^*$$

by selecting M_{rp}, M_{lp}, R_I, L_I, θ_{rI}, and θ_{lI} to do so. The factor W^2 is permitted to allow for the situation in which the noise output of the vertical seismometers is substantially different from that of the horizontals.

The solution is formally obtained by writing the noise sum expression and setting the derivatives equal to zero. To perform the algebra with minimum handling of subscripts, a change in notation will be used.

$$\begin{aligned} A &= R_I & \theta_A &= \theta_{rI} \\ B &= L_I & \theta_B &= \theta_{lI} \\ C &= R_p & \theta_c &= \theta_{rp} & M_c &= M_{rp} \\ D &= L_p & \theta_d &= \theta_{lp} & M_D &= M_{lp} \end{aligned} \qquad (1)$$

The decomposition equations are then

$$X = -E\left(M_D D e^{-i\Delta} \sin\theta_D + A \sin\theta_A\right) - B\cos\theta_B - M_c C \cos\theta_c e^{-i\Delta} + N_X \qquad (2a)$$

$$Y = -E\left(M_D D e^{-i\Delta} \sin\theta_D + A \cos\theta_A\right) + B \sin\theta_B + M_c C \sin\theta_c e^{-i\Delta} + N_Y \qquad (2b)$$

$$Z = M_D D e^{-i\Delta} + A + N_Z \qquad (2c)$$

$$N_X N_X^* = X X^* + E E^* D D^* \sin^2\theta_D M_D^2 + E E^* A A^* \sin^2\theta_A$$
$$+ B B^* \cos^2\theta_B + C C^* \cos^2\theta_C M_C^2$$
$$+ 2\,Re\{X E^* A^* \sin\theta_A + X B^* \cos\theta_B$$
$$+ E A \sin\theta_A B^* \cos\theta_B + C \cos\theta_C M_C e^{-i\Delta}[X^*$$
$$+ E^* D^* M_D e^{+i\Delta} \sin\theta_D + E^* A^* \sin\theta_A + B^* \cos\theta_B]$$
$$+ E D e^{-i\Delta} \sin\theta_D M_D [X^* + A^* E^* \sin\theta_A + B^* \cos\theta_B]\} \quad (3a)$$

$N_Y N_Y^*$ = same as $N_X N_X^*$, except that X becomes Y, sin becomes cos, and cos becomes $-\sin$. (3b)

$$N_Z N_Z^* = D D^* M_D^2 + A A^* + Z Z^* + 2Re[-Z D^* e^{+i\Delta} M_D$$
$$- Z A^* + D e^{-i\Delta} A^* M_D] \quad (3c)$$

The derivative of N^2 with respect to M_D is as follows:

$$\frac{\partial N^2}{\partial M_D} = W^2[2 D D^* M_D + 2Re\{D e^{-i\Delta}(A^* - Z^*)\}]$$
$$+ [2 E E^* D D^* \sin^2\theta_D M_D + 2Re\{D e^{-i\Delta} E \sin\theta_D (X^*$$
$$+ A^* E^* \sin\theta_A + B^* \cos\theta_B + C^* e^{+i\Delta} \cos\theta_C M_C)\}]$$
$$+ [2 E E^* D D^* \cos^2\theta_D M_D + 2Re\{D e^{-i\Delta} E \cos\theta_D (Y^*$$
$$+ A^* E^* \cos\theta_A - B^* \sin\theta_B - C^* e^{+i\Delta} \sin\theta_C M_C)\}]$$

This can be reduced by noting

$$\frac{\partial N^2}{\partial M_D} = 2D D^* (W^2 + E E^*) M_D$$
$$+ 2 Re\{E D e^{-i\Delta} C^* e^{+i\Delta} (\sin\theta_D \cos\theta_C - \cos\theta_D \sin\theta_C)\} M_C$$
$$+ 2 Re\{D e^{-i\Delta} [E X^* \sin\theta_D + E Y^* \cos\theta_D$$
$$+ A^* E^* E (\sin\theta_D \sin\theta_A + \cos\theta_D \cos\theta_A)$$
$$+ E B^* (\sin\theta_D \cos\theta_B - \cos\theta_D \sin\theta_B)$$
$$+ W^2 (A^* - Z^*)]\}$$

$$\frac{\partial N^2}{\partial M_D} = 2D D^* (W^2 + E E^*) M_D + 2 Re (E D e^{-i\Delta} C^* e^{+i\Delta}) \sin(\theta_D - \theta_C) M_C$$
$$+ 2 Re\{D e^{-i\Delta} [E X^* \sin\theta_D + E Y^* \cos\theta_D + A^* E^* E \cos(\theta_D - \theta_A)$$
$$+ E B^* \sin(\theta_D - \theta_B) + W^2 (A^* - Z^*)]\} \qquad (4)$$

Note that the first term on the right-hand side of Eq. (4) is linear in M_D and has a known coefficient; the second is linear in M_C and also has a known coefficient (which is very small since $\theta_D \approx \theta_C$); the third is dependent on the unknowns related to the interference. Now,

$$\frac{\partial N^2}{\partial M_C} = 2C C^* M_C \cos^2\theta_C + 2 Re\{C e^{-i\Delta} \cos\theta_C [X^*$$
$$+ E^* D^* e^{+i\Delta} \sin\theta_D M_D + E^* A^* \sin\theta_A + B^* \cos\theta_B]\}$$
$$+ 2C C^* M_C \sin^2\theta_C + 2 Re\{-C e^{-i\Delta} \sin\theta_C [Y^*$$
$$+ E^* D^* e^{+i\Delta} \cos\theta_D M_D + E^* A^* \cos\theta_A - B^* \sin\theta_B]\}$$

$$\frac{\partial N^2}{\partial M_C} = 2C\,C^* M_C + 2Re\{(E)\,e^{-i\Delta} C^* e^{+i\Delta} \sin(\theta_D - \theta_C) M_D$$
$$+ C\,e^{-i\Delta}[X^* \cos\theta_C - Y^* \sin\theta_C + E^* A^* \sin(\theta_A - \theta_C)$$
$$+ B^* \cos(\theta_B - \theta_C)]\} \qquad (5)$$

Equation (5) has the same properties of linearity as Eq. (4), with the roles of M_C and M_D reversed. If $M_C = M_D = M$,

$$\frac{\partial N^2}{\partial M} = \left[\frac{\partial N^2}{\partial M_C}\right]_{M_D} + \left[\frac{\partial N^2}{\partial M_D}\right]_{M_C}$$

$$\frac{\partial N^2}{\partial M} = 2[D\,D^*(W^2 + E\,E^*) + C\,C^*$$
$$+ 2Re\,(E^* D^* e^{+i\Delta} C\,e^{-i\Delta}) \sin(\theta_D - \theta_C)]M$$
$$+ 2Re\{\text{Remaining terms of Eqns. 4 and 5 which do not include } M\} \qquad (6)$$

In a similar manner, the partial derivatives of N^2 with respect to A, B, θ_A, and θ_B may be found. Since the partial derivatives of N^2 with respect to the real and imaginary parts of A (a_r and a_i, respectively) are both real, it is equally useful, but more convenient, to find

$$\frac{\partial N^2}{\partial a_r} + i\frac{\partial N^2}{\partial a_i}$$

$$= 2W^2[A - Z + D\, e^{-i\Delta} M_D]$$

$$+ 2[E\,E^* A \sin^2\theta_A + X\,E^* \sin\theta_A + \sin\theta_A\, B \cos\theta_B\, E^*$$

$$+ C \cos\theta_C\, M_C\, e^{-i\Delta} E^* \sin\theta_A + E\, D\, e^{-i\Delta} \sin\theta_D\, M_D\, E^* \sin\theta_A]$$

$$+ 2[E\,E^* A \cos^2\theta_A + Y\,E^* \cos\theta_A - \cos\theta_A\, B \sin\theta_B\, E^*$$

$$- C \sin\theta_C\, M_C\, e^{-i\Delta} E^* \cos\theta_A + E\, D\, e^{-i\Delta} \cos\theta_D\, M_D E^* \cos\theta_A]$$

$$\frac{\partial N^2}{\partial a_r} + i\frac{\partial N^2}{\partial a_i}$$

$$= 2(W^2 + E\,E^*)A + 2\sin(\theta_A - \theta_B)\, B\, E^*$$

$$+ 2\,E^* \sin(\theta_A - \theta_C)\, e^{-i\Delta} M_C\, C$$

$$+ 2[W^2 + E\,E^* \cos(\theta_D - \theta_A)]\, e^{-i\Delta} M_D\, D$$

$$+ 2[E^*(Y \cos\theta_A + X \sin\theta_A) - W^2 Z] \qquad (7)$$

Equation (7) is comprised of a term, linear in A with a known coefficient, (a term which would be zero under either of the two interference hypotheses mentioned previously) two terms linear in M_C and M_D with coefficients depending on the unknown θ_A, and a term in which the only unknown is θ_A.

Similarly,

$$\frac{\partial N^2}{\partial b_r} + i\frac{\partial N^2}{\partial b_i}$$

$$= 2[\cos^2\theta_B B + X\cos\theta_B + E D e^{-i\Delta}\sin\theta_D\cos\theta_B M_D$$

$$+ E A \sin\theta_A \cos\theta_B + C\cos\theta_B\cos\theta_C e^{-i\Delta} M_C]$$

$$+ 2[\sin^2\theta_B B - Y\sin\theta_B - E D e^{-i\Delta}\cos\theta_D \sin\theta_B M_D$$

$$- E A \cos\theta_A \sin\theta_B + C\sin\theta_B\sin\theta_C e^{-i\Delta} M_C]$$

$$\frac{\partial N^2}{\partial b_r} + i\frac{\partial N^2}{\partial b_i}$$

$$= 2B + 2\sin(\theta_A - \theta_B) E A + 2\cos(\theta_B - \theta_C) e^{-i\Delta} M_C C$$

$$+ 2\sin(\theta_D - \theta_B) E e^{-i\Delta} M_D D + 2(X\cos\theta_B - Y\sin\theta_B)$$

(8)

Equation (8) is linear in B, and A, but with a coefficient which is zero under the first interference hypothesis. [Eqn. (8) is irrelevent under the other hypothesis]. The equation is linear in M_C and M_D with coefficients depending on the unknown θ_B, and has one term in which the only unknown is θ_B.

Proceeding to find the derivatives of N^2 with respect to θ_A and θ_B,

$$\frac{\partial N^2}{\partial \theta_A} = 2 E E^* A A^* \sin\theta_A \cos\theta_A$$

$$+ 2 Re\left\{X F^* A^* + E A B^* \cos\theta_B + E D e^{-i\Delta} \sin\theta_D M_D A^* E^*\right\}\cos\theta_A$$

$$+ 2 Re\left\{C \cos\theta_C M_C e^{-i\Delta} E^* A^*\right\} \cos\theta_A$$

$$- 2 E E^* A A^* \sin\theta_A \cos\theta_A$$

$$- 2 Re\left\{Y E^* A^* - E A B^* \sin\theta_B + E D e^{-i\Delta} \cos\theta_D M_D A^* E^*\right\}\sin\theta_A$$

$$+ 2 Re\left\{C \sin\theta_C M_C e^{-i\Delta} E^* A^*\right\} \sin\theta_A$$

$$\frac{\partial N^2}{\partial \theta_A} = 2 Re\left\{A B^* E\right\} \cos(\theta_B - \theta_A)$$

$$+ 2 Re\left\{A^* E^* \left[X + E D e^{-i\Delta} \sin\theta_D M_D + C e^{-i\Delta} \cos\theta_C M_C\right]\right\}\cos\theta_A$$

$$+ 2 Re\left\{A^* E^* \left[-Y - E D e^{-i\Delta} \cos\theta_D M_D + C e^{-i\Delta} \sin\theta_C M_C\right]\right\}\sin\theta_A$$

(9)

Similarly,

$$\frac{\partial N^2}{\partial \theta_B} = - 2 B B^* \sin\theta_B \cos\theta_B$$

$$- 2 Re\left\{X B^* + E A \sin\theta_A B^* + E D' e^{-i\Delta} \sin\theta_D M_D B^*\right.$$

$$\left. + C \cos\theta_C e^{-i\Delta} M_C B^*\right\} \sin\theta_B$$

$$+ 2 B B^* \sin\theta_B \cos\theta_B$$

$$- 2 Re\left\{Y B^* + E A \cos\theta_A B^* + E D e^{-i\Delta} \cos\theta_D M_D B^*\right.$$

$$\left. - C \sin\theta_C e^{-i\Delta} M_C B^*\right\} \cos\theta_B$$

$$\frac{\partial N^2}{\partial \theta_B} = -2\,Re\,(E\,A\,B^*)\cos(\theta_A - \theta_B)$$
$$- 2\,Re\left\{B^*\left[Y - C\sin\theta_C\, e^{-i\Delta} M_C + E D\, e^{-i\Delta}\cos\theta_D M_D\right]\right\}\cos\theta_B$$
$$- 2\,Re\left\{B^*\left[X + C\cos\theta_C\, e^{-i\Delta} M_C + E D\, e^{-i\Delta}\sin\theta_D M_D\right]\right\}\sin\theta_B \qquad (10)$$

One hypothesis models interference as Rayleigh and Love waves from a known epicenter. Under this hypothesis, $\theta_A = \theta_B = \theta_I$, and Eqs. (9) and (10) become irrelevant.

Alternatively, if interference is Rayleigh wave motion from an unknown direction, Eq. (10) becomes irrelevant, and Eq. (9) can be simplified by using

$$B^* = 0 \qquad (11)$$

3.0 Application to Rayleigh/Love Wave Interference

Assuming that the interference consists of a combination of Rayleigh and Love waves from a known direction $\theta = \theta_A = \theta_B$, the equations derived above may be applied to find a minimum-noise solution for the signal magnitude, and also for the interfering wave amplitudes. Equations (7) and (8) may be set equal to zero, and by introducing the subscript n, for frequency, Eq. (6) may be summed over frequency and set equal to zero. For simplicity, S is symbolic of various <u>different</u> functions which may be defined by reference to Eqs. (6), (7), and (8), and K is symbolic of a subset of the known variables. The modified Eqs. (6), (7), and (8) are

$$\left[\sum_n S_n(K)\right] M + \sum_n Re\left[S_n(K) + S_n(K) A_n^* + S_n(K) B_n^*\right] = 0 \qquad (12)$$

$$S_n(K) A_n + S_n(K) M + S_n(K) = 0 \qquad (13)$$

$$B_n + S_n(K) M + S_n(K) = 0 \qquad (14)$$

Solving Eq. (13) for A_n, and Eq. (14) for B_n, and substituting the complex conjugates of these results into Eq. (12) gives

$$\left[\sum_n S_n(K)\right] M + \sum_n Re\left[S_n(K) + S_n(K) M\right] \qquad (15)$$

which is the same as

$$\left[\sum_n S_n(K)\right] M + \sum_n S_n(K) = 0 \qquad (16)$$

This symbolic equation has a very simple, closed-form solution for the minimum-noise value of M .

Having solved for M , it is possible to evaluate further minimumization of noise which might result from small changes in the "known" variables θ , τ , δ , and the ratio M_D/M_c . Results corresponding to alternate values of the "known" variables may be substituted into Eq. (2) via Eq. (3a-c), and those values producing minimum $\sum_N N^2$ may be taken as revised estimates of the "known variables.

4.0 Application to Rayleigh Coda Interference

Following a similar procedure, the results can be applied to Rayleigh coda interference. In this situation, the interference is assumed to be Rayleigh waves from unknown, frequency-dependent directions. In this formulation, B may be set equal to zero, and Eq. (6) may be summed over frequency. Eqs. (6), (7), and (9) become, symbolically,

$$\left[\sum_{n} S_n(K)\right] M + \sum_{n} \mathrm{Re}\left\{S_n(K) + A_n^* \left[S_n(K) + S_n(K)\cos\theta_{A,n} + S_n(K)\sin\theta_{A,n}\right]\right\} = 0 \quad (17)$$

$$S_n(K)\, A_n + S_n(K,M)\cos\theta_{A,n} + S_n(K,M)\sin\theta_{A,n} + S_n(K,M) = 0 \quad (18)$$

$$\mathrm{Re}\left\{A^* \left[S_n(K,M)\cos\theta_{A,n} + S_n(K,M)\sin\theta_{A,n}\right]\right\} = 0 \quad (19)$$

While the number of unknowns and the number of equations represented by Eqs. (17), (18), and (19) are equal, a closed-form solution is difficult to obtain. Instead, using an assumed value of M in Eq. (18), A_n may be solved for in terms of $\theta_{A,n}$ and substituted into Eq. (19), which may then be solved for $\theta_{A,n}$. After substituting $\theta_{A,n}$ back into Eq. (18) to find A_n, $\sum_n N_n^2$ can be evaluated in Eq. (2). This process may be repeated with different values for M until the minimum value of $\sum_n N_n^2$ is found.

Hence, the minimum-noise value of M can be found by a simple, single-variable search.

APPENDIX A: Curve Fitting of the VLP System Response

A.1 Summary

The published data on the Konigsberg (KON) very long period system response[15] was examined and curve fitted by a cascade of three identically tuned circuits. The amplitude vs period fit is based on

$$A = \frac{B_o^3}{\left[B_o^2 + \left(\tau_o/T - T/\tau_o\right)^2\right]^{3/2}}$$

in which

T is the period

τ_o is the resonant period

$B_o = 2h_o$, h_o is the damping constant.

As shown in Figures 21, 22, and 23, the resulting fit is quite good in spite of the fact that a complicated instrument is so simply represented.

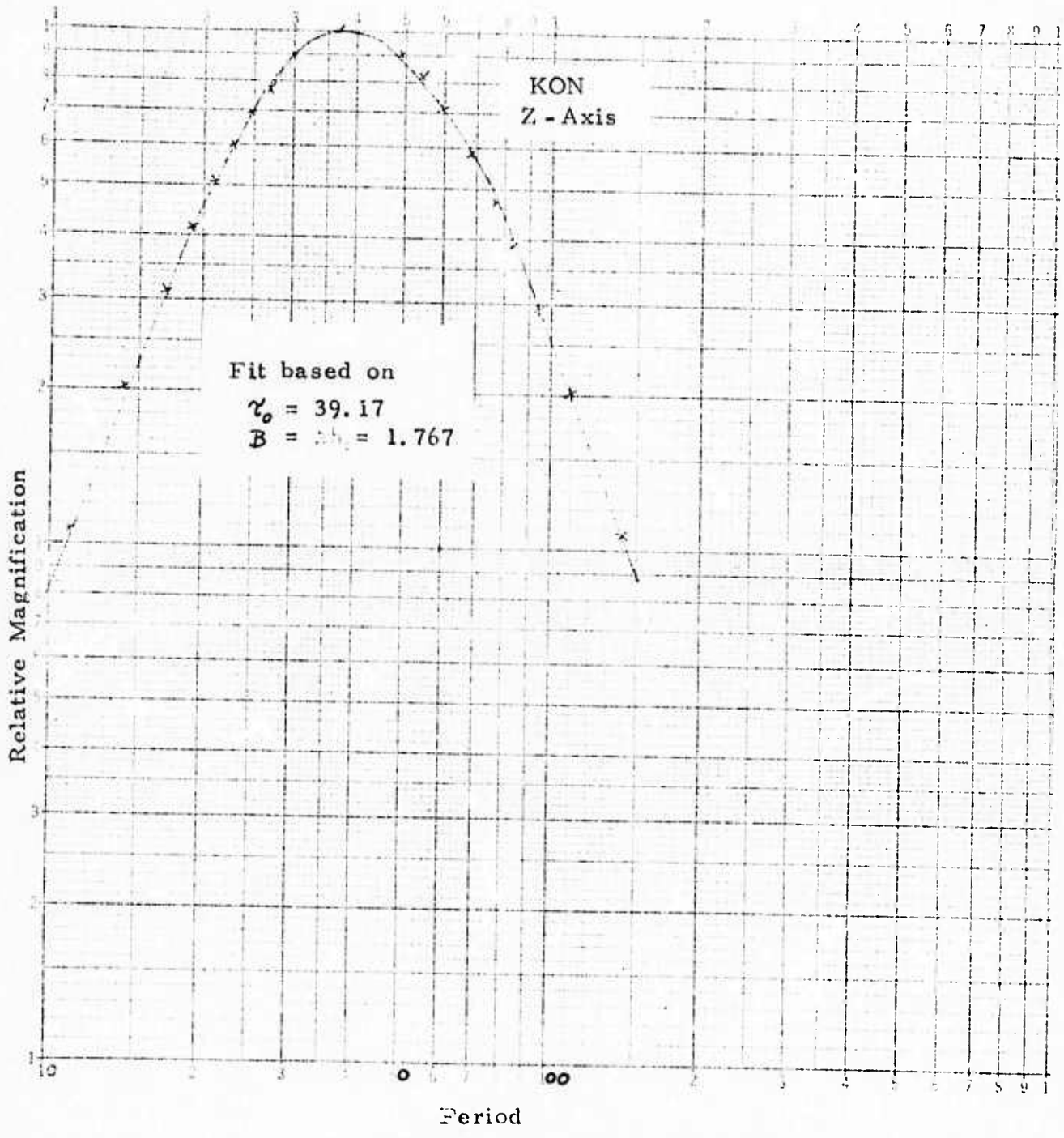

Fig. 21: Triple Tuned Model,
Curve Fitting of System Response

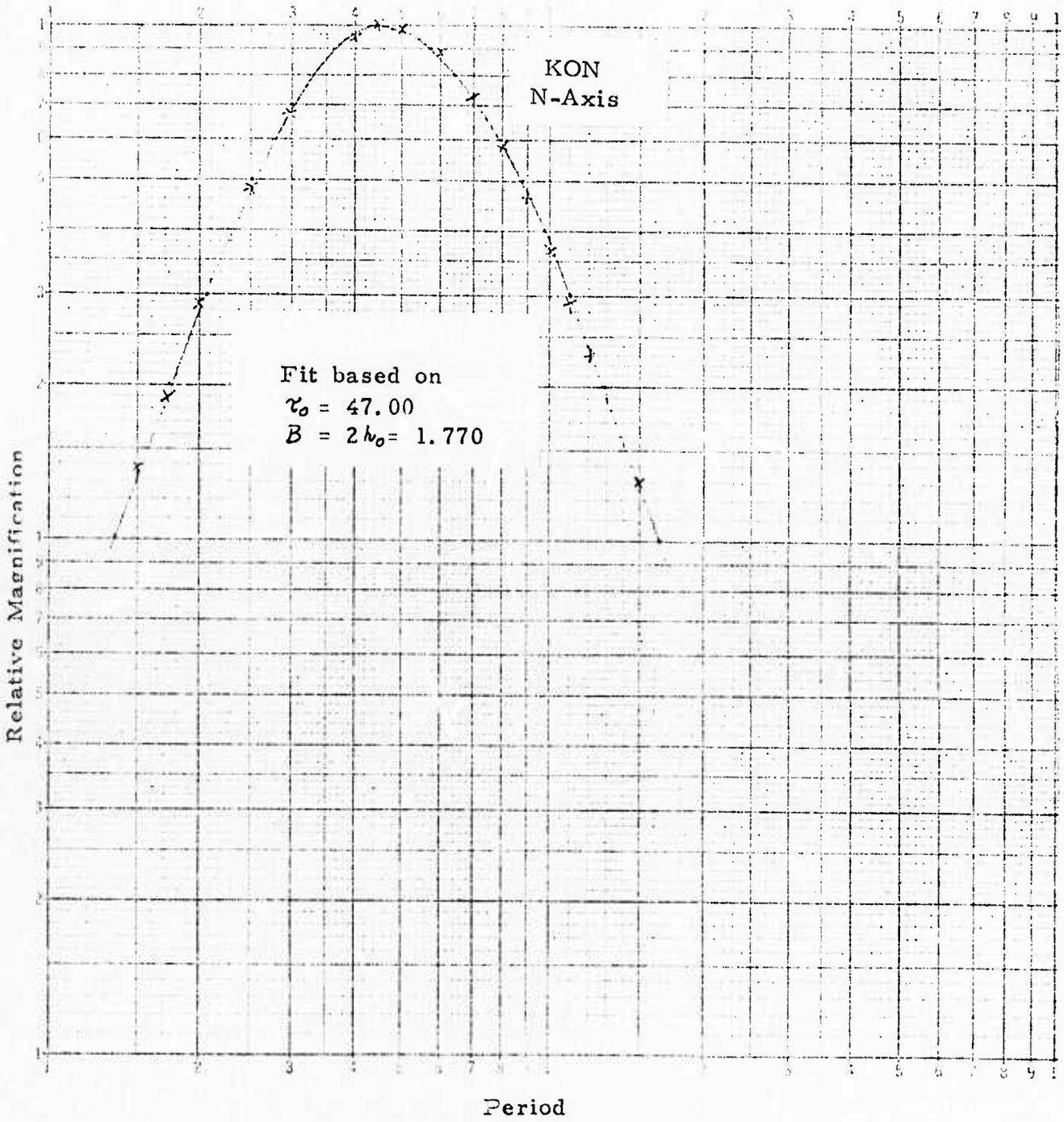

Fig. 22: Triple Tuned Model,
Curve Fitting of System Response

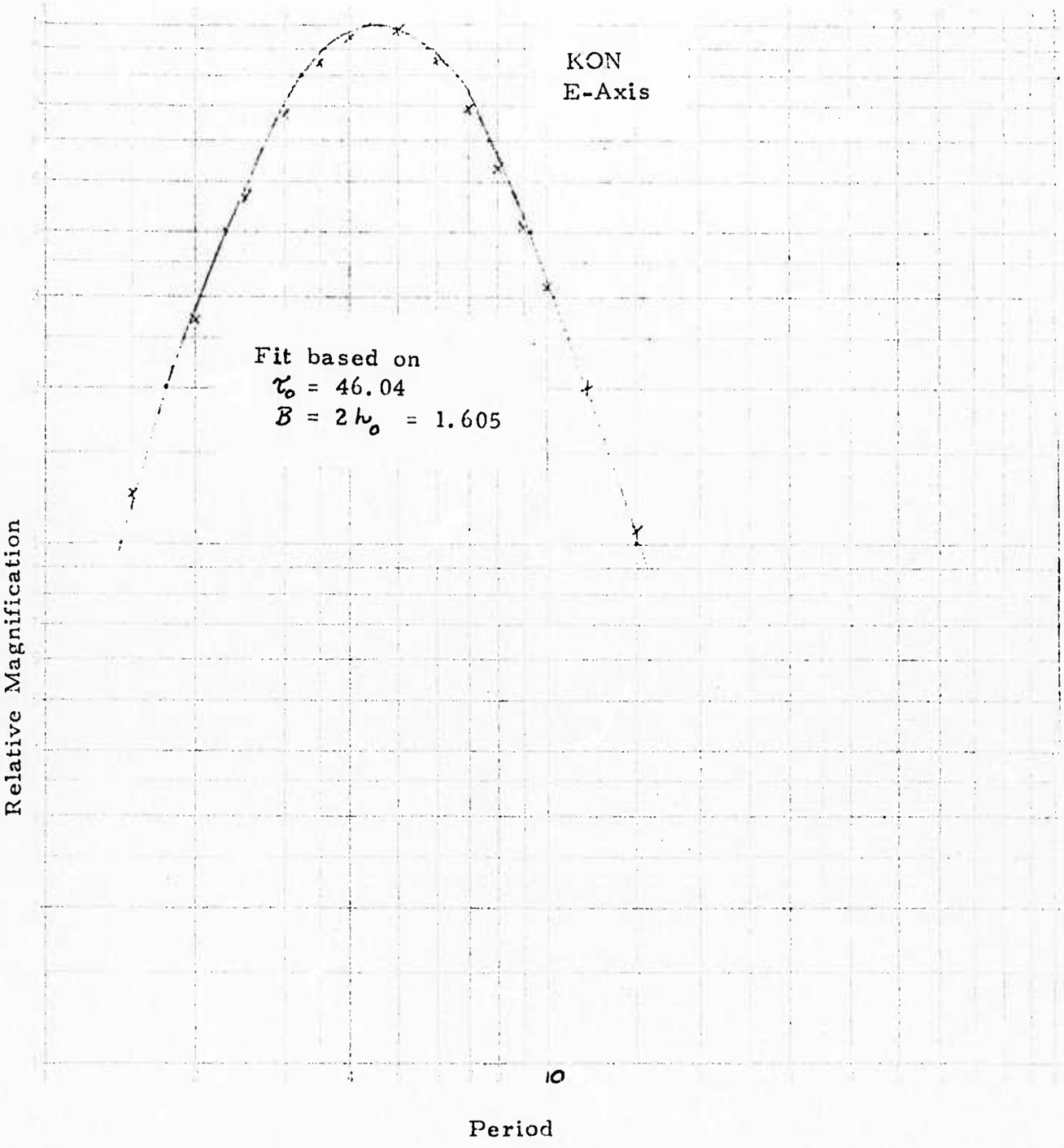

Fig. 23: Triple Tuned Model,
Curve Fitting of System Response

A.2 Method of Curve Fitting

The response of the seismometer and galvanometer alone is given by

$$R(s) = \frac{-k s^3}{(s^2 + 2h_1\omega_1 s + \omega_1^2)(s^2 + 2h_2\omega_2 s + \omega_2^2)}$$

in which (h_1 , ω_1) and (h_2, ω_2) are the damping constants and resonant frequencies of the seismometers and galvanometers. The amplitude vs period response is

$$R^2 = \frac{K^2 T^2}{\left[(1 - T^2/\gamma_1^2)^2 + 4h_1^2 T^2/\gamma_1^2\right]\left[(1 - T^2/\gamma_2^2)^2 + 4h_2^2 T^2/\gamma_2^2\right]}$$

The parameters of the vertical seismometers are

$$\gamma_1 \approx 30$$

$$\gamma_2 \approx 100$$

$$h_1 \approx h_2 \approx 1$$

This response is shown in Figure 24.

Comparison of the seismometer-galvanometer response with the overall response shows that the degree of extra filtering is considerable. While this is not unexpected, it does indicate that one might as well fit the overall response as try to imitate the

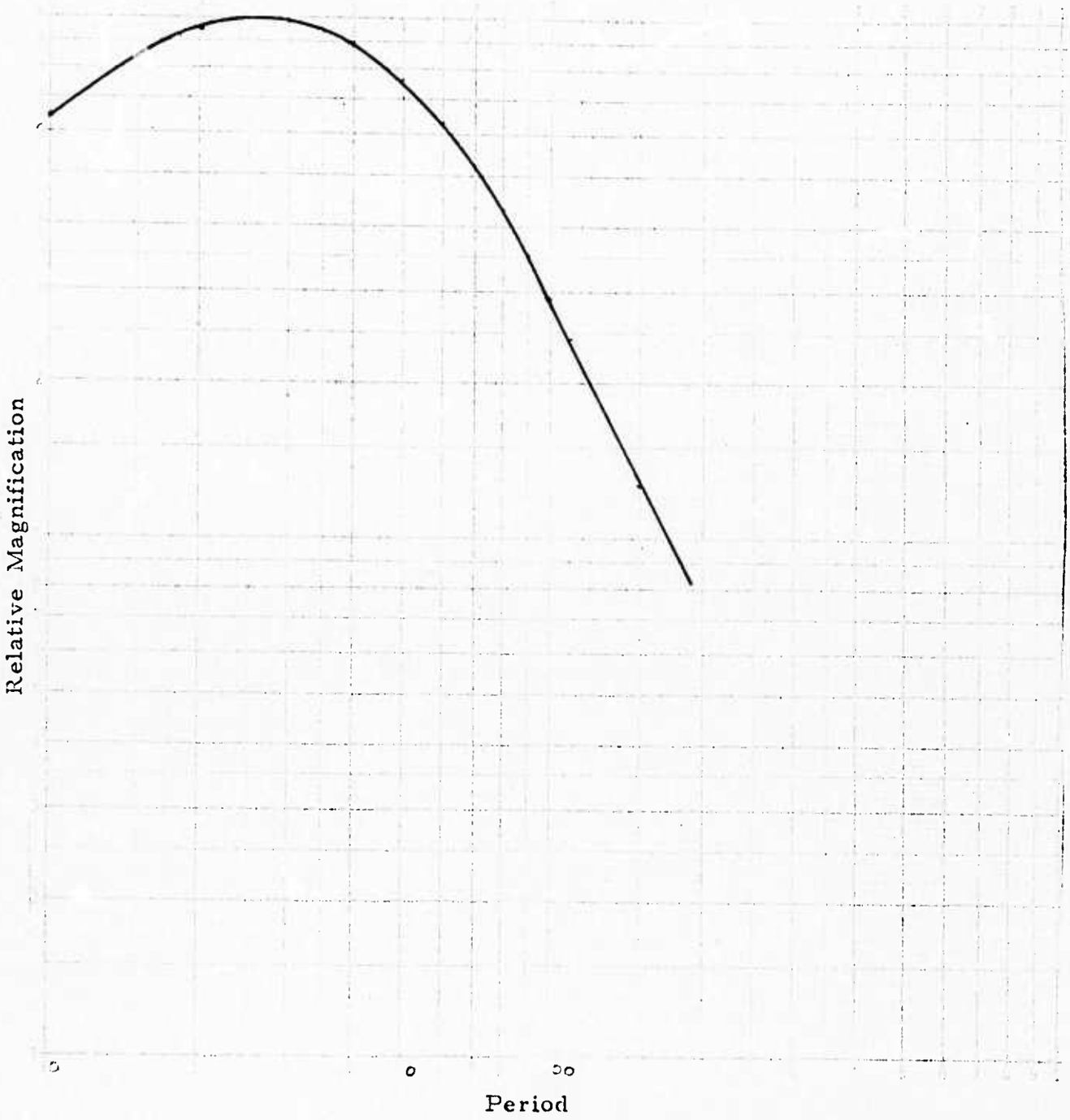

Fig. 24: Calculated Seismometer and Galvanometer Response

multi-stage filtering process with a mathematical expansion. For this reason, a direct synthesis of the overall response was made.

Examination of three axes shows that the amplitude curves are characterized by:

1. Geometry symmetry in period,
2. Skirt selectivities of 6 to 9 dB per octave.

The simplest network (fewest parameters) capable of fitting this type of bandpass is three cascaded identical single-tuned circuits.

A series, single-tuned circuit has the impedance function

$$Z(s) = R + sL + \frac{1}{sC}$$

and an admittance function

$$Y(s) = \frac{sC}{s^2LC + sRC + 1}$$

$$= \frac{s/L}{s^2 + s(R/L) + \frac{1}{LC}}$$

With $\omega_0 = 1/\sqrt{LC}$ the resonant frequency

$2h_0\omega_0 = R/L$ defining the damping factor

the form becomes

$$Y(s) \propto \frac{s}{s^2 + 2h_0\omega_0 s + \omega_0^2}$$

A more symmetrical form is

$$Y(s) \propto \frac{1}{(s/\omega_o + \omega_o/s) + 2h_o}$$

which translates into period

$$s = j\frac{2\pi}{T}$$

$$\omega_o = \frac{2\pi}{\tau_o}$$

$$Y(j\omega) \propto \frac{1}{2h_o + j(\omega/\omega_o - \omega_o/\omega)}$$

or $$Y\left(j\frac{2\pi}{T}\right) \propto \frac{1}{2h_o + j(\tau_o/T - T/\tau_o)}$$

The corresponding amplitude function, $A_1(T)$, for a single-tuned circuit is

$$A_1(T) = \frac{K}{\left[4h_o^2 + (\tau_o/T - T/\tau_o)^2\right]^{1/2}}$$

For three cascaded single-tuned circuits, the result is

$$A(T) = \frac{K^3}{\left[4h_o^2 + (\tau_o/T - T/\tau_o)^2\right]^{3/2}}$$

For convenience let

$$B = 2h_o$$

Then,

$$A(T) = \frac{B^3}{\left[B^2 + (\tau_o/T - T/\tau_o)^2\right]^{3/2}}$$

is the amplitude response of three cascaded single-tuned circuits, normalized to an $A(\tau)$ of unity at the peak $\tau_o = \tau$.

The procedure for curve fitting is:

1. Amplitude vs Period is read off the published data.

2. Geometric mean period is calculated for each amplitude level.

3. The average geometric mean period is selected as τ_o. Some improvement can be made in the fit, if desired, by ignoring the near peak values which are not accurate.

4. With τ_o known, a point estimate of B can be obtained from each pair of amplitude and period values

$$B = \left(\frac{A^{2/3}}{1 - A^{2/3}}\right)^{1/2} \left| \frac{\tau_o}{\tau} - \frac{\tau}{\tau_o} \right|$$

These are then averaged to give the estimate for B Some improvement is obtainable by ignoring those values corresponding to points near the peak.

If desired a minimum mean squared error fit could be made between the data and the response of the three single-tuned circuits. This is unnecessary, however, to prove that the data can be so fitted.

APPENDIX B: Leakage Effects in Evaluating the Spectrum and Analytic Signal of VLP Seismic Events

B.1 Summary

The evaluation of spectrum and/or the analytic function of the seismic signal is essential to the operation of mixed event seismic processors such as the Ellipticity Filter. The difficulties are accentuated for VLP signals because the negative frequency region can easily be smeared into the positive frequency region to give spurious results.

While the use of a uniform fader (window) is almost essential in the evaluation of the analytic function, the leakage effects are dramatic unless very long apertures are used. On the other hand, when only spectrum is desired, the cosine fader can be used and this weighting function permits small apertures to be used.

B.2 Discussion

One of the main difficulties to avoid in processing the very long period seismic signals is leakage which arises from the truncation effects of the DFT process. This leakage acts not only to smooth the spectrum, as is usual for all DFT processes, but because the signal content is of such low frequency, it also smears the negative frequency content into the positive frequency region.

The effect of negative frequency smearing, when a uniform fader is used, can be determined from Figures 25 and 26. For the system to have a dynamic range of 40 dB, a single DFT evaluation requires an fT product of 16; while a double DFT ratio evaluation (such as ellipticity) requires an fT product of 32. The corresponding apertures for a frequency component whose period is as large as 60 seconds are 960 and 1820 seconds. These apertures are quite long and the signal multipath cannot be expected to be stable in azimuth or in content over this duration.

The Hanning or Cosine Fader, on the other hand, as can be seen from Figures 25 and 26, require an fT product of 1.5 and 1.97 respectively. The corresponding apertures are then only 100 and 120 seconds respectively which is quite reasonable.

The first conclusion, therefore, is that the Hanning or Cosine Fader should be used for spectrum evaluations and thus provide the inputs for the frequency domain realizations of the Ellipticity Filter.

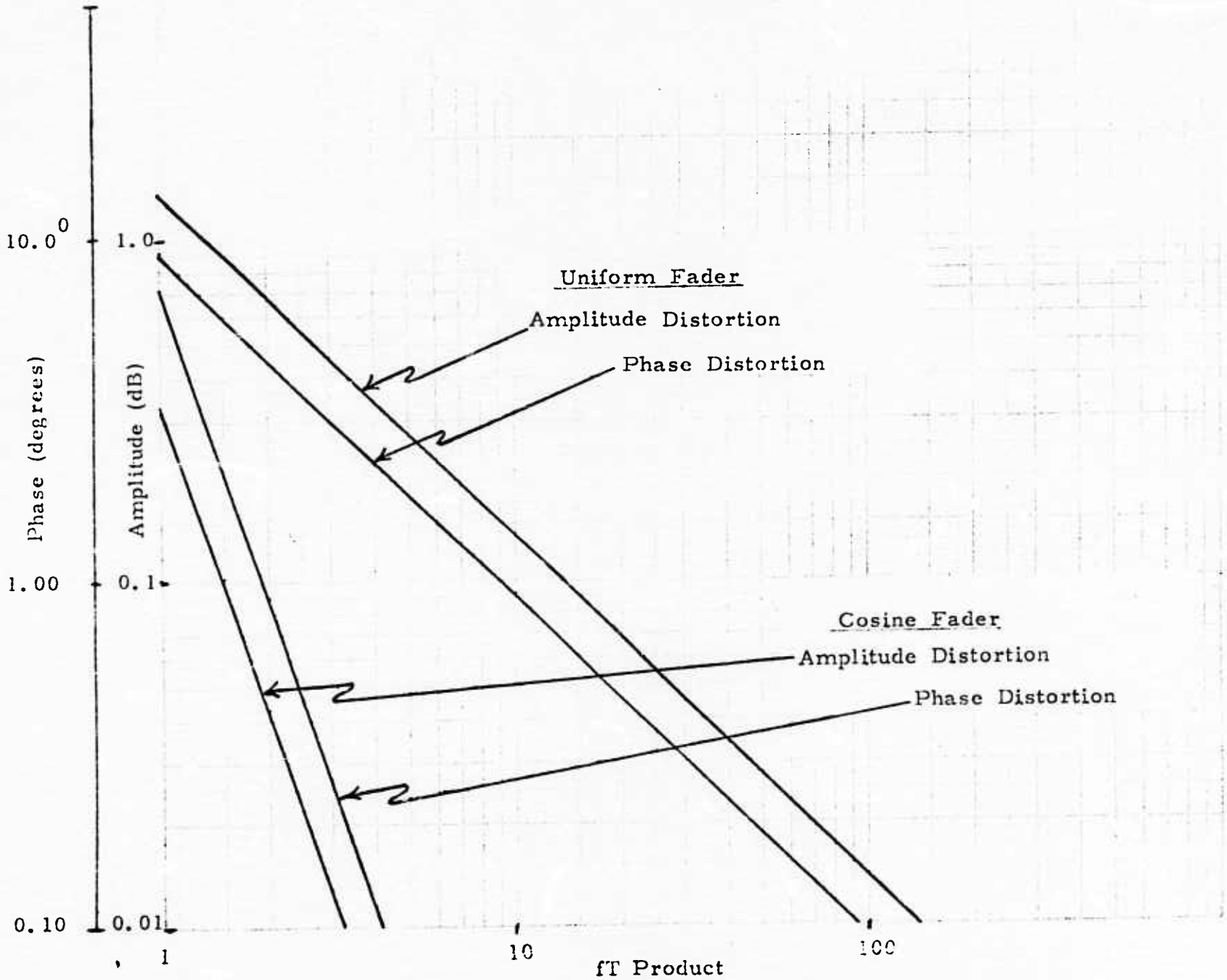

Fig. 25: Signal Distortion

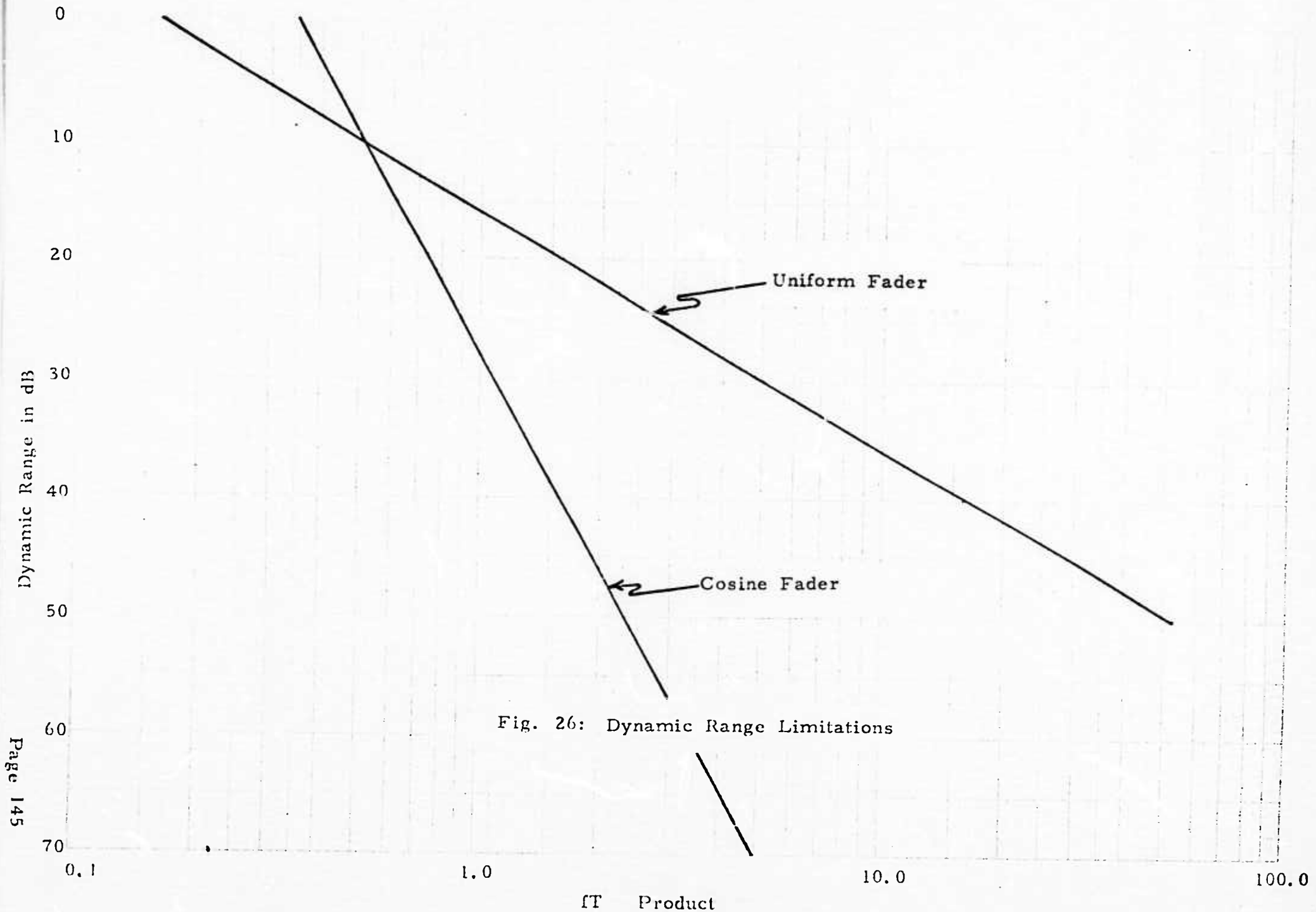

Fig. 26: Dynamic Range Limitations

Note, however, that the key advantage of the uniform fader is that the direct and inverse operations in sequence yield the original input. This is not true for the Cosine Fader. Thus, if one is instrumentizing time domain realizations of the Ellipticity Filter (using the DFT and the anlaytic function), the Uniform Fader is preferred. The sequence of operations is then:

1. Uniform Fader to obtain spectrum. Apertures of 1000 seconds are required.

2. Suppress the negative frequency output and take the inverse DFT (frequency filter here if desired.)

3. This gives the analytic function as an input to the time domain realization of the Ellipticity Filter.

4. If desired, the frequency domain realization can now be obtained by using reasonably short time apertures (200 seconds) and using the Cosine Fader to reduce smearing between the mixed events. This sequence, for the frequency domain realization, is cleaner (since there are no negative frequencies at this point) than using the Cosine Fader directly, but it is probably not necessary.

The frequency domain realizations can also be done at this point using a short time aperture uniform fader. There will be smearing between the positive frequency components of the mixed event, but the negative frequency smearing will be negligible.

B.3 Selection of the Fader

The large fT product required by the uniform aperture leads one to examine the benefits obtainable by using a different fader or aperture weighting function. Several alternatives exist (Hannon, p. 273-280)[16] The normalized windows are given in Table V.

Of the faders given, the Tukey-Hanning has the lowest sidelobes. This Hanning fader (Blackman and Tukey, p. 15 and p. 98)[13] has the unnormalized response

$$k(t) = \left(1 + \cos\frac{2\pi t}{T}\right)$$

$$K(f) = \frac{\sin \pi fT}{\pi fT} + \frac{1}{2}\frac{\sin \pi(f - 1/T)T}{\pi(f - 1/T)T} + \frac{1}{2}\frac{\sin \pi(f+\frac{1}{T})T}{\pi(f+\frac{1}{T})T}$$

$$= \frac{\sin \pi fT}{\pi fT} - \frac{1}{2}\left[\frac{\sin \pi fT}{\pi fT - \pi} + \frac{\sin \pi fT}{\pi fT + \pi}\right]$$

$$= \frac{\sin \pi fT}{\pi fT} \cdot \frac{\pi^2}{\pi^2 - (\pi fT)^2}$$

Thus, for large f

$$K(f) \rightarrow \frac{1}{\pi (fT)^3}$$

which is substantially better than the uniform fader. For this reason, as well as the low sidelobes present, the Hanning fader will be used.

Table V: Normalized Faders

	$k(x)$	$k(\lambda)$	Peak	Comments
Uniform	$1,\ \lvert x\rvert \le 1$ $0,\ \lvert x\rvert > 1$	$\frac{1}{\pi}\left(\frac{\sin\lambda}{\lambda}\right)$	$2/3\pi$	$k(x)$ is not continuous, spurious outputs are periodic in frequency.
Bartlett	$1-\lvert x\rvert,\ \lvert x\rvert \le 1$ $0,\ \lvert x\rvert > 1$	$\frac{1}{2\pi}\left(\frac{\sin\lambda/2}{\lambda/2}\right)^2$	$8/9\pi$	$k(\lambda)$ is always positive
Tukey-Hanning	$\frac{1}{2}(1+\cos\pi x),\ \lvert x\rvert \le 1$ $0,\ \lvert x\rvert > 1$	$\frac{\sin\lambda}{2\pi\lambda}\left(\frac{\pi^2}{\pi^2-\lambda^2}\right)$	$\frac{8}{105\pi}$	Low sidelobes. Commonly used
Parzen	$1-6x^2+6\lvert x\rvert^3,\ \lvert x\rvert \le \frac{1}{2}$ $2(1-\lvert x\rvert)^3,\ \frac{1}{2} \le \lvert x\rvert \le 1$ $0,\ 1 \le \lvert x\rvert$	$\frac{3}{8\pi}\left(\frac{\sin\lambda/4}{\lambda/4}\right)^4$		
Abel	$e^{-a\lvert x\rvert}$	$\frac{a}{\pi(a^2+\lambda^2)}$		Large computational load.
Daniell	$\frac{\sin\frac{1}{2}\pi x}{\frac{1}{2}\pi x}$	$\frac{1}{\pi},\ \lvert\lambda\rvert \le \pi/2$ $0,\ \lvert\lambda\rvert > \pi/2$		Large computational load.

B.4 Performance of the Uniform Fader

For a uniformly weighted time aperature (fader), the leakage can be evaluated as follows. For a sinusoid

$$X(t) = \cos(\omega_o t + \theta_o) = \frac{e^{j(\omega_o t + \theta_o)} + e^{-j(\omega_o t + \theta_o)}}{2}$$

the analytic function is

$$\tilde{x}(t) = e^{j(\omega_o t + \theta_o)}$$

The effect of the uniform time aperature on the analytic function is to give the spectral estimate

$$\underline{X}(j\omega) = \frac{1}{T}\int_{-T/2}^{+T/2} e^{j(\omega_o t + \theta_o)} e^{-j\omega t}\, dt$$

$$= \frac{e^{j\theta_o}}{T}\int_{-T/2}^{+T/2} e^{j(\omega_o - \omega)t}\, dt$$

$$= \frac{e^{j\theta_o}}{T} \cdot \frac{e^{j(\omega_o - \omega)T/2} - e^{-j(\omega_o - \omega)T/2}}{j(\omega_o - \omega)}$$

$$= e^{j\theta_o} \frac{\sin \pi(f_o - f)T}{\pi(f_o - f)}$$

This corresponds to the well understood

$$\frac{\sin \pi (f_o - f) T}{\pi (f_o - f)}$$

smearing of the true frequency transform.

There is, however, the second effect that the $\cos(\omega_o t + \theta_o)$ has its negative frequency content smeared as well. This can be seen by noting that the spectrum of the actual input, $X(t)$, is

$$\overline{X}(j\omega) = \left[e^{j\theta_o} \frac{\sin \pi (f_o - f) T}{\pi (f_o - f) T} + e^{-j\theta_o} \frac{\sin \pi (f_o + f) T}{\pi (f_o + f) T} \right]$$

This is diagramatically shown below

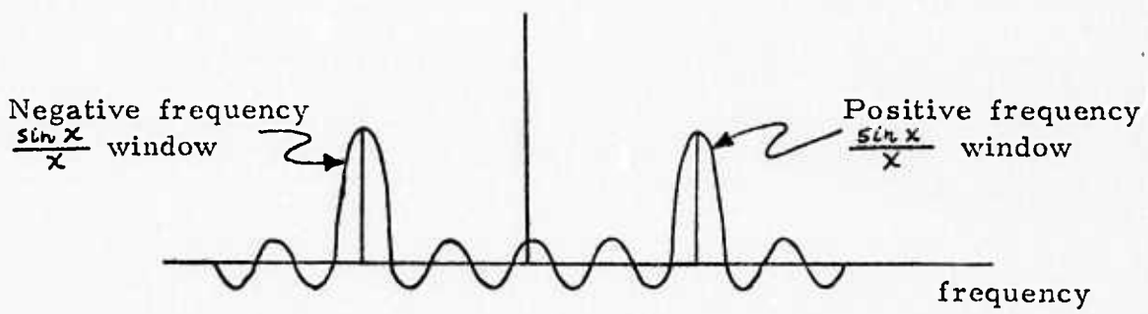

The total frequency window is the sum of the positive and negative frequency $\sin x/x$ windows and, hence, its shape is dependent on the frequency range being evaluated.

To numerically evaluate these effects, consider the lowest

frequency of interest to be f_ϕ Hz. Then,

$$\underline{X}(j\omega)\Big|_{f=f_\phi} = e^{j\theta_\phi} + e^{j\theta_\phi}\frac{\sin 2\pi f_\phi T}{2\pi f_\phi T}$$

The effect is zero when $f_\phi T$ is integer. This is as expected. For $f_\phi T$ not integer, the maximum effect is

$$\underline{X}(j\omega) = e^{j\theta_\phi} \pm \frac{e^{-j\theta_\phi}}{2\pi f_\phi T}$$

and the normalized result is a complex amplitude factor of

$$\left(1 \pm \frac{e^{-j2\theta_\phi}}{2\pi f_\phi T}\right)$$

The effect of this amplitude factor is phase angle dependent. The maximum amplitude effect occurs for $\theta_\phi = 0^\circ$,

$$\text{Maximum Amplitude Error} = \left(1 \pm \frac{1}{2\pi f_\phi T}\right)$$

The maximum phase error occurs for $\theta = \pm\pi/2$. The result is

$$\text{Maximum Phase Error} = \pm \tan^{-1}\frac{1}{2\pi f_\phi T} \quad \text{radians}$$

Two effects occur:

1. The signal itself is distorted in amplitude and phase.

For small errors, the maximum amplitude distortion in dB is

$$\text{Maximum Amplitude Error (dB)} = 20 \log_{10}\left(1 \pm \frac{1}{2\pi f_\beta T}\right)$$

$$= 20 \log_{10} e \ln\left(1 \pm \frac{1}{2\pi f_\beta T}\right)$$

$$\approx \frac{20 \log_{10} e}{2\pi f_\beta T}$$

$$\approx \frac{1.382}{f_\beta T}$$

The maximum phase error in degrees is

$$\text{Maximum Phase Error} \approx \frac{1}{2\pi f_\beta T} \text{ radians}$$

$$= \frac{360}{(2\pi)^2 f_\beta T} \text{ degrees}$$

$$= \frac{9.12}{f_\beta T} \text{ degrees}$$

Comparison of these two results show that a ten degree phase error criteria is equivalent to a 1.5 dB amplitude error.

2. The dynamic range of the system becomes limited because the larger signals obscure the smaller ones. The limit on the dynamic range (dB) is about

$$20 \log (2\pi f_{\phi} T)$$

These results are shown in Figures 25 and 26.

B.5 Performance of the Hanning or Cosine Fader

For a sinusoidal input

$$\cos(\omega_0 t + \theta_0)$$

the Hanning Fader smears the negative frequencies onto the positive frequencies so that the result is

$$\underline{X}(j\omega) = e^{j\theta_0} \frac{\sin \pi(f_0 - f)T}{\pi(f_0 - f)T} \cdot \frac{1}{1 - (f_0 - f)^2 T^2}$$

$$+ e^{-j\theta_0} \frac{\sin \pi(f_0 + f)T}{\pi(f_0 + f)T} \cdot \frac{1}{1 - (f_0 + f)^2 T^2}$$

Then, the amplitude distortion factor at $f_0 = f$ is

$$1 + e^{-j2\theta_0} \frac{\sin 2\pi f_0 T}{2\pi f_0 T} \cdot \frac{1}{1 - (2f_0 T)^2}$$

Then,

$$\text{Maximum Amplitude Error} = \left[1 \pm \frac{1}{2\pi f_0 T(1 - 4f_0^2 T^2)}\right]$$

while

$$\text{Maximum Phase Error} = \pm \tan^{-1} \frac{1}{2\pi f_0 T(1 - 4f_0^2 T^2)}$$

As for any fader there are two effects, distortion of the signal itself and limitations on the dynamic range.

1. Distortion of the signal is evaluated, as before, for small errors.

$$\text{Maximum Amplitude Factor in dB} \approx 20 \log \left(1 \pm \frac{1}{8\pi (f_0 T)^3}\right)$$

$$\approx \frac{20 \log_{10} e}{8\pi (f_0 T)^3}$$

$$\approx \frac{0.346}{(f_0 T)^3}$$

$$\text{Maximum Phase Factor} \approx \frac{1}{8\pi (f_0 T)^3} \text{ radians}$$

$$\approx \frac{45}{2\pi (f_0 T)^3} \text{ degrees}$$

$$\approx \frac{7.15}{(f_0 T)^3} \text{ degrees}$$

Comparison of these results show that a ten degree phase error is equivalent to about a 0.5 dB amplitude error.

2. Dynamic range limitations can be obtained by noting that the limit on the dynamic range in dB is

$$20 \log 8\pi (f_0 T)^3$$

which because of the cubed exponent is much better than that for a uniform fader.

These results are also shown in Figures 25 and 26.

ACKNOWLEDGMENTS

We would like to thank Dr. M. Nafi Toksoz of the Department of Earth and Planetary Sciences, Massachusetts Institute of Technology and Dr. Lynn Sykes and Dr. Keith McCamy of Lamont-Doherty Geological Observatory for their most helpful comments and suggestions at various stages of this effort.

Also we would like to thank Dr. Roy Greenfield of Pennsylvania State University and Dr. Eric Posmentier and Christina Mikulak of City College, New York for their assistance in the preparation of this paper.

Significant contributions have been made to this report Russell Gershman, Raymond Beaudin, and Isabella Tandy of the staff of Ocean & Atmospheric Science, Inc.

REFERENCES

1. Choy, G. and McCamy, K., "Enhancement of Long-Period Signals by Time Varying Adaptive Filters," Lamont-Doherty Geological Observatory, unpublished.

2. Alexander, S.S., "Long-Period Seismic Methods for Identifying Small, Underground Nuclear Explosions," Prepared for the Air Force Office of Scientific Research under the Sponsorship of Advanced Research Projects Agency, June 1969 to March 1973.

3. Sax, R.L. and Mims, C.M., "Rectilinear Motion Detection," Seismic Data Lab Report 118, ARPA Order 624, AF 33(657) 12447, March 1965.

4. Griffin, J.N., "Applications and Development of Polarization (REMODE) Filters," Prepared for Air Force Technical Applications Center under the Sponsorship of Advanced Research Projects Agency, February 1966 to February 1967.

5. Sykes, L.R., Ward, P.L., and Best, W., "High Gain, Long-Period Seismograph Station Instrumentation, Volume I and II," Lamont-Doherty Geological Observatory, Columbia University, 1971.

6. Savino, J., McCamy, K. and Hade, G., "Structures in Earth Noise Beyond 20 Seconds: A Window for Earthquakes," Bull. Seism. Soc. Amer., 62, 141, 1972a.

7. Savino, J.M., Murphy, A.J., Rynn, J.M.W., Tatham, R., Sykes, L.R., Choy, G.L. and McCamy, K., "Results from the High-Gain Long-Period Seismograph Experiment," Jour. Geophys. Res., 77, 1972.

8. Murphy, A.J., Savino, J., Rynn, J.M.W., Choy, G.L. and McCamy, K., "Observations of Long-Period (10 to 100 Sec) Seismic Noise at Several Worldwide Locations," J. Geophys. Res., 77, in press 1972.

9. Rynn, J.M.W., Savino, J., Tatham, R. Murphy, A.M. and Choy, G.L., "Detection Thresholds for Shallow Earthquakes Using High-Gain Seismograph Stations," (Abstract), Trans. Am. Geophys. Union, 53, 446, 1972.

REFERENCES (cont'd)

10. Greenfield, R.: "Some Notes on Long-Period Signals," Ocean & Atmospheric Science, Inc., Technical Report, TR 74-252, Prepared for the Air Force Office of Scientific Research under the Sponsorship of Advanced Research Projects Agency, Contract No. F44620-74-C-0066, November 26, 1974.

11. Posmentier, E., Gershman, R., and Harris, B.: "The Ellipticity Filter: A Proposed Solution to the Mixed Event Problem in Nuclear Seismic Discrimination," Ocean & Atmoshperic Science, Inc., Technical Report, TR 74-232, Prepared for the Air Force Office of Scientific Research under the Sponsorship of Advanced Research Projects Agency, Contract No. F44620-74-C-0066, September 7, 1974.

12. Harris, B.: "Quarterly Technical Report No. 3, Seismic Verification of Mixed Events, Ocean & Atmospheric Science, Inc., Technical Report, TR 75-271, Prepared for the Air Force Office of Scientific Research under the Sponsorship of Advanced Research Projects Agency, Contract No. F44620-74-C-0066, April 7, 1975

13. Blackman, R.B. and Tukey, J.W., "The Measurement of Power Spectrum," Dover Publications, Inc. (Reprint, 1959. Originally published by B.S.T.J., January 1958 and March 1958.

14. Boore, D.B. and Toksoz, M.N., "Rayleigh Wave Particle Motion and Crustal Structure," Bull. Seis. Soc. Am., 59: 331-346, 1969.

15. Lambert, D.G., Prahl, S.R., and Struass, A.C., "Evaluation of the Noise Characteristics and the Detection and Discrimination Capabilities of the Very Long Period Experiment (VLPE) Single Stations and the VLPE Network," Texas Instruments, Inc., Report No. ALEX(01)-STR-73-14, November 1, 1973.

16. Hannan, E.J., "Multiple Time Series," John Wiley and Sons, Inc., 1970.